Electronic Thesis and Dissertation Repository

10-29-2021 2:00 PM

# Creating Tools to Study the Signaling and Function of the Adhesion Family of GPCRs

Victor M. Mirka, *The University of Western Ontario*

Supervisor: Ramachandran, Rithwik, *The University of Western Ontario*
A thesis submitted in partial fulfillment of the requirements for the Master of Science degree in Physiology and Pharmacology
© Victor M. Mirka 2021

## Recommended Citation

# Abstract

Adhesion GPCRs (aGPCRs) are difficult to study because they are activated by mechanical force. aGPCRs are autoproteolytically cleaved into N-terminal and C-terminal fragments. Mechanical force removes the N-terminal fragment revealing a tethered ligand activating the receptor. Proteinase Activated Receptors (PARs) are N-terminally cleaved by proteinases revealing a tethered ligand activating the receptor. We hypothesized the tethered ligand of aGPCRs could be revealed by replacing the N-terminal fragment with a PAR N-terminus. We fused the PAR2 N-terminus to the C-terminal fragments of four aGPCRs: CD97, EMR2, GPR56, and BAI1. PAR2-aGPCR chimeric receptors dose dependently recruited G-proteins and β-arrestins, supporting our hypothesis. Peptides made to mimic the tethered ligand, are sufficient to activate receptors. We developed a method for predicting aGPCR tethered ligand mimicking peptides and tested the approach for CD97. We found SSFAILMAH-NH$_2$ to be a potent CD97 activating peptide. In this thesis we developed two novel methods for studying the illusive aGPCRs.

# Keywords

# Summary for Lay Audience

The various systems of our bodies are controlled through an intercellular communication network mediated by soluble chemical messengers. These chemical messengers relay information throughout our bodies by binding receptors expressed on the surface of our cells. Exogenous molecules, drugs, can be made to mimic these chemical messengers, which can then bind cell surface receptors to modulate bodily functions and treat disease. G-protein coupled receptors (GPCRs) are the largest targets of FDA approved drugs, with around 25-36% of all FDA approved drugs targeting GPCRs. Despite this fact, the second largest GPCR subfamily, the adhesion GPCRs (aGPCRs), are not targeted by a single FDA approved drug. These receptors are attractive drug targets as they have been shown to be involved in brain development, the immune system, inflammatory diseases, and many different cancers. Lack of drug development at these receptors stems from the fact that they are activated in a two-cell system by mechanical force. As their mechanism of action is very difficult to reproduce and control in a laboratory setting, in this thesis we set out to design tools to enable their study. We designed a method in where aGPCRs could be activated by proteolytic cleavage instead of mechanical force, allowing receptor activation to be controlled by adjusting the concentration of enzyme. Further, we determined a method of predicting aGPCR agonist peptides. We then tested our two new methods on four of the more well studied aGPCRs: CD97 (ADGRE5), EMR2 (ADGRE2), GPR56 (ADGRG1), and BAI1 (ADGRB1). Both methods proved to be very effective and based on our result we believe they can be applied to study the whole family of 33 aGPCRs.

# Co-Authorship Statement

All data presented in this thesis was completed by Victor Mirka in the laboratory of Dr. Rithwik Ramachandran. Dr. Rithwik Ramachandran provided guidance on experimental design, data analysis, interpretation, and manuscript preparation for all chapters.

Chapter 1:

Chapter 1 contains components of a book chapter in press written by Victor Mirka and Dr. Rithwik Ramachandran. Victor Mirka contributed to all figures, tables, and manuscript preparation.

Mirka V, Ramachandran R. (2021) Allosteric modulation of tethered ligand activated receptors. ELSEVIER. In press.

Chapter 2 and 3:

Dr. Arundhasa Chandrabalan completed all peptide synthesis with design directions from Victor Mirka and Dr. Rithwik Ramachandran. Victor Mirka completed all bioluminescence resonance energy transfer, TANGO, and confocal experiments described with guidance from Dr. Arundhasa Chandrabalan, Dr. Pierre Thibeault, and Dr. Rithwik Ramachandran.

Chapter 3 contains components of a book chapter in press written by Victor Mirka and Dr. Rithwik Ramachandran. Victor Mirka contributed to all figures, tables, and manuscript preparation.

Mirka V, Ramachandran R. (2021) Allosteric modulation of tethered ligand activated receptors. ELSEVIER. In press.

# Acknowledgments

First, I would like to thank my supervisor Dr. Rithwik Ramachandran. In my fourth year you took a risk on me as a thesis student as I didn't have any prior hands-on lab experience. This one-year commitment quickly turned into three, and I have nothing but positive things to say about my experience in your lab. Your unique approach of allowing every student in your lab to choose their own project I feel brings out the best in people.

Next, I would like to thank the current and past members of the Ramachandran lab: Dr. Arundhasa Chandrabalan, Dr. Hiroyuki Igarashi, Dr. Pierre Thibeault, Samantha Ingham, Junbo Wang, Varunaavee Sivashanmugathas, and Darsh Shah. All of your guidance over the past three years has been greatly appreciated.

Finally, I would like to thank my Parents and brother. Without your continued support nothing that I have achieved would be possible.

# Table of Contents

# List of Figures

# List of abbreviations

| | |
|---|---|
| 3-α-DOG | 3-α-acetoxydihydrodeoxygedunin |
| μg | Microgram |
| μM | Micromolar |
| A | Alanine |
| aGPCR | Adhesion G-protein coupled receptor |
| AKT | Protein kinase B |
| AP-2 | Adaptor protein 2 |
| ATP | Adenosine triphosphate |
| BAI1 | Brain-specific angiogenesis inhibitor 1 |
| BFPP | Bilateral frontoparietal polymicrogyria |
| BRET | Bioluminescence resonance energy transfer |
| C | Cystine |
| $Ca^{2+}$ | Calcium |
| cAMP | Cyclic adenosine monophosphate |
| CaS | Calcium sensing receptor |
| CD97 | Cluster of differentiation 97 |
| cGMP | Cyclic guanosine monophosphate |
| Cl | Chloride |
| CNS | Central nervous system |
| CREB | Cyclic AMP response element binding protein |
| CRD | Cysteine rich domain |
| CRISPR | Clustered regularly interspaced short palindromic repeats |
| C-terminus | Carboxy-terminus |
| CTF | C-terminal fragment |

| | |
|---|---|
| D | Aspartic acid |
| DAG | Diacylglycerol |
| DDT | Dichloro-diphenyl-trichloroethane |
| DHA | Docosahexaenoic acid |
| DMEM | Dulbecco's modified Eagle's medium |
| DMSO | Dimethylsulfoxide |
| DNA | Deoxyribonucleic acid |
| E | Glutamic acid |
| E-cadherin | Epithelial cadherin |
| ECL | Extracellular loop |
| EDTA | Ethylenediaminetetraacetic acid |
| EGFR | Epidermal growth factor receptor |
| EMR2 | Epidermal growth factor-like module-containing mucin like hormone receptor-like 2 |
| ER | Endoplasmic reticulum |
| ERK/MAPK | Extracellular receptor kinase/Mitogen activated protein kinase |
| F | Phenylalanine |
| FDA | Food and drug administration |
| FSH | Follicle stimulating hormone |
| G | Glycine |
| GABA | Gama-Aminobutyric acid |
| GAP | GTPase accelerating protein |
| GAIN | GPCR autoproteolysis inducing domain |
| GDP | Guanosine diphosphate |
| GEF | Guanine nucleotide exchange factor |
| GIRK | G-protein regulated inward rectifier potassium channels |

| | |
|---|---|
| GPCR | G-protein coupled receptor |
| GPR56 | G-protein coupled receptor 56 |
| GPS | GPCR autoproteolysis site |
| GRK | G-protein coupled receptor regulator kinase |
| GSK-3β | Glycogen synthase kinase 3β |
| GTP | Guanosine triphosphate |
| H | Histidine |
| H | Hydrogen |
| HBSS | Hanks' balanced salt solution |
| HEK293 | Human embryonic Kidney 293 |
| HEPES | 4-(2-hydroxethyl)-1-piperazineethanesulfonic acid |
| I | Isoleucine |
| ICL | Intracellular loop |
| IL | Interleukin |
| $IP_3$ | Inositol triphosphate |
| K | Lysine |
| L | Leucine |
| LB | Luria broth |
| LH | Luteinizing hormone |
| LRP | Lipoprotein receptor protein |
| M | Methionine |
| Mg | Magnesium |
| mg | Milgram |
| MHC | Major histocompatibility complex |
| mL | Milliliter |
| mM | Millimolar |

| | |
|---|---|
| mm | Millimeter |
| N | Nitrogen |
| $Na^+$ | Sodium |
| NAM | Negative allosteric modulator |
| NFAT | Nuclear factor of activated T-cells |
| nM | Nanomolar |
| N-terminus | Amino-terminus |
| NTF | N-terminal fragment |
| Opti-MEM | Optimized minimal essential medium |
| P | Proline |
| PAM | Positive allosteric modulator |
| PAR | Proteinase activated receptor |
| PAR2-KO | PAR2 knock out |
| PBS | Phosphate buffered saline |
| PKA | Protein kinase A |
| PKC | Protein kinase C |
| Phe(4-Me) | 4-Methyl-L-phenylalanine |
| PI3K | Phosphoinositide 3-kinase |
| $PIP_2$ | Phosphatidylinositol 4,5-bisphosphate |
| PLC-$\beta$ | Phospholipase C$\beta$ |
| PLL | Pentraxin/Laminin/neurexin/sex hormone binding globulin-like domain |
| Q | Glutamine |
| R | Arginine |
| RGS | Regulators of G-protein signaling |
| RhoA | Ras homolog family member A |

| | |
|---|---|
| RLuc | Renilla luciferase |
| RNA | Ribonucleic acid |
| ROCK | Rho-associated protein kinase |
| RFP | Red fluorescent protein |
| S | Serine |
| SAG | Smoothened ligand |
| SEM | Standard error of the mean |
| SRE | Serum response element |
| SRF | Serum response factor |
| T | Threonine |
| TM | Transmembrane domain |
| TSH | Thyroid stimulating hormone |
| V | Valine |
| VFT | Venous flytrap |
| VIP | Vasoactive intestinal peptide |
| W | Tryptophan |
| WNT | Wingless/Int-1 |
| Y | Tyrosine |

# Chapter 1

# 1 Introduction

## 1.1 Regulation of cellular signaling

Multicellular organisms require efficient intercellular communication to control cellular proliferation, migration, differentiation, survival and homeostasis[1]. Cells can communicate through direct cell-cell and cell-matrix interactions or through secreted signaling molecules[1,2]. The interaction of E-cadherin with the epidermal growth factor receptor (EGFR) is an important example of direct cell-cell signaling[3,4]. The homophilic interaction of two E-cadherin molecules on neighboring cells allows E-cadherin to interact with and inhibit the kinase function of the EGFR[3,4]. EGFR kinase signaling is an important cell proliferation pathway and is often dysregulated in cancer[3,4].

A major component of intercellular signaling is mediated by the diffusion of chemical messengers, which act on cell surface receptors leading to intracellular changes[1]. The signaling of secreted molecules can be differentiated based on the distance the signal must travel[1,2]. In autocrine signaling, a secreted signaling molecule acts back on the same cell that produced it[1,2]. For example, after a T cells has recognized its appropriate major histocompatibility complex (MHC)-peptide antigen complex it begins to release interleukin 2 and express high affinity interleukin 2 receptors[5]. This autocrine interleukin 2 signaling is important for initiating the clonal expansion of activated T cells for the future coordination of the adaptive immune response[5].

When a cell releases a signaling molecule which then acts on a nearby cell, this is considered paracrine signaling[1,2]. An example of paracrine signaling is when neurotransmitters released from the nerve terminal of one neuron cross the synaptic cleft and act on the receptors of post synaptic neurons[2]. In Parkinson's disease, degeneration of dopaminergic neurons in the substantia nigra causes the loss of important inhibitory dopamine paracrine signaling in the neostriatum, leading to involuntary movements[6].

Endocrine signaling occurs when a signaling molecule is secreted into the circulation and acts on a distant cell[1,2]. The release of thyroid stimulating hormone (TSH) from the anterior pituitary, which then travels through the circulation to bind TSH receptors on thyroid follicular cells is an example of endocrine signaling[7]. TSH signaling at thyroid follicular cells is an important regulator of thyroid hormone production, and its dysregulation commonly results in cancer[7]. Exogenous molecules, drugs, can be made to mimic these endogenous chemical messengers to modulate homeostatic processes[2]. Many disease states are the result of homeostatic dysregulation and can therefore be treated by the use of exogenous drugs[8].

## 1.2   Major receptor families

Cellular receptors can be broadly separated into four families: ligand gated ion channels, enzyme-linked receptors, intracellular receptors, and G-protein coupled receptors[9]. As G-protein coupled receptors were the primary focus of this thesis they will be explained in detail and only a brief description will be provided for the other three receptor families.

### 1.2.1   Ligand gated ion channels

Ligand gated ion channels are generally pentameric integral membrane proteins which form a ligand gated membrane spanning pore[9,10]. Upon ligand binding the receptor undergoes a conformational change, opening the pore, and allowing the selective passive flow of ions down their electrochemical gradient across the plasma membrane[9,10]. Of the four major receptor family's ligand gated ion channels have the shortest response durations, lasting only a few milliseconds[9,10]. As an example, in post-natal neurons upon the binding of the neurotransmitter Gama-Aminobutyric acid (GABA), the $GABA_A$ receptor opens a chloride selective channel[11]. Chloride moving into the cell down its electrochemical gradient hyperpolarizes the cell, and this basic mechanism is the primary way inhibitory signaling is transduced in the brain[11]. The balance of excitatory and inhibitory signaling in the brain is vital for homeostasis[11]. Dysregulation of $GABA_A$ receptors inhibitory signaling in the brain, can lead to an excess of excitatory signaling, resulting in diseases such as epilepsy[11].

## 1.2.2    Enzyme-linked receptors

Enzyme-linked receptors are generally single pass transmembrane proteins with an extracellular ligand binding domain and an intracellular region that either has intrinsic enzyme activity or associates directly with an enzyme[9,12]. Upon ligand binding the receptor undergoes a conformational change that either activates the intrinsic enzyme or recruits one to its intracellular binding domain[9,12]. The duration of enzyme-linked receptor responds is generally on the scale of minutes to hours[9,12]. Most enzyme-linked receptors fall under the category of receptor tyrosine kinases, where the receptor contains an intracellular kinase domain capable of phosphorylating itself and other effector proteins to initiate signaling cascades upon ligand binding[9,12]. The insulin receptor is an example of a receptor tyrosine kinase, however unlike most it exists as a preformed dimer[13]. Upon insulin binding the two receptors intracellular kinase domains come in contact and begin to phosphorylate each other[13]. These phosphorylated tyrosine residues form docking site for other kinase effector proteins to continue the signaling cascade[13]. Dysregulated insulin receptor signaling is known to contribute to the development of diseases such as type 2 diabetes[13].

## 1.2.3    Intracellular receptors

Intracellular receptors are located primarily in the cytoplasm and nucleus and are activated by cell permeant lipophilic ligands, such as hormones[9]. Unlike the other receptor families, intracellular receptors directly regulate gene expression by physically binding DNA and acting as transcription factors[9]. Upon ligand binding a prebound inhibitory protein is generally released, allowing receptor dimerization and translocation to the nucleus for DNA binding[9]. Because intracellular receptors primarily regulate changes in gene transcription their signaling duration is on the scale of hours to days[9]. The estrogen receptor can be an example of an intracellular receptor[14]. Upon estrogen binding the pool of intracellular estrogen receptors, the receptor undergoes a conformational change causing the release of inhibitory heat shock proteins, revealing of a DNA binding domain, and allowing receptor dimerization[14]. The dimerized receptors then translocate from the cytoplasm to the nucleus and bind the promoters of specific genes to positively or negatively regulate their expression[14].

## 1.3   G-protein coupled receptors

G Protein-coupled receptors (GPCRs) are the largest family of membrane proteins in the human genome[15,16] and have evolved to respond to diverse stimuli[17]. GPCRs are also major targets for therapeutic drugs with estimates showing between 25-36% of all FDA approved drugs targeting GPCRs[18]. These receptors are characterized by their extracellular N-terminus and ligand binding site, seven transmembrane spanning domains, and intracellular C-terminus and transducer binding site[19,20]. Classically GPCR activation is triggered by the binding of a ligand to the extracellular ligand binding site, which induces conformational changes in the receptor that allows the intracellular binding of transducers, such as heterotrimeric G proteins and arrestins[19,20] (Fig 1). The duration of signaling events produced by GPCRs are on the scale of seconds to minutes[9].
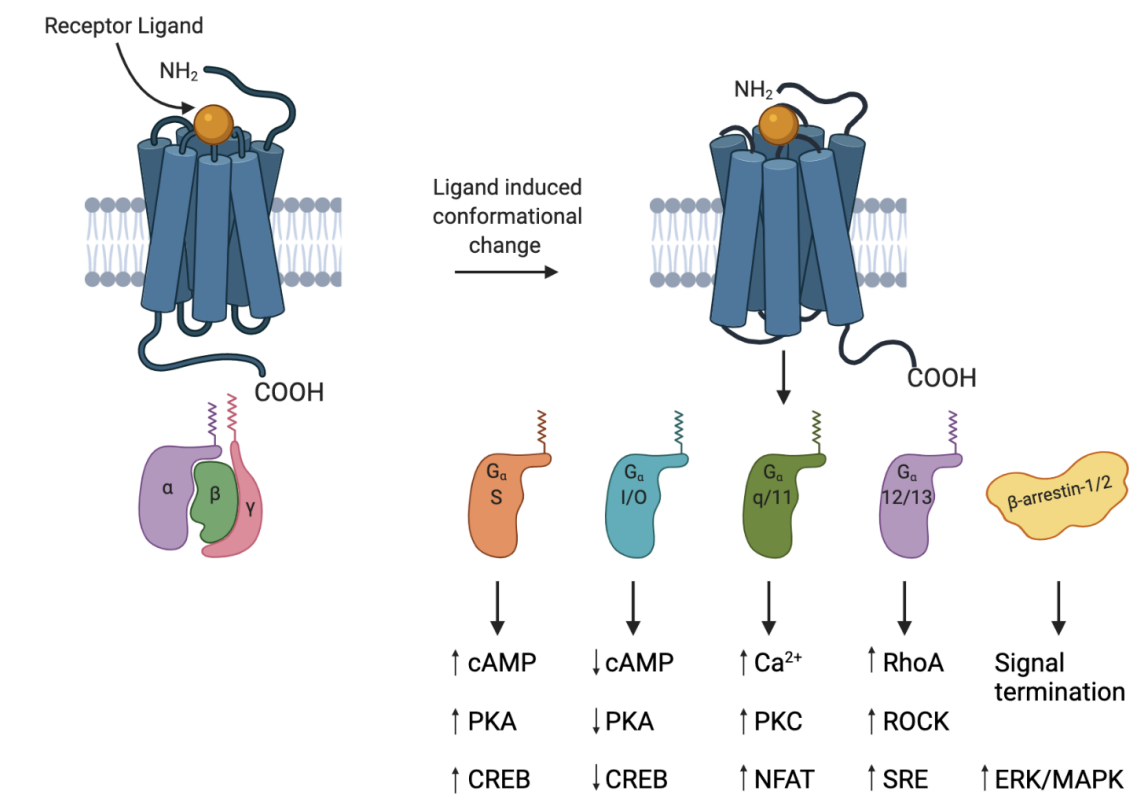
**Figure 1. General activation mechanism for most GPCRs**. A ligand binds the receptor causing a conformational change, leading to receptor activation. The activated receptor is then able to recruit one or more of the five major families of effectors proteins $G_{\alpha S}$, $G_{\alpha i/o}$, $G_{\alpha q/11}$, $G_{\alpha 12/13}$, and β-arrestin 1/2. The type of effect protein then determines the distinct change in cellular signaling that will occur. Figures were generated using the program Biorender (https://biorender.com).

## 1.3.1 Allosteric transitions

Allosteric transitions describe the change in receptor conformation from the inactive to active state. These events are best understood for Rhodopsin family (class A) GPCRs, as they have the most solved ligand and effector bound structures in various conformational states[21,22]. The general structural changes involved in the allosteric transition to the active state are an outward movement of transmembrane domain 6 (TM6), an inward movement of TM5 and TM7, a rotation of TM3, a constriction of the orthosteric site, and an opening of an intracellular transducer binding site[21–25]. These structural changes are mediated by a conserved set of microswitches including CWxP, NPxxY, PIF, and D(E)RY. Located in TM6, $W^{6.48}$ (Ballesteros Weinstein numbering in superscript [26]) of the CWxP motif in class A GPCRs is thought to function as a "toggle switch" between the inactive and active states[22,24]. Located in TM7, the NPxxY motif stabilizes the inactive state of Rhodopsin family GPCRs by forming a hydrogen bond network, via $N^{7.49}$, with water molecules and an allosteric $Na^+$ ion. Upon ligand binding, TM7 moves inward, and this hydrogen bonding network is broken. In the active state the NPxxY motif instead mediates the packing of TM3 to TM7[22]. The PIF motif, which is located in TM6, interacts with the toggle switch residue $W^{6.48}$ to help mediate the outward movement of TM6 upon ligand binding[22]. Located in TM3, the D(E)RY motif, or ionic lock switch, stabilizes the inactive state by forming a salt bridge between $R^{3.50}$ and $E^{6.30}$ of TM6. Ligand binding breaks this salt bridge, allowing the outward movement of TM6[22].

## 1.3.2 GPCR effector proteins

Interaction of the GPCR intracellular face with signaling effectors determines the second messenger signaling pathways that are activated to affect changes in cellular function[20]. Five types of effector proteins cause the majority of signaling downstream of GPCRs[19,27–30]. These are the four different types of heterotrimeric G-proteins and the β-arrestins[19,27–30]. The heterotrimeric G-protein is made up of $G_\alpha$, $G_\beta$ and $G_\gamma$ subunits[19,27,28]. The $G_\beta$ and $G_\gamma$ subunits exist as a dimer and are therefore usually referred to as $G_{\beta\gamma}$[19,27,28]. The $G_\alpha$ subunit contains a GTPase domain and guanine nucleotide binding site, which in the inactive state is bound to GDP[19,27,28]. The heterotrimeric G-protein is anchored at the plasma membrane by lipid modifications on the $G_\alpha$ and $G_\gamma$ subunits; however, whether

the heterotrimeric G-protein is pre-coupled to the receptor seems to be receptor and G-protein dependent[19,27,28]. Although there are many different types of $G_\alpha$, $G_\beta$ and $G_\gamma$ subunits, the different families of heterotrimeric G-protein are characterized by the type of $G_\alpha$ subunit [19,27,28]. The four different families of G-proteins are $G_s$, $G_{i/o}$, $G_{q/11}$, and $G_{12/13}$. Although cross talk between pathways occurs, each type of G-protein generally employs different effector proteins to cause distinct changes in cellular function. The primary function of GPCRs is to act as guanine nucleotide exchange factors (GEFs) for heterotrimeric G-proteins, where the pre-bound GDP on the $G_\alpha$ subunit is exchanged for GTP[19,27,28]. This exchange activates the G-protein, causing dissociation of the $G_\alpha$ subunit from $G_{\beta\gamma}$, allowing both to engage downstream effectors proteins[19,27,28]. Signaling via the $G_\alpha$ subunit is terminated by both its own low activity GTPase and by effectors such as regulators of G-protein signaling (RGS) proteins, which act as GTPase accelerating proteins (GAPs)[19,27,28]. The inactive $G_\alpha$ subunit then binds up free $G_{\beta\gamma}$ subunits to terminate its signaling and reform the heterotrimeric G-protein for future signaling events[19,27,28].

## 1.3.2.1    The $G_s$ family of G-proteins

The $G_s$ (stimulatory) family of alpha subunits includes $G_{sS(short)}$, $G_{sL(Long)}$, and $G_{olf(olfactory)}$[27,28]. $G_{sL(Long)}$ is a splice variant from the same gene as $G_{sS(short)}$ that contains a longer N-terminal region[27,28]. $G_{sS}$ is ubiquitously expressed, whereas the expression of $G_{sL}$ and $G_{olf}$ are restricted to neuroendocrine cells and the olfactory epithelium, respectfully[27,28]. Once activated, the primary effector protein activated by the $G_s$ family is adenylate cyclase[27,28]. Adenylate cyclase converts ATP into the second messenger signaling molecule cyclic AMP[27,28] (cAMP). Therefore, a common method of determining $G_s$ activation is to measure an increase in cellular cAMP levels. cAMP can then activate protein kinase A (PKA), which can phosphorylate a number of downstream effector proteins[27,28]. Cyclic AMP response element binding protein (CREB) is an important transcription factor that when activated by PKA can increase the expression of genes involved in cell proliferation, survival and differentiation[27,28]. Therefore, another common way of determining $G_s$ activation is measuring the activity of a luciferase

reporter gene under the control of CREB[31]. cAMP can also open cation ligand gated ion channels in the olfactory epithelium[27,28].

## 1.3.2.2    The G$_{i/o}$ family of G-proteins

The G$_{i/o}$ (inhibitory/other) family of G-proteins consists of G$_{i1}$, G$_{i2}$, G$_{i3}$, G$_{oA}$, G$_{oB}$, G$_z$, G$_{gustducin}$, G$_{transducin-r(rod)}$, and G$_{transducin-c(cone)}$[27,28]. G$_{i1}$ and G$_{i2}$ are widely distributed while G$_{i3}$ is ubiquitously expressed[27,28]. The expression of G$_{oA}$ and G$_{oB}$ are restricted to neurons and neuroendocrine cells, respectively[27,28]. G$_z$ expression is restricted to neurons and platelets, whereas G$_{gustducin}$ is expressed in taste cells and intestinal brush boarder cells[27,28]. G$_{transducin-r}$ is expressed in retinal rod cells and taste cells, while G$_{transducin-c}$ is expressed in rental cone cells[27,28]. Opposite to G$_s$, G$_{i1-3}$ inhibit the activity of adenylate cyclase to reduce cellular concentrations of cAMP. Therefore, a common method of determining G$_{i/o}$ activation is to measure decreases in intracellular cAMP levels. The signaling of G$_{oA}$ and G$_{oB}$ is generally thought to occur through their G$_{\beta\gamma}$ subunit, which can activate G-protein regulated inward rectifier potassium channels (GIRKs) and inhibit voltage dependent calcium channels[27,28]. Due to the high expression of G$_{i/o}$ family G-proteins (especially G$_o$), they are thought to be the primary G-proteins which signal through their G$_{\beta\gamma}$ subunit[27,28]. Unlike other members of the G$_i$ subfamily, G$_z$ and G$_{gustducin}$ can reduce cellular levels of cAMP by activating cAMP specific phosphodiesterase, which catalase the breakdown of cAMP[27,28]. G$_z$ can also inhibit adenylate cyclase to decrease cAMP levels, and interestingly unlike G$_{i1-3}$ this inhibition is pertussis toxin insensitive[27,28]. Similar to G$_z$ and G$_{gustducin}$, G$_{transducin-r}$ and G$_{transducin-c}$ inhibit the production of a cyclic second messenger by activating a phosphodiesterase, however, they inhibit the production of cyclic GMP through the activation cGMP specific phosphodiesterase[27,28].

## 1.3.2.3    The G$_{q/11}$ family of G-proteins

The G$_{q/11}$ subfamily contains of G$_q$, G$_{11}$, G$_{14}$, G$_{15}$, and G$_{16}$. G$_q$ and G$_{11}$ show ubiquitous expression, whereas G$_{14}$ expression is restricted to the kidney, lung, liver, and spleen[27,28]. G$_{15}$ is the murine homolog whereas G$_{16}$ is the human, and shows expression restricted to hematopoietic cells[27,28]. The primary effector activated by the G$_{q/11}$ family of G-proteins is    phospholipase    Cβ    (PLC-β),    which    cleaves    the    signaling    membrane    lipid

phosphatidylinositol 4,5-bisphosphate (PIP$_2$) into inositol triphosphate (IP$_3$) and diacylglycerol (DAG)[27,28]. IP$_3$ can then open ligand gated ion channels on the endoplasmic reticulum (ER) to increase levels of intracellular calcium[27,28]. Therefore, a common method of determining G$_{q/11}$ activation is measuring changes in intracellular calcium levels. The calcium released from the ER can then act back upon ER calcium channels to further increase intracellular calcium levels, a process known as calcium induced calcium release[27,28]. Increased levels of intracellular calcium can then go onto activate a host of different effector proteins, such as the transcription factor nuclear factor of activated T-cells (NFAT)[27,28]. Therefore, another common way of determining G$_{q/11}$ activation is measuring the activity of a luciferase reporter gene under the control of NFAT[31]. DAG remains associated with the plasma membrane, where it is able to activate effector proteins such as protein kinase C (PKC)[27,28]. Through the binding of intracellular calcium molecules and DAG, PKC becomes fully activated and is able to phosphorylate various effector proteins[27,28].

## 1.3.2.4　The G$_{12/13}$ family of G-proteins

The G$_{12/13}$ subfamily consists of just G$_{12}$ and G$_{13}$, both of which show ubiquitous expression[27,28]. Once activated the G$_{12/13}$ family of G-proteins generally activate the effector protein RhoGEF1, which exchanges GDP for GTP on RhoA[27,28,32]. RhoA is then able to bind and activate Rho-associated protein kinase (ROCK), which phosphorylates a number downstream cytoskeletal effector proteins involved in cell movement and shape change[27,28,32]. RhoA/ROCK can also activate the transcription factor serum response factor (SRF) which binds genes with serum response elements (SRE) to control processes such as cell growth and survival[31]. Therefore, common methods of determining G$_{12/13}$ activation are measuring the activity of RhoA and the activity of a luciferase reporter gene under the control of SRF[31].

## 1.3.2.5　The β-arrestin family of proteins

At the level of the receptor, signaling is terminated through receptor desensitization and internalization[29,30,33,34]. Serine and threonine residues on the receptors C-terminus can be phosphorylated by G-protein coupled receptor regulator kinases (GRKs), and through

negative feedback by PKA and PKC[29,30,33,34]. These phosphorylated residues become binding sites for the β-arrestins. The four types of β-arrestin are arrestin 1, arrestin 4, β-arrestin 1 (arrestin 2), and β-arrestin 2 (arrestin 3)[29]. The expression of the visual arrestins, arrestin 1 and arrestin 4, are restricted to rod and cone cells, respectfully, whereas β-arrestin 1 and β-arrestin 2 are expressed ubiquitously[29]. The binding of β-arrestin blocks G-proteins from binding the receptors intracellular transducer site, therefore uncoupling the receptor from G-protein dependent downstream signaling[29,30,33,34]. Adaptor protein 2 (AP-2) and clathrin bind β-arrestin and direct the receptor to clathrin coated pits[33,34]. Dynamin activation then causes internalization of the receptor-clathrin complex into endosomes[33,34]. The receptor can either be recycled to the membrane for future signaling events or sent to the lysosome for degradation[33,34]. β-arrestin can also cause G-protein independent receptor signaling by acting as a docking scaffold for effector proteins such as extracellular receptor kinase/mitogen activated protein kinase (ERK/MAPK), which can phosphorylate a number of transcription factors which control the expression of genes involved in cell proliferation, differentiation, and survival[29,30,33,34].

## 1.3.3    Major GPCR subfamilies

GPCRs can be separated into four major subfamilies: class A rhodopsin-like, class B secretin-like/adhesion, class C metabotropic glutamate-like, and class F frizzled/smoothened[35]. Alternatively, they can be categorized in a similar way using the GRAFS system: Glutamate, Rhodopsin, Adhesion, Frizzled, Secretin[35]. The major difference in these naming systems being the separation of the two types of class B receptors, secretin and adhesion, into two different subfamilies in the GRAFS system, likely due to the difference in activation mechanism. Both systems are often used in GPCR literature, therefore when explaining the different subfamilies of GPCRs both systems will be referenced for clarity.

## 1.3.3.1    Class A rhodopsin-like receptors

The class A rhodopsin-like receptors are by far the largest GPCR subfamily, with around 719 members separated into three major subfamilies[1]. Receptors in the first subfamily

utilize a ligand binding site deep within their transmembrane domains to bind small molecule ligands such as neurotransmitters, signaling lipids, and odorants[1]. Subfamily 2 binds mainly protein ligands such chemokines and tethered ligands through a more exposed binding site which includes the extracellular loops[1]. Tethered ligands will be discussed in detail in following sections on proteinase activated receptors and adhesion GPCRs. Subfamily 3 utilizes its larger extracellular region to bind lower weight hormones such as luteinizing hormone (LH), follicle stimulating hormone (FSH), and thyroid stimulating hormone[1].

## 1.3.3.2 Class B secretin-like/adhesion receptors

Class B secretin-like/adhesion receptors are characterized by their extremely large extracellular regions, which are often larger than the membrane imbedded and intracellular receptor regions[1,36]. These receptors can be separated into two major subfamilies based on mechanism of action. Through their large extracellular regions, subfamily B1 secretin-like receptors can bind the C-terminus of high molecular weight peptides hormones such as secretin, glucagon, and vasoactive intestinal peptide (VIP)[1,36]. This interaction allows the peptide hormones N-terminus to adopt a α-helical structure and interact strongly with a transmembrane domain binding site leading to receptor activation[36]. This process is known as the two-domain model of activation for class B receptors[36]. Subfamily B2 adhesion receptors large extracellular regions are removed by mechanical force through the binding of various transmembrane and extracellular matrix proteins such as integrins, collagen, and sugars[37]. Removal of the extracellular region then reveals a tethered ligand similar to the mechanism of proteinase activated receptors[37], which are discussed in detail in the section 1.4.

## 1.3.3.3 Class C metabotropic glutamate-like receptors

The family of class C receptors contains members such as the metabotropic glutamate receptors, $GABA_B$ receptors, taste receptors, and calcium sensing receptor (CaSR)[1,38]. These receptors utilize a unique mechanism of action, where an extracellular Venus flytrap (VFT) domain is used to bind ligands[38]. The two lobed VFT domain remains open until ligand binding, where it undergoes a conformational change to a closed position

which brings the lobes closer together leading to receptor activation[38]. Although the other families of GPCRs can form various combinations of homo and heterodimers, for class C metabotropic glutamate-like receptors dimerization is a requirement for receptor activation[1,38].

### 1.3.3.4    Class F frizzled/smoothened receptors

The frizzled and smoothened receptors make up the class F subfamily of GPCRs[1,39–41]. These receptors are important regulators of development and are therefore often dysregulated in cancer[1,39–41]. The ligands of the frizzled receptors are the 19 different wingless/Int-1 (WNT) family of proteins[39,40]. WNT proteins bind a cysteine rich domain (CRD) on the extracellular region of frizzled receptors using both their lipid modified thumb and index finger domains[39,40]. The activation of frizzed receptors by WNT proteins also require the recruitment of lipoprotein receptor related protein (LRP) co-receptors[39,40]. Under resting conditions, smoothened receptors are inhibited by the 12 transmembrane domain protein Patch[39,41]. Upon binding of the hedgehog family of proteins to the hedgehog receptor, Patch, it is internalized and degraded[39,41]. The loss of patch inhibition is sufficient for smoothened receptor activation; however, the CRD domain binding ligand oxysterol and transmembrane domain binding smoothened ligand (SAG) can contribute to great levels of receptor activation[39,41].

## 1.4   Tethered ligand activated GPCRs

While GPCRs ligands are diverse, for the most part they are soluble molecules, such as hormones or neurotransmitters, that diffuse freely and find their cognate receptors[42]. An exception to this rule is in instances where the ligand is physically attached to the receptor. Such ligands are often referred to as tethered ligands or tethered agonists and are an example of a non-classical GPCR activation mechanism, due to the irreversible nature of such receptor activation. There are two prominent examples of GPCR families that can be activated by tethered ligands, the first are the four-member family of Proteinase Activated Receptors (PARs)[43] and the other is the adhesion family of GPCRs (aGPCRs)[44]. In the case of both PARs and aGPCRs the receptors contain within their sequence a receptor activating motif that is masked in the inactive receptor and unmasked

by activators to reveal the tethered ligand. The tethered ligand binds the orthosteric site intramolecularly to trigger signaling[45,46] (Fig 2, Fig 3, and Fig 4).
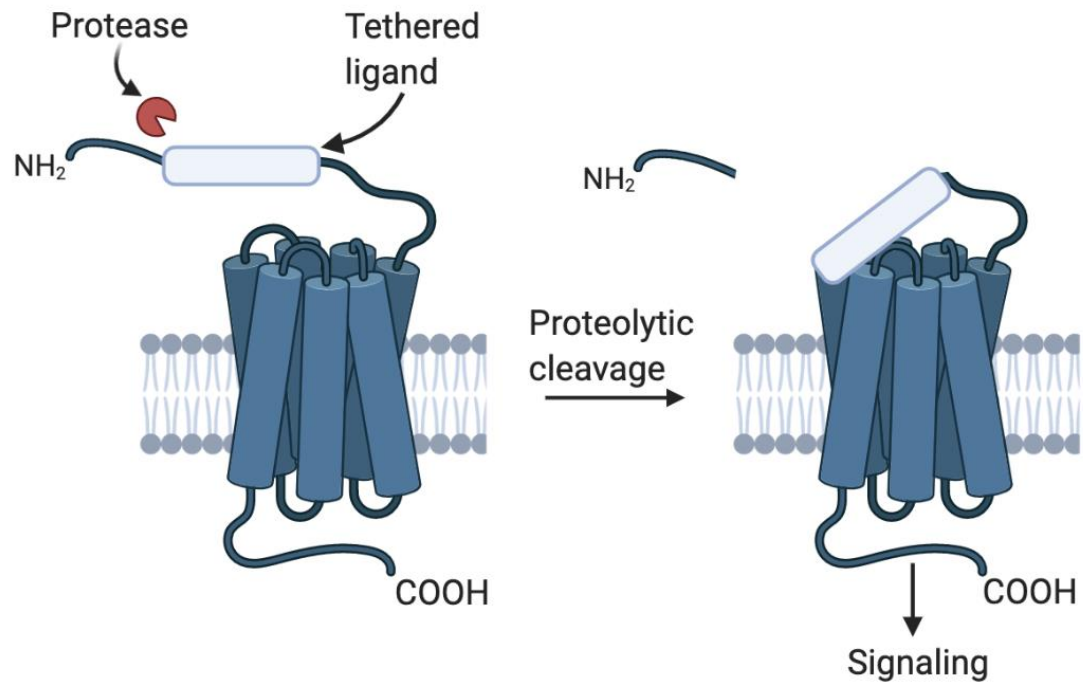
**Figure 2. PAR receptor mechanism of activation**. Proteinases, such as trypsin and thrombin, are able to cleave the receptors N-terminus revealing a normally hidden tethered ligand which then binds and activates the receptor. Figures were generated using the program Biorender (https://biorender.com).
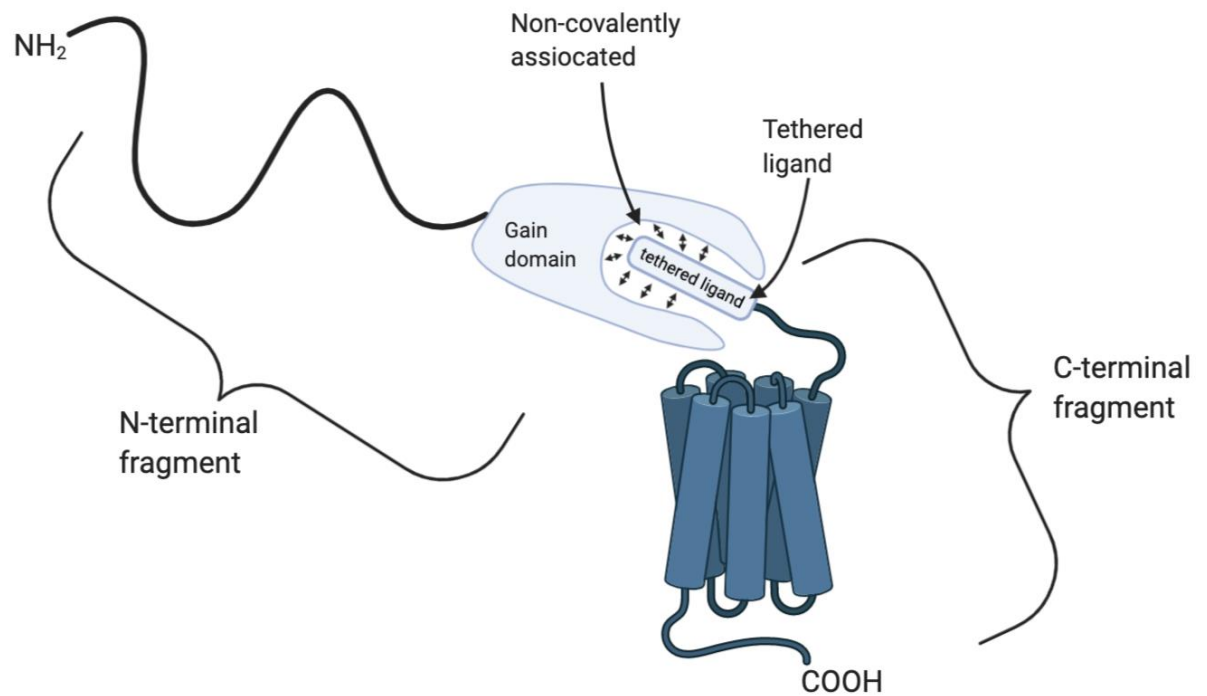
**Figure 3. Basic structure of an adhesion GPCR**. The receptors N-terminal fragment remains strongly non-covalently associated with the membrane imbedded C-terminal fragment. When mechanical force is applied to the N-terminal fragment these non-covalent interactions are broken and the two fragments sperate. Figures were generated using the program Biorender (https://biorender.com).
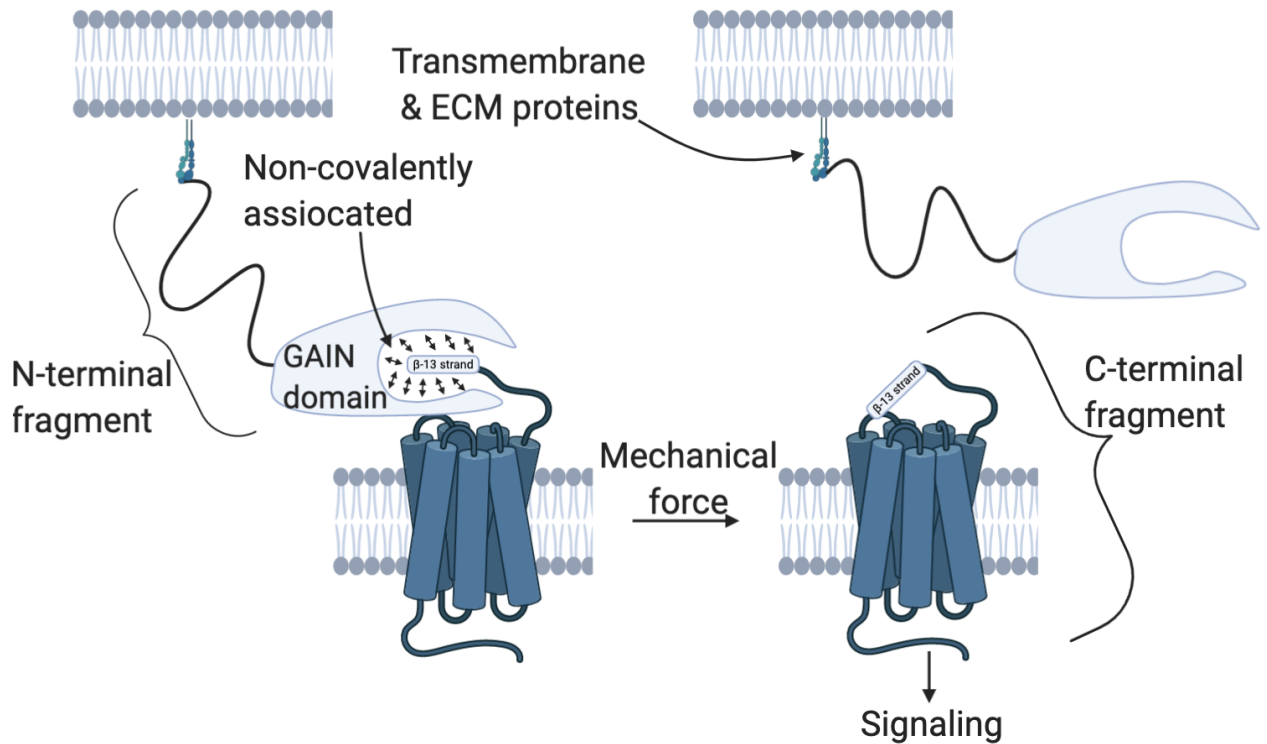
**Figure 4. Adhesion GPCR mechanism of activation**. Adhesion GPCR endogenous ligands tend to be transmembrane and extracellular matrix proteins. When expressed on neighboring cells these proteins can bind the N-terminal fragment and induce mechanical force. Once the N-terminal fragment is removed a normally hidden tethered ligand is able to bind and activate the receptor. Figures were generated using the program Biorender (https://biorender.com).

## 1.4.1   Proteinase Activated Receptors (PARs)

The PAR family is made up of 4 class A Rhodopsin like GPCRs: PAR1, PAR2, PAR3, and PAR4[43]. Because of their importance in platelet function and inflammation, PARs are exciting targets for new anti-thrombotic and anti-inflammatory agents. The tethered ligands of PARs are encoded in their N-termini. Various proteinases are able to cleave specific sites on the PAR N-terminus, revealing tethered ligands capable of binding the orthosteric site and activating receptor signaling (Fig 2)[47,48]. PAR1, PAR3 and PAR4 N-termini contain thrombin cleavage sites (R41/S42 for PAR1, K38/T39 for PAR3 and R47/G48 for PAR4) which reveal the canonical tethered ligands SFLLRN…., TFRGAP…. and GYPGQV…. respectively, while PAR2 is N-terminally cleaved by trypsin at R35/S36, revealing the SLIGKV…. tethered ligand. The tethered ligands in all cases bind intramolecularly and in the case of PAR1, PAR2 and PAR4 activate receptor coupled second messenger signaling cascades[48]. The ability of PAR3 to signal independently has been questioned and this receptor may primarily act as a co-factor for other PARs[49].

Despite being activated by this unusual proteolytic mechanism, PARs are fundamentally peptide receptors and the ability of synthetic peptides to act as surrogate activators of the PARs was made soon after their discovery. Short 5-6 amino acid synthetic peptides have now been developed for PAR1 (TFLLR-NH$_2$), PAR2 (SLIGRL-NH$_2$) and PAR4 (AYPGKF-NH$_2$) allowing specific activation and study of individual PARs, particularly in cells that express multiple members of this family that respond to a common activating enzyme. Peptides mimicking the PAR3 tethered ligand (TFRGAP-NH$_2$) activate PAR1 and PAR2[48].

## 1.4.2   Adhesion GPCRs (aGPCRs)

### 1.4.2.1   Tethered ligand mediated signaling

aGPCRs are a family of 33 receptors which are further divided into 9 subfamilies[46,50,51]. With GPCRs being such a major target of FDA approved drugs, one would assume all the major subfamilies are involved in current drug development. Surprisingly the second largest GPCR subfamily, the adhesion GPCRs (aGPCRs), are not currently targeted by a

single FDA approved drug[52]. These receptors are dysregulated in many cancers, neurological disorders, and inflammatory diseases[53–56]. An absence of drug development at these receptors can be explained by their unusual structure and mechanism of action (Fig 3 and Fig 4)[57]. Similar to PARs, many aGPCRs can be activated by tethered ligands encoded in their N-termini[46]. The mechanism by which the aGPCR tethered ligand is revealed is however distinct from the PARs. aGPCRs are autoproteolytically cleaved at a GPCR autoproteolysis site (GPS) within their GPCR autoproteolysis inducing domain (GAIN) during endoplasmic reticulum biosynthesis and trafficking to the cell membrane[50]. The resulting N-terminal fragment (NTF) of the receptor remains non-covalently associated to the membrane imbedded C-terminal fragment (CTF)[50]. Mechanical force applied to the NTF enable its removal, revealing the tethered ligand (sometimes referred to as the *statchel*) in the CTF, which binds intramolecularly to activate receptor signaling[50,57]. The NTF of aGPCRs are large and diverse, encoding binding sites for various molecules, such as transmembrane and extracellular matrix proteins[50]. As an example, GPR56 (ADGRG1) was recently shown to be the collagen receptor in platelets. Type III collagen tethered to the extracellular matrix binds the NTF of GPR56[58]. As the affinity for the interaction of collagen to the extracellular matrix is stronger than the non-covalent forces tethering the two receptor fragments, the NTF of GPR56 is removed, revealing the tethered ligand, TYFAVLM…[59], which then binds the orthosteric site and activates receptor signaling.

As with the PARs, synthetic peptides mimicking the tethered ligand are also able to activate aGPCRs. Peptide libraries based on the aGPCR stalk region (beginning of CTF to TM1) of many aGPCRs have been studied to show the utility of these peptides and to provide further support for tethered agonism as an activation mechanism common to many aGPCRs[59–61]. The consensus from these studies is that the first 7 amino acids of the CTF, which are highly conserved, likely form the core tethered ligand (consensus sequence = TXFAVLM). However, for many aGPCRs such 7 amino acid peptides are not agonistic. It is thought that predicted turn elements in many aGPCR stalk regions that lie outside of core sequence have important roles in conferring agonistic properties. This is illustrated nicely when comparing GPR56, which has no predicted stalk region turn elements, and is activated by a peptide consisting of the first 7 CTF amino acids,

TYFAVLM to GPR110 (ADGRF1), which has many predicted stalk region turn elements, and is only activated by longer peptides containing these turn elements[59].

## 1.4.2.2    Tethered ligand independent signaling

Although tethered ligand meditated signaling is thought to be their primary mechanism of action, there is evidence that adhesion GPCRs can be activated in a tethered ligand independent manner[46,62–65]. Ligands binding to allosteric regions of the NTF are able to induce conformational changes leading to receptor activation. Signaling through the BAI1 (ADGRB1) receptor, synaptamide and monobodies targeting the GAIN and Pentraxin/Laminin/neurexin/sex hormone binding globulin-like (PLL) domains of the NTF are the best examples of such mechanisms[62–64]. Recently, aGPCRs have also been shown to be activated by more classic allosteric modulation mechanisms. Glucocorticoids allosterically binding the 7 transmembrane bundle of GPR97 (ADGRG3) and inducing conformation changes leading to receptor activation, is so far the only example of such a mechanism[65].

A truncation of the BAI1 receptor, where the entire extracellular region up until the first transmembrane domain was removed showed no decrease in activity compare to both full length receptor and truncated receptors where the proposed tethered ligand was exposed[62]. If tethered agonism was its mechanism of activation, then this truncation should have drastically decreased its activity[62]. This would suggest that upon removal of BAI1's N-terminal fragment the receptor undergoes a conformational change to a more active state to initiate signaling.

Synaptamide is an endogenous metabolite of the omega-3-fatty acid Docosahexaenoic acid (DHA) that was recently shown to activate the aGPCR GPR110[64,66]. Synaptamide activation of GPR110 induces $G_s$ mediated changes in cAMP, increasing neurogenesis, synaptogenesis, and neurite growth[64,66]. Neither mutation preventing GAIN domain cleavage, H565 to A, or tethered ligand activity, T567 to A, were shown to effect synaptamide mediated GPR110 signaling[64]. Synaptamide was also shown to not affect orthosteric tethered ligand mediated signaling, therefore it is an allosteric agonist and not a positive allosteric modulator (PAM)[64]. Using chemical crosslinking, mass spectrometry,

and molecular modeling synaptamide was found to bind a long channel between subdomains A and B of the GAIN domain[64]. Modeling predicts this binding site to have a polar exposed region and a hydrophobic core[64]. Mutation of predicted synaptamide interacting residues Q511, N512, Y513 to alanine decreased synaptamide mediated changes in cAMP and double mutations of Q511/N512 and N512/Y513 to alanine completely abolished synaptamide induced signaling[64]. These interacting residues are however not conserved in other closely related aGPCRs[64]. Also, the interface between subdomains A and B is much smaller in structures of other aGPCR N-terminal fragments[59,64]. Future work is needed to determine if other aGPCRs utilize a similar allosteric GAIN subdomain interface binding site.

Monobodies are synthetic proteins based on the human fibronectin type-III scaffold that have been used extensively to help stabilize proteins for structural studies. Monobodies created to determine the crystal structure of GPR56's N-terminal fragment were found to act as both allosteric agonists and inverse agonists[63]. The α5 monobody, which targets both the GAIN and PLL domains of mouse GPR56, is an allosteric inverse agonist that inhibits SRE reporter gene signaling below baseline levels[63]. Similarly, the β1 monobody is an allosteric inverse agonist that targets both the GAIN and PLL domains and inhibits SRE reporter gene signaling below baseline but targets human GPR56[63]. The β7 monobody targets only the PLL domain of human GPR56 and acts as an allosteric agonist by increasing SRE reporter gene signaling above baseline levels[63]. Neither mutation preventing GAIN domain cleavage or tethered ligand function affected the signaling of these monobodies[63]. Therefore, these monobodies act as allosteric agonists and inverse agonists and not as negative allosteric modulators (NAMs) or PAMs. In the future, designing monobodies targeting the GAIN and PLL domains of other aGPCRs could enable the study of structure and signaling for many orphan aGPCRs.

Recently, GPR97 was found to be activated by several different glucocorticoids[65]. Prednisolone, dexamethasone, beclomethasone, prednisone, cortisol, cortisone, and 11-deoxyocortisol were all shown to increase GPR97 mediated $G_{i/o}$ signaling[65]. Beclomethasone and cortisol were able to activate C-terminal fragment only GPR97 8-30 times more than full length receptor[65]. This observation suggests glucocorticoids function

as ago-PAMs of GPR97. Ago-PAMs are defined as allosteric modulators that have activity with and without the presence of orthosteric agonists. Structures of beclomethasone and cortisol bound to GPR97 determined a long ellipsoidal shaped allosteric binding site within the 7 transmembrane domain bundle created by residues from TM1-3, TM5-7, ECL2, and ECL3[65]. Therefore, glucocorticoids seem to activate GPR97 like more conventional allosteric modulators. Mutations of glucocorticoid interacting residues Y406, W421, L498, F345, W490, I494, and N510 to alanine all decreased cortisol and beclomethasone mediated GPR97 $G_{i/o}$ signaling[65]. Interestingly, 7/14 residues involved with glucocorticoid binding to GPR97 are conserved across the G subfamily, and 5/14 are conserved across all aGPCRs[65]. This suggests other aGPCRs may share a similar allosteric site, and that other members of the G family may also bind glucocorticoids. A previous small molecule library screen of another G subfamily member, GPR56, identified 3-α-acetoxydihydrodeoxygedunin (3-α-DOG) as a partial agonist[67]. Glucocorticoids and 3-α-DOG share a similar 4 ring steroid-like structure. This further supports the idea that other G subfamily members may share a similar allosteric site that interacts with steroid-like molecules.

## 1.5   aGPCRs of interest

In this thesis we chose to design tools for studying the four aGPCRs CD97, EMR2, GPR56, and BAI1. We chose these four receptors as they are four of the more well studied members of the family and because they are involved in physiological processes and diseases that are of particular interest to our lab.

### 1.5.1   CD97 (ADGRE5)

Cluster of differentiation 97, CD97 (ADGRE5), is part of the E subfamily and was one of the first aGPCRs to be discovered in the early 1990's[68]. CD97's known endogenous ligands are CD55/decay accelerating factor, CD90/thymocyte differentiation antigen 1, chondroitin sulfate B, and integrins $\alpha_v\beta_3$ and $\alpha_5\beta_1$[50]. CD97 has been shown to be expressed in the bone, hematopoietic cells, heart, lungs, intestine, pancreas, kidney, bladder, uterus, skeletal muscle, epididymis, and adipocytes[50,69]. This receptor has been shown to be involved in immune cell function, gut epithelial cell biology, and many

different cancers[53,55,56,70–74]. A single nucleotide polymorphism (T64C) in the CD97 promoter has been associated with the development of colitis[71]. Further, the CD97 gene is part of an inflammatory bowel disease susceptibility locus on chromosome 19[75,76]. When CD97 was overexpressed in a mouse model of colitis, there was an attenuation of the disease and an apparent protection from the development of colorectal cancer[71]. The colonic cells of mice overexpressing CD97 were shown to have increased lateral cell-cell junctions[71]. As colitis is a disease that damages the colonic epithelial barrier, it was hypothesized that CD97 signaling may have increased colonic lateral cell contacts resulting in the apparent protection from the disease[71]. Colonic cells from mice overexpressing CD97 also had significantly more membrane associated β-catenin[71]. β-catenin is normally a component of lateral cell junctions, but when the cellular barrier is compromised this protein internalizes and translocates to the nucleus to increase the expression of genes involved in colorectal carcinogenesis[71,72]. CD97 has been shown to be involved in many innate and adaptive immune responses such as immune cell migration, proliferation, and mobilization from the bone marrow[50,77–79]. Overexpression of CD97 leads to increased tumor proliferation, migration and invasiveness and poor clinical outcomes in various cancers including colorectal, hepatic, breast, thyroid, gastric and prostate[53,55,56,70–74].

## 1.5.2    EMR2 (ADGRE2)

Epidermal growth factor-like module-containing mucin like hormone receptor-like 2, EMR2 (ADGRE2), and CD97 were the first adhesion GPCRs to be discovered[68]. Currently, the only known endogenous ligand for EMR2 is chondroitin sulfate B[50]. As EMR2 is not expressed in mice it has been difficult to characterize its expression, however it is known to be expressed in the lungs, breast, brain, bone, and hematopoietic cells[50,53]. This receptor is also a member of the E subfamily and is involved in immune cell functions, such as neutrophil migration, degranulation, and cytokine secretion[50,80,81]. EMR2 has been shown to be overexpressed in various cancers such as lung, breast and brain[50,53].

### 1.5.3    GPR56 (ADGRG1)

Of the 33 adhesion GPCRs, G-protein coupled receptor 56 (GPR56) is probably the most well studied. This is likely due the fact loss of function mutations in GPR56 results in the rare hereditary congenital brain disorder bilateral frontoparietal polymicrogyria (BFPP)[82–86]. Patients with BFPP exhibit significant developmental and motor delay, seizures, ataxia, language and visual impairment[82–86]. GPR56 is vital in the development of the cerebral cortex, where by binding collagen III it guides newly formed neurons to stop migrating once they have reached the pial membrane[82–86]. Loss of function mutations in GPR56 causes the over migration of neurons through the pial membrane resulting in BFPP[82–86]. The known endogenous ligands of GPR56 are collagen III and transglutaminase II[50,53]. In the brain GPR56 is expressed in oligodendrocytes, gilia cells, microglia, and neural progenitor cells[50]. GPR56 is also expressed in the bone, platelets, lymphocytes, Schwann cells, liver, thyroid, testis, intestines, prostate, skin, and skeletal muscle[50,53]. Other than its important role in cerebral development, GPR56 was recently shown to be important for platelet activation[58]. GPR56 knockout mice show a significant lack of hematopoietic stem cells in the bone marrow but an accumulation in the spleen, liver and peripheral blood[87]. This suggests GPR56 has a role in immune cell compartmentalization, likely through binding adhesive molecules such as collagen III, keeping GPR56 expressing cells in the bone marrow. Male GPR56 knockout mice were found to be infertile due to improper testicular basal lamina formation leading to dysfunction of the seminiferous tubules[88]. GPR56 has been shown to be overexpressed in various cancers such as bone, skin, colorectal and prostate[50,53].

### 1.5.4    BAI1 (ADGRB1)

Brain-specific angiogenesis inhibitor 1, BAI1 (ADGRB1), is a member of the B subfamily and binds the endogenous ligands phosphatidylserine and matrix metalloprotease 14[50,53]. The receptor is expressed in macrophages, astrocytes, microglia, skeletal muscle, heart, central and peripheral neurons, kidneys, and breast[50,53]. On phagocytes such as macrophages, BAI1 binds phosphatidylserine on apoptotic cells and lipopolysaccharide on gram-negative bacteria to initiate their phagocytosis[89,90]. In skeletal muscle, BAI1 promotes the fusion of myoblasts into muscle fibers[91]. In the brain, BAI1

expression levels have been shown to regulate synaptogenesis[92]. As the name suggests BAI1 inhibits angiogenesis, therefore it is not surprising this receptor is downregulated in various cancers such as brain, lung, breast, colorectal, and renal[50,53].

## 1.6   Tools for studying aGPCR signaling and function

Based on the observation that removal of the N-terminal fragment activates aGPCRs, truncated receptors where only the C-terminal fragment is expressed have been used to study aGPCR signalling[50,59,61]. These truncated receptors have two main limitations. First, they have low surface expression because they do not have an N-terminal signal sequence. Second, lacking the N-terminal fragment means they are expressed as pre-activated receptors. Therefore, methods of measuring signaling are limited to time independent accumulation assays, such as gene reporter assays. The GPCR field has generally moved away from using gene reporter assays, as they measure downstream signaling outcomes that are prone to crosstalk. Therefore, it is generally preferred to use assays that time dependently show the recruitment of receptor proximal effector proteins. We sought to create a system where we could measure the time dependent recruitment of aGPCR effector proteins and maintain proper surface expression of the receptor. Since removal of the N-terminal fragment is fundamental to the activation of aGPCRs, we reasoned that using an alternative method to remove the N-terminal fragment would also allow study of receptor-effector coupling. Since PAR receptors also signal through proteolytic unmasking of a tethered ligand, we reasoned that a PAR2-aGPCR chimera would enable trypsin mediated cleavage of the receptor N-terminus to trigger signaling through these receptors. ***Therefore, we hypothesized that a PAR2-aGPCR chimeric receptors would enable study of receptor-proximal aGPCR signaling events.***

As mentioned above, peptides made to mimic certain lengths of the stalk region have been shown to activate many different aGPCRs. These aGPCRs include: GPR56, GPR110, GPR126 (ADGRG6), GPR133 (ADGRD1), GPR64 (ADGRG2), GPR114 (ADGRG5), GPR116 (ADGRF5) and LPHN1 (ADGRL1)[59,61,93,94]. However, tethered ligand mimicking peptide has yet to be made for CD97. By analyzing these past studies, we reasoned it was possible to predict the sequence of a CD97 tethered ligand mimicking

peptide. ***Therefore, we hypothesized that a peptide made to mimic a certain length of the CD97 stalk region could be used to activate and study receptor signaling.***

**<u>The two specific aims of this thesis are to:</u>**

1. Create trypsin activated PAR2-CD97, PAR2-EMR2, PAR2-GPR56, and PAR2-BAI1 chimeric receptors as tools to study aGPCR signaling

2. Design and test a tethered ligand mimicking peptide capable of activating CD97.

# Chapter 2

## 2 Methods

## 2.1 Chemicals and reagents

Unless stated otherwise, all chemicals and reagents were obtained from ThermoFisher Scientific (Hampton, New Hampshire, United States), Millipore-Sigma (Burlington, Massachusetts, United States), or BioShop Canada Inc. (Burlington, Ontario, Canada). Porcine pancreatic trypsin (EC# 3.4.21.4) was purchased from Sigma Aldrich (St. Louis, Michigan, United States). A maximum specific activity of 20 000 units/mg was used to determine trypsin concentrations in molar as previously described[95] (1unit/mL converts to around 2nM). Trypsin stock solutions were prepared in 25mM 4-(2-hydroxethyl)-1-piperazineethanesulfonic acid (HEPES) and diluted down to working concentrations in Hanks' balanced salt solution (HBSS). SLIGRL-$NH_2$ was produced and purchased from Genscript (Piscataway, New Jersey, United States). SSFAILMAH-$NH_2$ was synthesized using solid phase peptide synthesis at the Luyt Laboratory in Victoria hospital as previously described[96]. SLIGRL-$NH_2$ was diluted in 25mM HEPES and HBSS, whereas SSFAILMAH-$NH_2$ was dissolved in 100% dimethylsulfoxide (DMSO). For experiments SSFAILMAH-$NH_2$ stock solutions were made in 100% DMSO and then diluted to the proper assay condition concentrations using HBSS pre-warmed to 37ºC. Therefore, each concentration of SSFAILMAH-$NH_2$ contained the same amount of DMSO (6%). SSFAILMAH-$NH_2$ diluted in less than 6% DMSO precipitated out of solution. Vehicle control for all SSFAILMAH-$NH_2$ assays consisted of HBSS with 6% DMSO. These higher concentrations of DMSO are required for aGPCR tethered ligand mimicking peptides, such as SSFAILMAH-$NH_2$, due to their highly hydrophobic nature[59].

## 2.2 Molecular cloning and constructs

PAR2-adhesion GPCR chimeric receptors for CD97, EMR2, GPR56, and BAI1 were designed using the program Benchling (https://benchling.com) (San Francisco, California, United States) and sequence verified synthetic genes were obtained (Integrated DNA Technologies, Coralville, Iowa, United States). PAR2-aGPCR chimeric

receptors were cloned into the pcDNA3.1+ vector (ThermoFisher Scientific, Waltham, MA) using Not1 and Xho1 restriction enzymes (New England Biolabs, Whitby, Ontario, Canada), as previously described[97,98]. In brief, chimeric receptors in their provided IDT AMP vector (Integrated DNA Technologies, Coralville, Iowa, United States) were incubated overnight at 37ºC with Not1 and Xho1 restriction enzymes in NEB 3.1 buffer (New England Biolabs, Whitby, Ontario, Canada). Chimeric receptor inserts were isolated by gel electrophoreses on a 1.5% agarose gel (Sigma Aldrich, St. Louis, Michigan, United States). Chimeric receptor insert DNA was gel purified (Qiagen, Hilden, Germany) and incubated overnight at 16ºC with T4 ligase (New England Biolabs, Whitby, Ontario, Canada) and Not1 and Xho1 digested pcDNA3.1+ vector. After ligation, chimeric receptors in pcDNA3.1+ were transformed into max efficiency DH5α cells (Invitrogen; ThermoFisher Scientific, Waltham, Massachusetts, United States) and grown overnight on 100µg/mL ampicillin (BioShop Canada Inc., Burlington, Ontario, Canada) Luria broth (LB) (ThermoFisher Scientific, Hampton, New Hampshire, United States) plates. Single colonies were selected and grown overnight in Terrific broth (TB) (Sigma Aldrich, St. Louis, Michigan, United States) containing 100µg/mL ampicillin. Chimeric receptors in pcDNA3.1+ were miniprep (Qiagen, Hilden, Germany) purified and sent for sequencing. Enhanced yellow fluorescent protein (eYFP) (Clontech, Takara Bio, San Jose, CA)[99] was cloned onto the C-terminus of the PAR2-aGPCR chimeric receptors using Xho1 and Xba1 restriction enzymes (New England Biolabs, Whitby, Ontario, Canada), as previously described[97,98]. In brief, aGPCR chimeric receptors in pcDNA3.1+ were incubated overnight at 37ºC with Xho1 and Xba1 restriction enzymes in NEB CutSmart buffer (New England Biolabs, Whitby, Ontario, Canada). Chimeric receptor in pcDNA3.1+ were separated from the DNA fragments between Xho1-Xba1 by gel electrophoreses on a 1.5% agarose gel. Chimeric receptors in pcDNA3.1+ digested with Xho1 and Xba1 were gel purified and incubated overnight at 16ºC with T4 ligase and Xho1 and Xba1 digested eYFP. After ligation, eYFP tagged chimeric receptors in pcDNA3.1+ were transformed into max efficiency DH5α cells and grown overnight on 100µg/mL ampicillin LB plates. Single colonies were selected and grown overnight in TB containing 100µg/mL ampicillin. eYFP tagged chimeric receptors were miniprep purified and sent for sequencing. Renilla luciferase-tagged β-arrestins 1 and 2 constructs

were a kind gift from Dr. Michel Bouvier (University of Montreal)[96,100]. Renilla luciferase tagged $G_\alpha$ proteins were a kind gift from Dr. Bryan Roth (University of North Carolina, Chapel Hill)[101]. PAR2 and CD97 TANGO constructs were a kind gift from Dr. Bryan Roth (University of North Carolina, Chapel Hill, NC)[102] and were obtained from Addgene (Watertown, Massachusetts, United States). Sequence verified constructs were transformed into sub cloning efficiency DH5α cells (Invitrogen; ThermoFisher Scientific, Waltham, Massachusetts, United States) for amplification and grown overnight on 100µg/mL ampicillin LB plates. Single colonies were selected and grown overnight in TB containing 100µg/mL ampicillin. DNA was first purified using miniprep, and once sequence verified DNA was purified in larger quantities using midiprep (Qiagen, Hilden, Germany). All constructs were verified by Sanger sequencing (London Regional Genomics Centre, University of Western Ontario).

## 2.3   Cell lines and culturing conditions

All cell culture media and reagents were purchased from ThermoFisher Scientific (Waltham, MA) unless otherwise stated. PAR2 knock out (PAR2-KO) Human Embryonic Kidney 293 cells (HEK293) (ATCC; Manassas, Virginia United States) were maintained in Dulbecco's modified Eagle's medium (DMEM) supplemented with 10% fetal bovine serum, 100µg/µL penicillin streptomycin, and 1% sodium pyruvate. PAR2-KO HEK293 cells were previously generated using CRISPR/Cas9 targeting[100]. In brief, the specific guide RNA CCCCAGCAGCCACGCCGCGC was cloned into the lentiCRISPR v2 vector (Addgene, Watertown, Massachusetts, United States). HEK293 cells were transfected with the specific guide RNA using X-tremegene9 and grown in selection media containing 5 µg/mL puromycin. Deficiency of PAR2 was determined by calcium signaling assays with PAR2 agonists trypsin and SLIGRL-NH$_2$[100].

To generate stable cell lines expressing PAR2-aGPCR chimeras PAR2-KO cells were transiently transfected with either PAR2-CD97, PAR2-EMR2, PAR2-GPR56, or PAR2-BAI eYFP tagged chimeric receptors. At 72 hours post transfection cells were switched to antibiotic selection media. The antibiotic selection media consisted of DMEM supplemented with 600µg/mL G418 sulfate (Geneticin; ThermoFisher Scientific, Waltham, Massachusetts, United States), 10% fetal bovine serum, 100µg/µL penicillin

streptomycin, and 1% sodium pyruvate. After 4 weeks of culture in G418 selection media, eYFP expressing cells were selected by flow cytometry (FACSAria III; London Regional Flow Cytometry Facility).

HTLA cells were a kind gift from Dr. Gilad Barnea (Brown University)[103]. HTLA cells were maintained in DMEM supplemented with 10% fetal bovine serum, 100µg/µL penicillin streptomycin, 1% sodium pyruvate, 5µg/mL puromycin, 200µg/mL hygromycin B, and 500µg/mL G418 sulfate.

HEK293 cells were maintained in DMEM supplemented with 10% fetal bovine serum, 100µg/µL penicillin streptomycin, and 1% sodium pyruvate.

Subsequently all cell lines were sub-cultured every 48 hours using enzyme-free isotonic (pH 7.4) phosphate buffered saline (PBS) supplemented with 1mM ethylenediaminetetraacetic acid (EDTA) to detach cells. PBS-EDTA was then removed by centrifugation. Trypsin EDTA was not used for subculturing as it would activate PAR2-aGPCR chimeric receptors, or endogenously expressed PAR receptors which could affect experimental results. Cells were then resuspended with appropriate growth medium and counted using trypan blue and a hemocytometer.

For BRET and TANGO experiments, 700000 cells/well were plated in six well plates and transiently transfected with X-tremegene9 in optimized minimal essential medium (Opti-MEM). After 24 hours post-transfection cells were transferred into 96-well white bottom plates at a seeding density of 35000 cells/well. BRET and TANGO experiments were performed 48 hours post-transfection. For confocal microscopy experiments, 35000 cells were seeded in 35-mm glass bottom culture dishes (MatTek Corporation, Ashland, MA) coated with 0.05mg/ml poly D-lysine and imaged 48 hours after seeding. Each experiment was performed in either duplicate or triplicate a minimum of three times, on three different days, and with three separate transfections (N=3).

## 2.4 Confocal microscopy

PAR2-KO cells stably expressing either PAR2-CD97, PAR2-EMR2, PAR2-GPR56, or PAR2-BAI1 eYFP tagged chimeric receptors were seeded at a density of 35000 cells and

cultured on 35mm glass bottom dishes for imaging. Before seeding, glass bottom dishes were coated with 0.05mg/ml poly D-lysine. Cells were imaged 48 hours after plating on a Nikon Eclipse Ti2-E spinning disk confocal microscope (Minato City, Tokyo, Japan) at 60x magnification to determine the cellular localization of PAR2-aGPCR chimeric receptors.

## 2.5 Bioluminescence resonance energy transfer 1 assay for β-arrestin recruitment

The ability of PAR2-aGPCR chimeric receptors to recruit β-arrestins 1 and 2 was assessed using a bioluminescence resonance energy transfer 1 (BRET1) assay (Fig 5 and Fig 6)[96,104]. The BRET1 assay consists of the BRET pair eYFP and RLuc proteins. The chimeric receptors were C-terminally tagged with eYFP and β-arrestins 1 and 2 were tagged with RLuc. During RLuc catalysis of coelenterazine H to coelenteramide (NanoLight Technology, Pinetop, AZ) light is emitted at the wavelength that can excite eYFP. BRET is dependent on the distance between the donor luciferase and acceptor fluorophore. Upon addition of receptor activating drug, receptor recruitment of β-arrestin brings the eYFP and RLuc tags into close proximity resulting in an energy transfer to eYFP and an increase in fluorescence[96,104]. Receptor β-arrestin coupling was confirmed if agonist dose dependent changes in the ratio of eYFP fluorescence/RLuc luminescence was observed[96,104].

PAR2-KO or HEK293 cells were transfected with either 1µg of eYFP tagged PAR2-CD97, PAR2-EMR2, PAR2-GPR56, or PAR2-BAI1 chimeric receptors and 100ng of β-arrestin-RLuc 1 or 2 using a 3:1 ratio of Opti-MEM to X-tremegene9. One day post transfection cells were transferred into a 96-well white plate and seeded at a density of 35000 cells per well. The next day media was aspirated and replaced with 0.3-300nM trypsin or 0.3-300µM SSFAILMAH-NH$_2$. After 10 minutes of drug treatment cells were treated with 5µM coelenterazine H. After 20 minutes of drug treatment plates were read using a Berthold Mithras LB 940 plate reader and BRET ratios of eYFP fluorescence/RLuc luminescence were determined. NET BRET was then calculated by subtracting the vehicle control BRET ratio from all other samples. Dose response curves were generated using three parameter log agonist vs response non-linear regression

analysis on Graphpad prism 8 with error bars representing the standard error of the mean (SEM).

**Figure 5. Principle of β-arrestin recruitment bioluminescence resonance energy transfer 1 (BRET1) assay for trypsin**. The PAR2-aGPCR chimeric receptor of interest is C-terminally tagged with eYFP and β-arrestin 1 and 2 are tagged with RLuc and transiently expressed in PAR2-KO HEK293 cells. Upon the addition of agonist and RLuc substrate coelenterazine H, β-arrestin is recruited to the receptor. The proximity of eYFP to the RLuc mediated catalysis of coelenterazine H to coelenteramide causes an energy transfer to eYFP, creating an increase in fluorescence. If a ligand recruits β-arrestin to the receptor there should be dose dependent changes in the BRET ratio of eYFP fluorescence/RLuc luminescence. Figures were generated using the program Biorender (https://biorender.com).
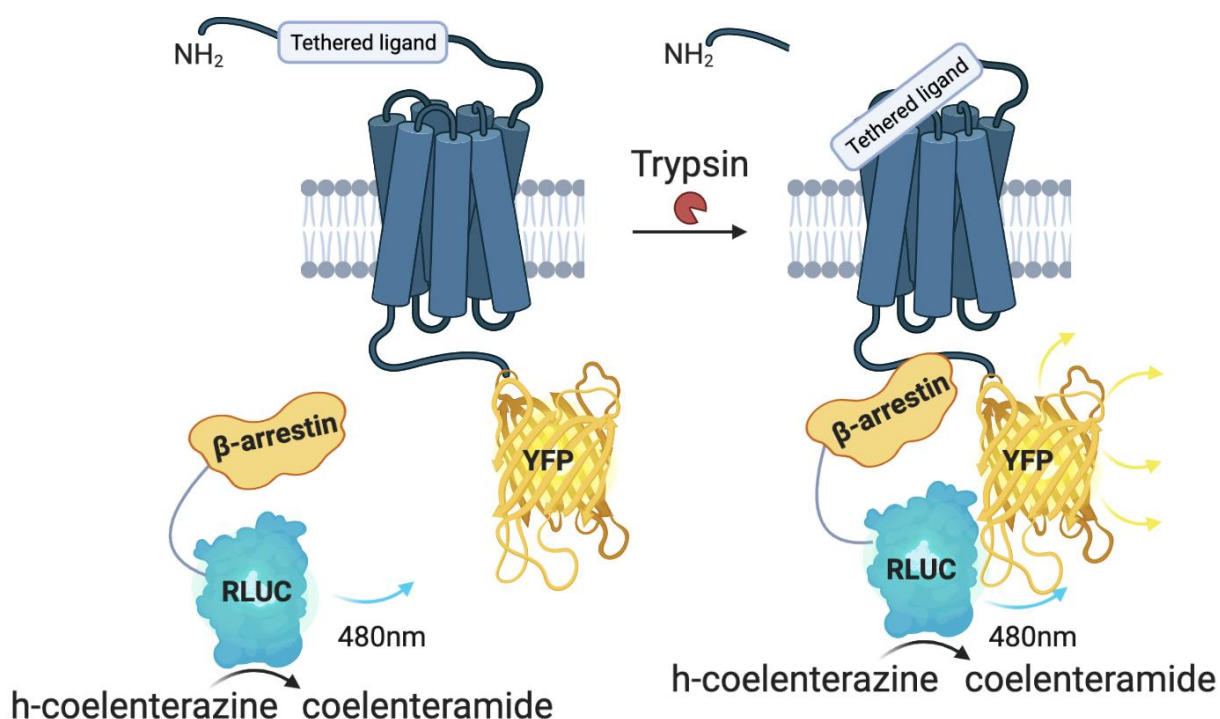
**Figure 6. Principle of β-arrestin recruitment bioluminescence resonance energy transfer 1 (BRET1) assay for peptides**. The PAR2-CD97 chimeric receptor is C-terminally tagged with eYFP and β-arrestin 1 and 2 are tagged with RLuc and transiently expressed in HEK293 cells. Upon the addition of agonist and RLuc substrate coelenterazine H, β-arrestin is recruited to the receptor. The proximity of eYFP to the RLuc mediated catalysis of coelenterazine H to coelenteramide causes an energy transfer to eYFP, creating an increase in fluorescence. If a ligand recruits β-arrestin to the receptor there should be dose dependent changes in the BRET ratio of eYFP fluorescence/RLuc luminescence. Figures were generated using the program Biorender (https://biorender.com).
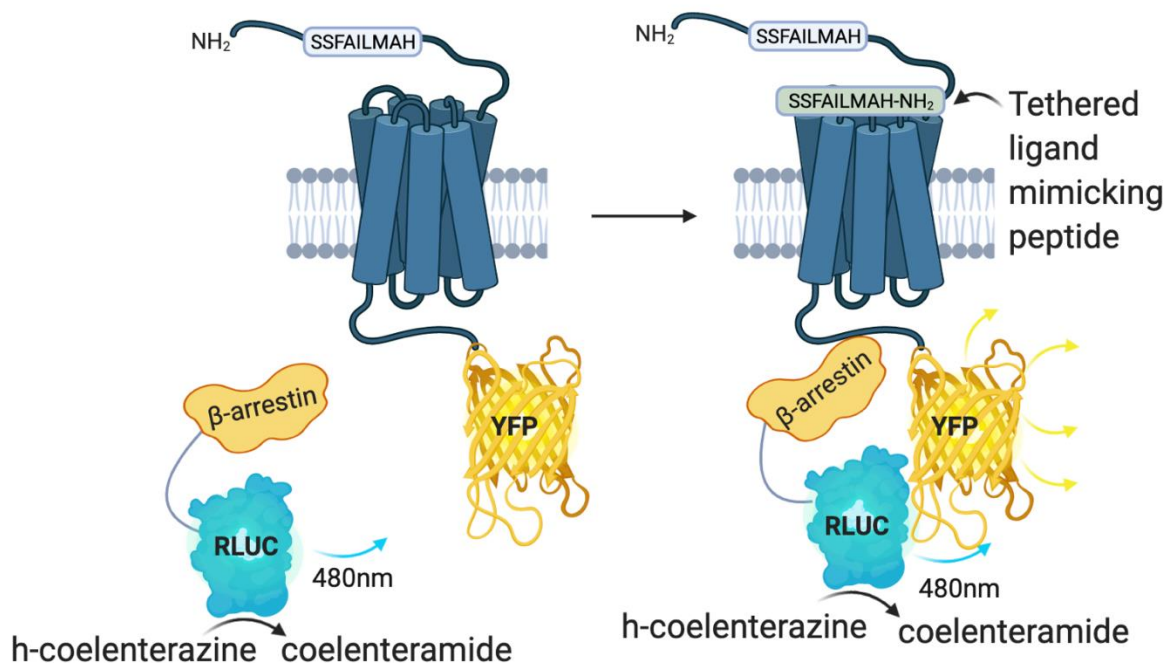
## 2.6 Bioluminescence resonance energy transfer 1 assay for G-protein recruitment

The ability of PAR2-aGPCR chimeric receptors to recruit various $G_\alpha$ proteins was assessed using a bioluminescence resonance energy transfer 1 (BRET1) assay (Fig 7)[104,105]. The chimeric receptors were C-terminally tagged with eYFP and $G_{sS(short)}$, $G_{sL(Long)}$, $G_{i1}$, $G_{i2}$, $G_{i3}$, $G_{oA}$, $G_{oB}$, $G_z$, $G_{gustducin}$, $G_q$, $G_{11}$, $G_{15}$, $G_{12}$ and $G_{13}$ $\alpha$ subunits tagged with RLuc were adapted from the TRUPATH biosensor platform[101]. Upon addition of drug and RLuc substrate coelenterazine H, if the receptor recruits the G-protein of interest, the close proximity of eYFP to the RLuc mediated catalysis of coelenterazine H to coelenteramide causes an energy transfer to eYFP, creating an increase in fluorescence[104,105]. Receptor G-protein coupling was confirmed if dose dependent changes in the ratio of eYFP fluorescence/RLuc luminescence was observed[104,105]. PAR2-KO cells were transfected with 1µg of eYFP tagged PAR2-CD97, PAR2-EMR2, PAR2-GPR56, or PAR2-BAI1 chimeric receptors and 100ng of the $G_\alpha$-protein of interest using a 3:1 ratio of Opti-MEM to X-tremegene9. One day post transfection cells were transferred into a 96-well white plate and seeded at a density of 35 000 cells per well. The next day media was aspirated and replaced with 5µM coelenterazine H diluted in HBSS and incubated at 37ºC for 5 minutes. After 5 minutes of incubation with coelenterazine H cells were treated with 0.3-300nM trypsin and plates were immediately read using a Berthold Mithras LB 940 plate reader and BRET ratios of eYFP fluorescence/RLuc luminescence were determined. NET BRET was then calculated by subtracting the lowest recorded BRET ratio from all samples. All points before the lowest recorded BRET ratio were excluded. Dose response curves were generated using three parameter log agonist vs response non-linear regression analysis on Graphpad prism 8 and error bars represent SEM.
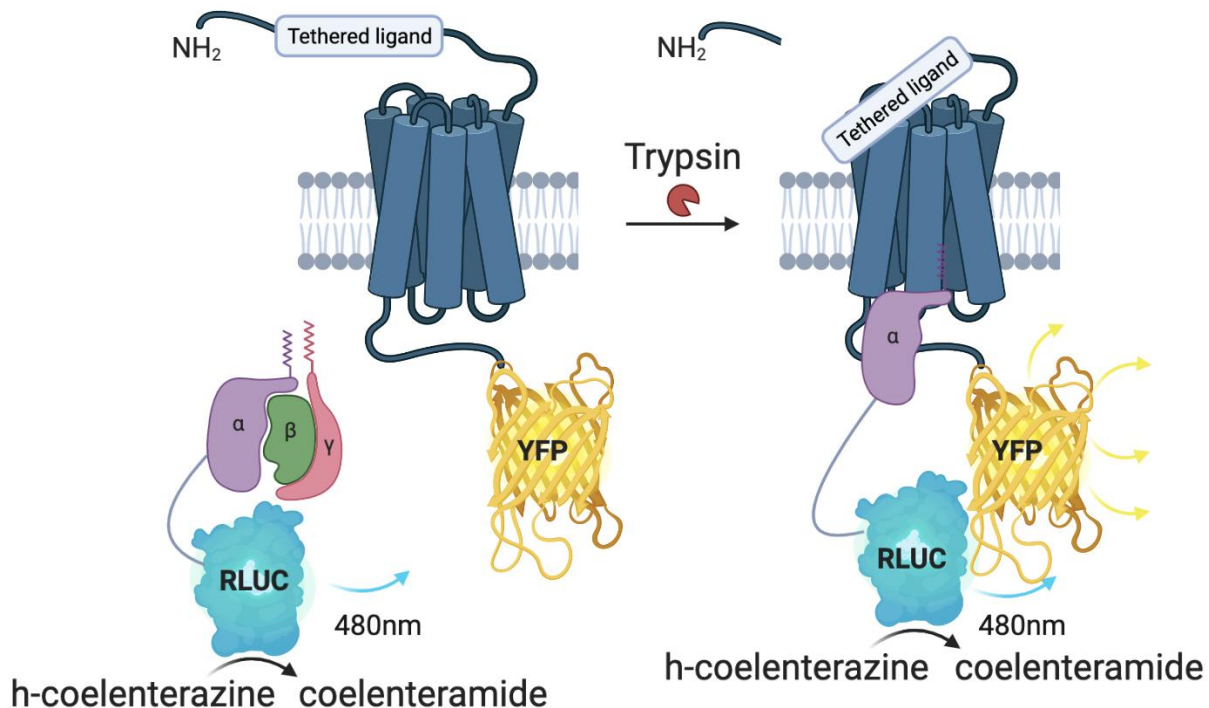
**Figure 7. Principle of G-protein recruitment bioluminescence resonance energy transfer 1 (BRET1) assay for trypsin**. The PAR2-aGPCR chimeric receptor of interest is C-terminally tagged with eYFP and the $G_\alpha$ subunit of interest is tagged with RLuc and transiently expressed in PAR2 KO HEK293 cells. Upon the addition of agonist and RLuc substrate coelenterazine H, the $G_\alpha$ subunit of interest is recruited to the receptor. The proximity of eYFP to the RLuc mediated catalysis of coelenterazine H to coelenteramide causes an energy transfer to eYFP, creating an increase in fluorescence. If a ligand recruits the $G_\alpha$ subunit of interest to the receptor there should be dose dependent changes in the BRET ratio of eYFP fluorescence/RLuc luminescence. Figures were generated using the program Biorender (https://biorender.com).

## 2.7 TANGO assay

The TANGO assay quantifies receptor activation by measuring the recruitment of β-arrestin 2 (Fig 8)[102,103,106]. β-arrestins are proteins involved in the desensitization of GPCRs and are preferentially recruited to activated receptors[29,30,33,34]. The assay requires HTLA cells and transfection with a TANGO receptor construct[102,103,106]. HTLA cells are HEK293 cells which express β-arrestin 2 tagged with the TEV protease and a firefly luciferase reporter gene under the control of the tTA transcription factor[102,103,106]. A TANGO receptor construct has the receptor of interest C-terminally fused at a TEV cleavage site to the tTA transcription factor[102,103,106]. If the ligand of interest is able to activate the receptor, β-arrestin 2 will be recruited[102,103,106]. When in close proximity to the receptor the TEV protease will allow tTA to be released and increase the expression of the luciferase receptor gene[102,103,106]. By treating cells with the luciferase substrate D-luciferin, changes in luminescence can be measured[102,103,106]. Cells were transfected with 1µg of the PAR2 or CD97 TANGO construct using a 3:1 ratio of Opti-MEM to X-tremegene9. One day post transfection cells were lifted in serum free media and seeded into a 96-well white plate at a density of 35 000 cells per well. Peptide agonists SLIGRL-$NH_2$ and SSFAILMAH-$NH_2$ were then added in concentrations ranging from 0.3-300µM and incubated with cells for 24 hours. After 24 hours of drug treatment, drug and media were carefully aspirated and replaced with Glo reagent. Glo reagent consisted of 0.14 mg/mL D-luciferin, 1.1mM ATP, 2.5% v/v Triton-x100, 5mM dichloro-diphenyl-trichloroethane (DDT), 75mM NaCl, 3mM MgCl, 108mM Tris-HCl, 42mM Tris-Base, and HBSS[102,106]. After 20 minutes of incubation with Glo reagent plates were read using a Berthold Mithras LB 940 plate reader and luminescence values were recorded. Luminescence values were normalized, with the HBSS blank set at 0% and the highest recorded luminescence set at 100%. Dose response curves were generated using three parameter log agonist vs response non-linear regression analysis on Graphpad prism 8 and error bars represent SEM.
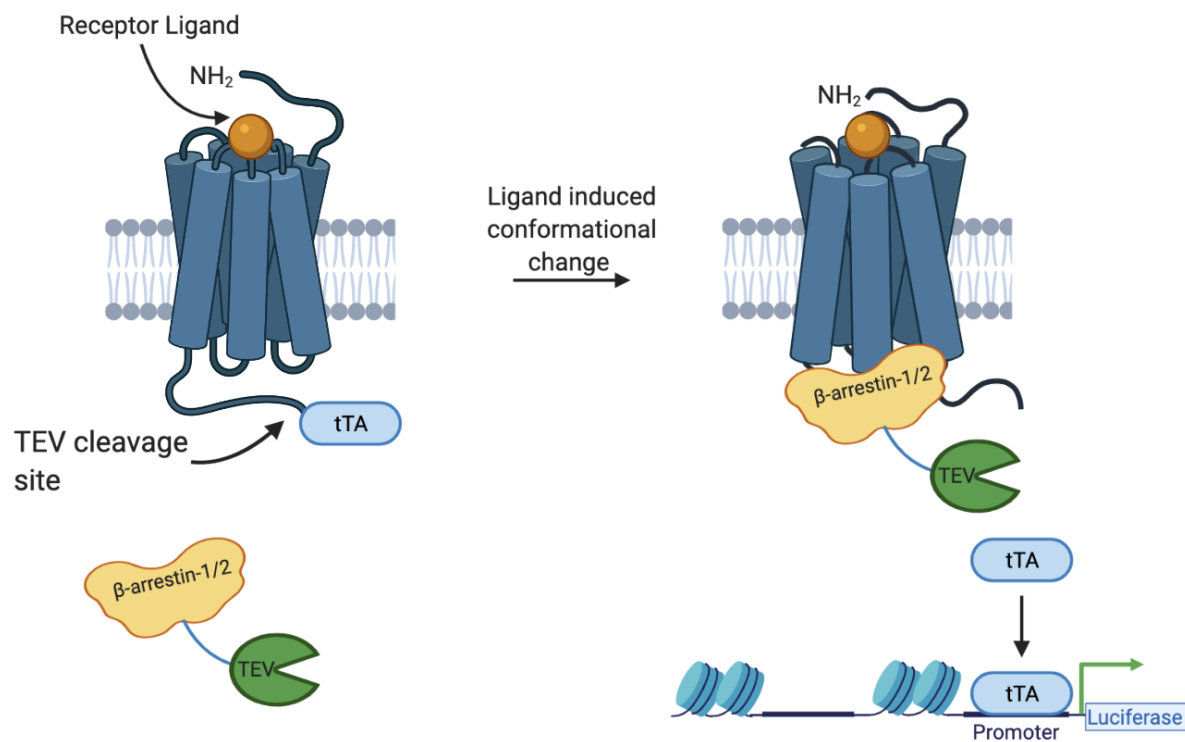
**Figure 8. Principle of the TANGO assay**. The receptor is C-terminally fused at a TEV protease cleavage site to the tTA transcription factor and transiently expressed in HLTA cells. HTLA cells are HEK293 cells which express β-arrestin 2 tagged with the TEV protease and a firefly luciferase reporter gene under the control of the tTA transcription factor. If the ligand tested is able to activate the receptor, β-arrestin is recruited to the receptor. This allows TEV to cleave tTA free of the receptor, where it translocates to the nucleus and increases the expression of the luciferase reporter gene. Figures were generated using the program Biorender (https://biorender.com).

# Chapter 3

# 3 Results and discussion

## 3.1 Results

### 3.1.1 PAR2-aGPCR chimeric receptor design

As mentioned in chapter 1 PARs are also activated by a tethered agonist, but instead of mechanical forces, the PAR tethered agonist is revealed by proteolytic cleavage of the receptor N-terminus[48]. As removal of the aGPCR N-terminal fragment has been shown to be important for receptor activation[46], we reasoned that replacing the N-terminal fragment of aGPCRs with the N-terminus of a PAR receptor would enable proteolytic unmasking of the aGPCR C-terminal fragment. To enable protease cleavage at a specific site, recognition sites for different proteases can be engineered into proteins[107]. Depending on the protease used, introduction of these tags can leave an exogenous residue on the protein of interest after cleavage[107]. Since the sequence of the revealed C-terminal fragment is critical for activation of signaling we wanted to establish a method that did not result in any changes to the revealed aGPCR sequence. PARs can be N-terminally cleaved by thrombin and trypsin, with PAR1 being the high affinity thrombin receptor and PAR2 being the high affinity trypsin receptor[48]. Therefore, we examined thrombin and trypsin cleavage site specificities to determine which PAR receptor N-terminus could be fused to the C-terminal fragments of aGPCRs to produce cleavage sites which leave no exogenous sequence behind.

### 3.1.1.1 Thrombin PAR1-aGPCR chimeric receptor approach

We first examined the cleavage specificity of the PAR1 agonist thrombin. The canonical thrombin cleavage site for PAR1 is between residues R41 and S42[48]. Fluorescence-based cleavage assays studying thrombin P1, P1', and P2' cleavage site specificities revealed that for high affinity thrombin cleavage P1 must be R, P1' must be S, and P2' must be F[108]. Protease cleavage sites P1, P1', and P2' are described using the Schechter and Berger nomenclature[109]. Therefore, in our system P1 would be the last residue of the PAR1 N-terminus, R41, and P1' and P2' would be the first two residues of the aGPCR C-

terminal fragment. By aligning the stalk regions for all 33 aGPCRs using the GPCRdb alignment tool (https://gpcrdb.org) (Fig 9) we found that only 9/33 aGPCRs have P1'=S, only 1/33 have P2'=F, and 0/33 have both P1'=S and P2'=F. Therefore, the PAR1 N-terminus cannot be fused to any aGPCR C-terminal fragment to create thrombin activated receptors without changing the sequence of aGPCR C-terminal fragments. Recently a group of researchers made a thrombin activated PAR1-LPHN3 (ADGRL3) chimeric receptor[110]. To achieve sufficient thrombin cleavage, they had to change the first residue of the LPHN3 stalk region from T to S and put in a frame shift mutation by deleting the second residue, N[110]. This therefore created the thrombin cleavage site P1=R, P1'=S, and P2'=F for their PAR1-LPHN3 chimeric receptor[110]. Although these researchers claim their approach can be more broadly applied to study other aGPCRs[110], this approach will only work if the first two residues of the aGPCR C-terminal fragment are changed to P1'=S and P2'=F. As the downstream signaling of many aGPCRs has yet to be determined, and it is known that changes to individual amino acids in the tethered ligand can influence signaling outcomes[59], it is not ideal to change the first two residues of this highly conserved sequence when studying aGPCR signaling. A second major limitation of this study relates to the endogenous expression of the thrombin activated GPCR PAR1 in the cell lines used to study the chimeric PAR1-LPHN3 receptor[110]. The methods used to study signaling measured the interaction of G proteins with downstream effectors, and not the direct interaction of G proteins with the receptor[110]. As PAR1 is endogenously expressed in HEK293 cells it is possible they were simply measuring the thrombin mediated response of the canonical thrombin receptor, PAR1.

**Figure 9. Alignment of all 33 adhesion GPCRs stalk regions**. The stalk region corresponds to the beginning of the C-terminal fragment to the first transmembrane domain. Highlighted in yellow is the β-13 strand, which creates the key non-covalent interactions holding the receptor together and also appears to contain the tethered agonistic for adhesion GPCRs. Highlighted in blue are predicted turn elements, which seemed to be required in tethered ligand mimicking peptides for proper activity. The majority of adhesion GPCRs stalk regions begin with either a S or T residue (highlighted in red), allowing the creation of a trypsin cleavage site when fused to the first 36 amino acids of PAR2. Alignment of all 33 aGPCR stalk regions was done using the GPCRdb alignment tool (https://gpcrdb.org).

### 3.1.1.2 Trypsin PAR2-aGPCR chimeric receptor approach

As the PAR1 thrombin activated approach would require substantial changes and optimization for each aGPCR chimeric receptor, we next examined the cleavage specificity of the PAR2 agonist trypsin. The canonical trypsin cleavage site for PAR2 is between residues R36 and S37[48]. Referring back to our alignment of the 33 aGPCR stalk regions we found that the C-terminal fragments of 27/33 aGPCRs begin with either a S or T residue (Fig 9). Another fluorescence-based cleavage assay which looked at trypsin P1' and P2' residue specificity determined that trypsin cleaves all of the 19 possible P2' residues as long as P1=R and P1'=S[111]. They also found that trypsin cleaves 12/19 possible P2' residues as long as P1=R and P1'=T[111]. Therefore, 26/27 of the aGPCRs that have stalk regions beginning with either S or T can be made into trypsin activated receptors without any changes to the receptors C-terminal fragment. This can be done by fusing the first 36 amino acids of PAR2, ending in R36, with the C-terminal fragment of an aGPCR beginning with S37 or T37. Further, 2/6 aGPCR stalk regions that do not begin with S or T can still form trypsin cleavage sites when fused to the PAR2 N-terminus. Therefore, our PAR2-aGPCR chimeric receptor approach can be used to make trypsin activated receptors for 29/33 aGPCRs without making any changes to the receptors C-terminal fragment. Upon the addition of trypsin, the PAR2 N-terminus would be removed and the aGPCR C-terminal fragment would be exposed via a mechanism that is almost identical to the canonical PAR activation mechanism (Fig 10). These chimeric receptors could then be time dependently activated with nM concentrations of trypsin to study aGPCR signaling. As mentioned in chapter 1 a limitation of the truncated receptor method is that they show low cell surface expression because they lack an N-terminal signal sequence. However, our PAR2-aGPCR chimeric receptors should show normal cell surface expression as they contain the PAR2 N-terminal signal sequence[112]. Further, to ensure we were measuring the response of the aGPCR of interest and not endogenously expressed PARs, all our signaling experiments measured the direct interaction of the chimeric receptor with effector proteins and were done in PAR2-KO cells that are devoid of the trypsin responsive receptor PAR2.
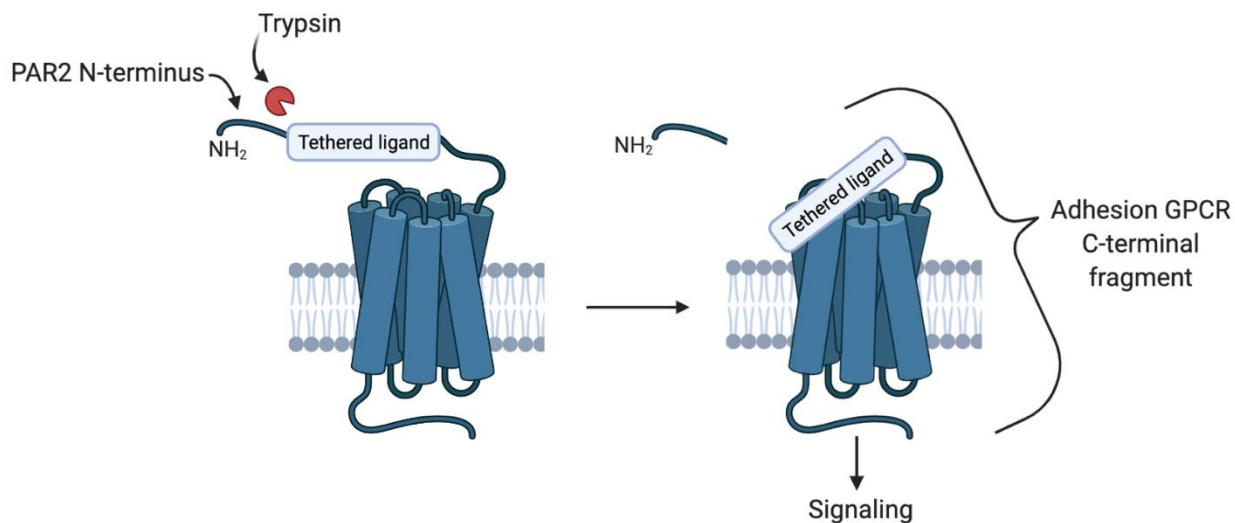
**Figure 10. Illustration of our PAR2-aGPCR chimeric receptor design**. The first 36 amino acids of PAR2 are fused to the C-terminal fragment of the aGPCR of interest. Upon the addition of nM concentrations of trypsin, the PAR2 N-terminus is removed allowing either the tethered agonist or conformational change to activate the receptor. Figures were generated using the program Biorender (https://biorender.com).

## 3.1.2    PAR2-CD97, PAR2-EMR2, PAR2-GPR56, PAR2-BAI1 chimeric receptors

As mentioned in chapter 1, we chose to study CD97, EMR2, GPR56, and BAI1 because they are 4 of the more well studied aGPCRs, and all have significant relevance in normal physiology and disease. Further, these receptors are representative members of 3 aGPCR subfamilies. The PAR2-CD97 chimeric receptor has a trypsin cleavage site of P1=R, P1'=S, and P2'=S. The PAR2-EMR2 chimeric receptor has a trypsin cleavage site of P1=R, P1'=S, and P2'=S. The PAR2-GPR56 chimeric receptor has a trypsin cleavage site of P1=R, P1'=T, and P2'=Y. The PAR2-BAI1 chimeric receptor has a trypsin cleavage site of P1=R, P1'=S, and P2'=T. Therefore 3 of our 4 chimeric receptors have unique trypsin cleavage sites (Fig 11), which supports the wide applicability of our approach to the receptor family as a whole.
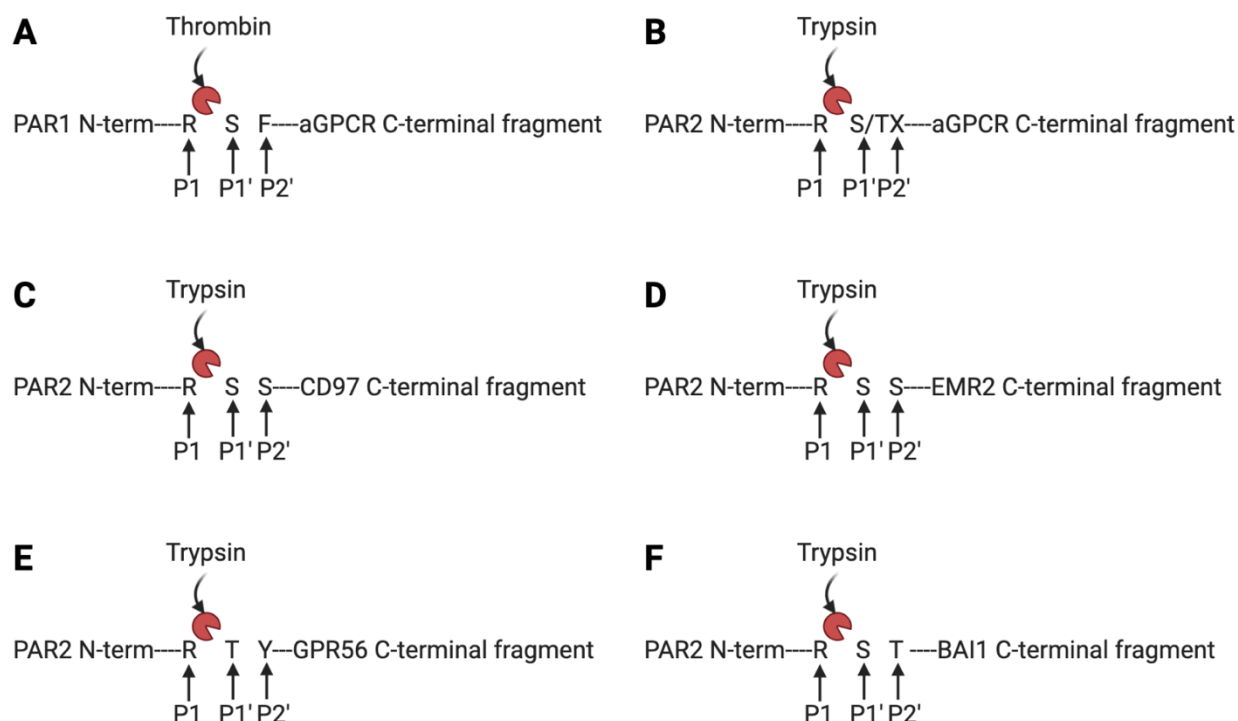
**Figure 11. Illustrations of protease cleavage specificities and PAR2-aGPCR chimeric receptor cleavage sites**. A) Thrombin cleavage specificity. Thrombin requires P1=R, P1'=S, and P2'=F for high affinity cleavage. B) Trypsin cleavage site specificity. Trypsin will cleave any of the possible P2' residues as long as P1=R and P1'=S. Trypsin will also cleave 12/19 of the possible P2' residues as long as P1=R and P1'=T. C) PAR2-CD97 chimeric receptor design. The first 36 amino acids of PAR2 ending in R36 were fused to the C-terminal fragment of CD97, with P1=R, P1'=S, and P2'=S. D) PAR2-EMR2 chimeric receptor design. The first 36 amino acids of PAR2 ending in R36 were fused to the C-terminal fragment of EMR2, with P1=R, P1'=S, and P2'=S. E) PAR2-GPR56 chimeric receptor design. The first 36 amino acids of PAR2 ending in R36 were fused to the C-terminal fragment of GPR56, with P1=R, P1'=T, and P2'=Y. F) PAR2-BAI1 chimeric receptor design. The first 36 amino acids of PAR2 ending in R36 were fused to the C-terminal fragment of BAI1, with P1=R, P1'=S, and P2'=T. Figures were generated using the program Biorender (https://biorender.com).

### 3.1.3    aGPCR chimeric receptor expression

PAR2-KO cells stably expressing either PAR2-CD97, PAR2-EMR2, PAR2-GPR56, or PAR2-BAI1 eYFP tagged chimeric receptors were analyzed by confocal microscopy to determine their cellular localization (Fig 12). PAR2-CD97, PAR2-EMR2, and PAR2-BAI1 chimeric receptors all appeared to be expressed on the cell membrane. However, the PAR2-GPR56 chimeric receptor appeared to be mainly expressed inside the cell.
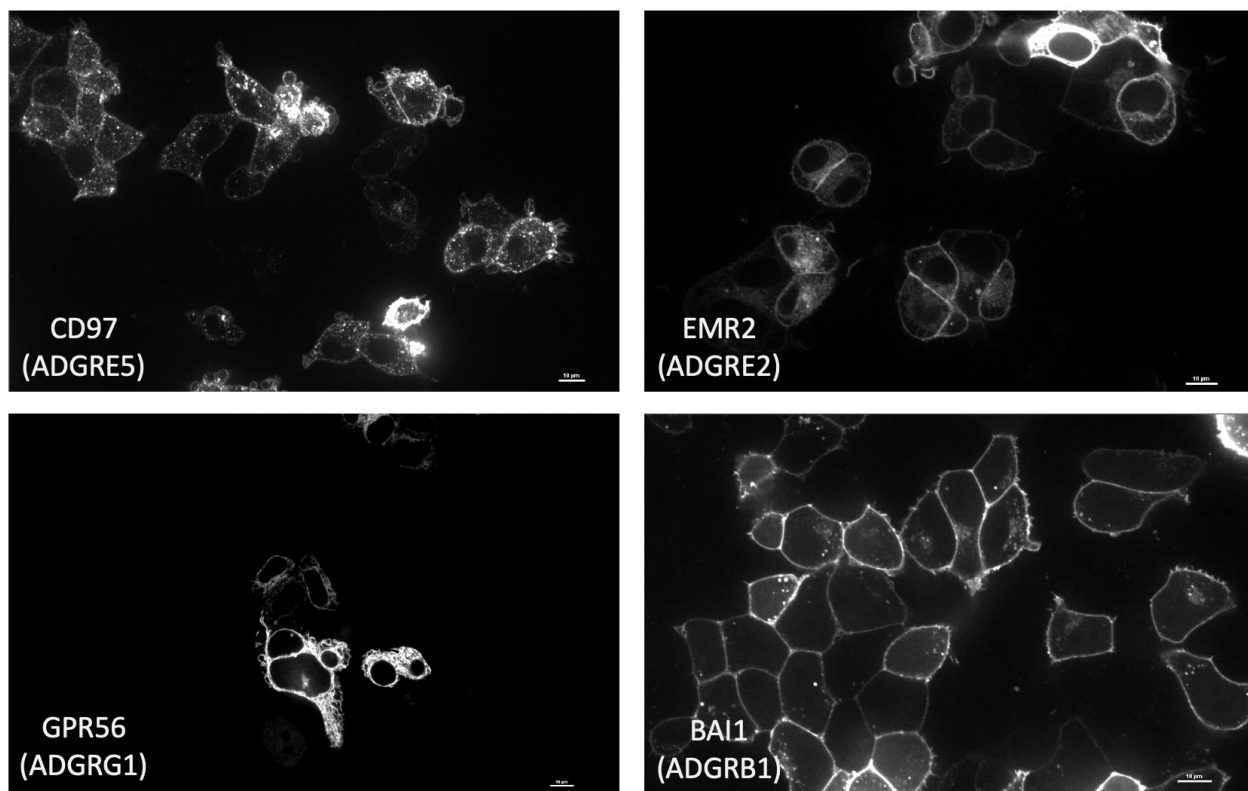
**Figure 12. PAR2-aGPCR chimeric receptor expression in PAR2-KO stable cells** (N=3). PAR2-KO cells stably expressed eYFP tagged PAR2-CD97, EMR2, GPR56, and BAI1 chimeric receptors were cultured on 35mm glass bottom dishes for imaging. Cells were imaged on a Nikon spinning disk confocal microscope at 60x magnification to determine cellular localization of PAR2-aGPCR chimeric receptors.

### 3.1.4 CD97 β-arrestin and G-protein recruitment profile

BRET1 assays with eYFP tagged PAR2-CD97 chimeric receptor as the photon acceptor and 16 different RLuc tagged β-arrestin (β-arrestin 1 and 2) and G-protein ($G_{12}$, $G_{13}$, $G_q$, $G_{11}$, $G_{15}$, $G_{i1}$, $G_{i2}$, $G_{i3}$, $G_{oA}$, $G_{oB}$, $G_z$, $G_{gustducin}$, $G_{sS(short)}$, $G_{sL(Long)}$) effectors as the photon donor were done to determine the effector coupling profile of CD97 (Fig 13). When treated with increasing concentrations of trypsin CD97 was able to cause dose-dependent increases in the BRET ratio of eYFP fluorescence/RLuc luminescence for both β-arrestin 1 ($EC_{50}$=61.59nM) and 2 ($EC_{50}$=136.5nM). When treated with increasing concentrations of trypsin CD97 also caused dose-dependent increases in the BRET ratio of eYFP fluorescence/RLuc luminescence for $G_{12}$ ($EC_{50}$=48.85nM), $G_{13}$ ($EC_{50}$=169.1nM), $G_q$ ($EC_{50}$=78.83nM), $G_{11}$ ($EC_{50}$=87.10nM), $G_{15}$ ($EC_{50}$=1092nM), $G_{i1}$ ($EC_{50}$=65.73nM), $G_{i2}$ ($EC_{50}$=23.10nM), $G_{i3}$ ($EC_{50}$=91.31nM), $G_{oA}$ ($EC_{50}$=110.6nM), $G_{oB}$ ($EC_{50}$=80.90nM), $G_z$ ($EC_{50}$=67.27nM), $G_{gustducin}$ ($EC_{50}$=155.5nM), $G_{sL(Long)}$ ($EC_{50}$=250.0nM), and $G_{sS(short)}$ ($EC_{50}$=568.8nM).

**Figure 13. β-arrestin and G-protein recruitment profile of CD97** (N=3-5). Bioluminescence resonance energy transfer 1 (BRET1) assays where the PAR2-CD97 chimeric receptor tagged with eYFP acted as the photon acceptor and 16 different RLuc tagged β-arrestin (β-arrestin 1 and 2) and G-protein ($G_{12}$, $G_{13}$, $G_q$, $G_{11}$, $G_{15}$, $G_{i1}$, $G_{i2}$, $G_{i3}$, $G_{oA}$, $G_{oB}$, $G_z$, $G_{gustducin}$, $G_{sS(short)}$, $G_{sL(Long)}$) effectors acted as the photon donor. For β-arrestin recruitment assays PAR2-CD97 chimeric receptors were transiently expressed in PAR2-KO HEK293 cells and treated for 20 minutes with 0.3-300nM trypsin. CD97 was able to cause dose-dependent increases in the BRET ratio of eYFP fluorescence/RLuc luminescence for both β-arrestin 1 ($EC_{50}$=61.59nM) and 2 ($EC_{50}$=136.5nM). For G-protein recruitment assays PAR2-CD97 chimeric receptors were transiently expressed in PAR2-KO HEK293 cells and treated with 0.3-300nM trypsin. CD97 was also able to cause dose-dependent increases in the BRET ratio of eYFP fluorescence/RLuc luminescence for $G_{12}$ ($EC_{50}$=48.85nM), $G_{13}$ ($EC_{50}$=169.1nM), $G_q$ ($EC_{50}$=78.83nM), $G_{11}$

$(EC_{50}=87.10nM)$, $G_{15}$ $(EC_{50}=1092nM)$, $G_{i1}$ $(EC_{50}=65.73nM)$, $G_{i2}$ $(EC_{50}=23.10nM)$, $G_{i3}$ $(EC_{50}=91.31nM)$, $G_{oA}$ $(EC_{50}=110.6nM)$, $G_{oB}$ $(EC_{50}=80.90nM)$, $G_z$ $(EC_{50}=67.27nM)$, $G_{gustducin}$ $(EC_{50}=155.5nM)$, $G_{sL(Long)}$ $(EC_{50}=250.0nM)$, and $G_{sS(short)}$ $(EC_{50}=568.8nM)$.

### 3.1.5 EMR2 β-arrestin and G-protein recruitment profile

BRET1 assays with eYFP tagged PAR2-EMR2 chimeric receptor as the photon acceptor and 16 different RLuc tagged β-arrestin (β-arrestin 1 and 2) and G-protein ($G_{12}$, $G_{13}$, $G_q$, $G_{11}$, $G_{15}$, $G_{i1}$, $G_{i2}$, $G_{i3}$, $G_{oA}$, $G_{oB}$, $G_z$, $G_{gustducin}$, $G_{sS(short)}$, $G_{sL(Long)}$) effectors as the photon donor were done to determine the effector coupling profile of EMR2 (Fig 14). When treated with increasing concentrations of trypsin EMR2 was able to cause dose-dependent increases in the BRET ratio of eYFP fluorescence/RLuc luminescence for both β-arrestin 1 ($EC_{50}$=44.35nM) and 2 ($EC_{50}$=28.90nM). When treated with increasing concentrations of trypsin EMR2 was also able to cause dose-dependent increases in the BRET ratio of eYFP fluorescence/RLuc luminescence for $G_{12}$ ($EC_{50}$=92.01nM), $G_{13}$ ($EC_{50}$=162.8nM), $G_q$ ($EC_{50}$=209.8nM), $G_{11}$ ($EC_{50}$=95.71nM), $G_{15}$ ($EC_{50}$=185.4nM), $G_{i1}$ ($EC_{50}$=79.28nM), $G_{i2}$ ($EC_{50}$=115.4nM), $G_{i3}$ ($EC_{50}$=123.9nM), $G_{oA}$ ($EC_{50}$=75.90nM), $G_{oB}$ ($EC_{50}$=144.9nM), $G_z$ ($EC_{50}$=249.5nM), $G_{gustducin}$ ($EC_{50}$=100.9nM), $G_{sL(Long)}$ ($EC_{50}$=155.6nM), and $G_{sS(short)}$ ($EC_{50}$=74.45nM).

**Figure 14. β-arrestin and G-protein recruitment profile of EMR2** (N=3-5). Bioluminescence resonance energy transfer 1 (BRET1) assays where the PAR2-EMR2 chimeric receptor tagged with eYFP acted as the photon acceptor and 16 different RLuc tagged β-arrestin (β-arrestin 1 and 2) and G-protein ($G_{12}$, $G_{13}$, $G_q$, $G_{11}$, $G_{15}$, $G_{i1}$, $G_{i2}$, $G_{i3}$, $G_{oA}$, $G_{oB}$, $G_z$, $G_{gustducin}$, $G_{sS(short)}$, $G_{sL(Long)}$) effectors acted as the photon donor. For β-arrestin recruitment assays PAR2-EMR2 chimeric receptors were transiently expressed in PAR2 KO HEK293 cells and treated for 20 minutes with 0.3-300nM trypsin. EMR2 was able to cause dose-dependent increases in the BRET ratio of eYFP fluorescence/RLuc luminescence both β-arrestin 1 ($EC_{50}$=44.35nM) and 2 ($EC_{50}$=28.90nM). For G-protein recruitment assays PAR2-EMR2 chimeric receptors were transiently expressed in PAR2-KO HEK293 cells and treated with 0.3-300nM trypsin. EMR2 was able to cause dose-dependent increases in the BRET ratio of eYFP fluorescence/RLuc luminescence for $G_{12}$ ($EC_{50}$=92.01nM), $G_{13}$ ($EC_{50}$=162.8nM), $G_q$ ($EC_{50}$=209.8nM), $G_{11}$ ($EC_{50}$=95.71nM), $G_{15}$

(EC$_{50}$=185.4nM), G$_{i1}$ (EC$_{50}$=79.28nM), G$_{i2}$ (EC$_{50}$=115.4nM), G$_{i3}$ (EC$_{50}$=123.9nM), G$_{oA}$ (EC$_{50}$=75.90nM), G$_{oB}$ (EC$_{50}$=144.9nM), G$_z$ (EC$_{50}$=249.5nM), G$_{gustducin}$ (EC$_{50}$=100.9nM), G$_{sL(Long)}$ (EC$_{50}$=155.6nM), and G$_{sS(short)}$ (EC$_{50}$=74.45nM).

### 3.1.6     GPR56 β-arrestin and G-protein recruitment profile

BRET1 assays with eYFP tagged PAR2-GPR56 chimeric receptor as the photon acceptor and 16 different RLuc tagged β-arrestin (β-arrestin 1 and 2) and G-protein ($G_{12}$, $G_{13}$, $G_q$, $G_{11}$, $G_{15}$, $G_{i1}$, $G_{i2}$, $G_{i3}$, $G_{oA}$, $G_{oB}$, $G_z$, $G_{gustducin}$, $G_{sS(short)}$, $G_{sL(Long)}$) effectors as the photon donor were done to determine the effector coupling profile profile of GPR56 (Fig 15). When treated with increasing concentrations of trypsin GPR56 was able to cause dose-dependent increases in the BRET ratio of eYFP fluorescence/RLuc luminescence for both β-arrestin 1 ($EC_{50}$=25.00nM) and 2 ($EC_{50}$=24.41nM). When treated with increasing concentrations of trypsin GPR56 was also able to cause dose-dependent increases in the BRET ratio of eYFP fluorescence/RLuc luminescence for $G_{12}$ ($EC_{50}$=59.14nM), $G_{13}$ ($EC_{50}$=78.16nM), $G_q$ ($EC_{50}$=85.33nM), $G_{11}$ ($EC_{50}$=65.99nM), $G_{15}$ ($EC_{50}$=17.79nM), $G_{i1}$ ($EC_{50}$=148.5nM), $G_{i2}$ ($EC_{50}$=841.5nM), $G_{i3}$ ($EC_{50}$=151.5nM), $G_{oA}$ ($EC_{50}$=47.23nM), $G_{oB}$ ($EC_{50}$=69.99nM), $G_z$ ($EC_{50}$=892.0nM), $G_{gustducin}$ ($EC_{50}$=702.3nM), $G_{sL(Long)}$ ($EC_{50}$=52.52nM), and $G_{sS(short)}$ ($EC_{50}$=49.84nM).
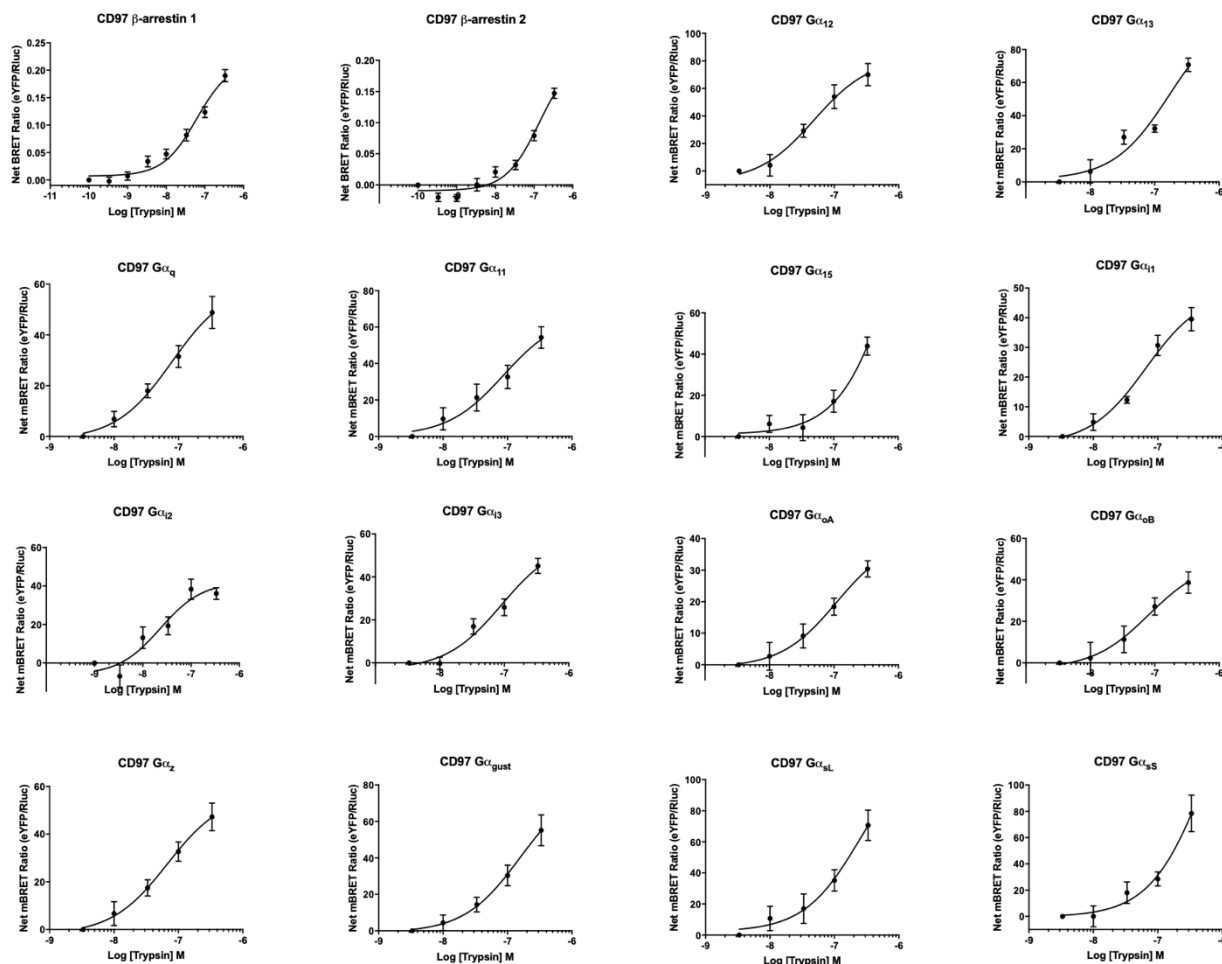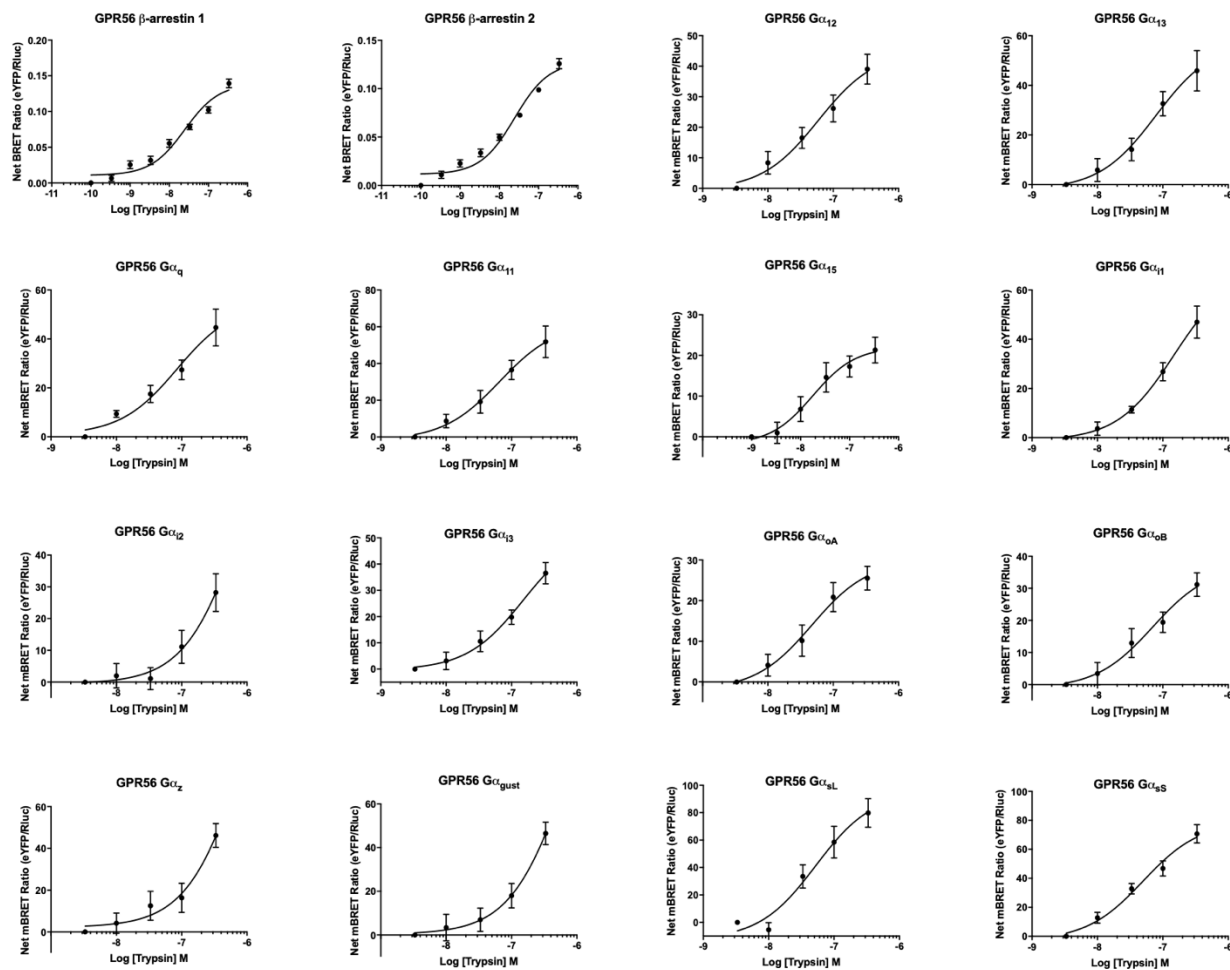
**Figure 15. β-arrestin and G-protein recruitment profile of GPR56** (N=3-5). Bioluminescence resonance energy transfer 1 (BRET1) assays where the PAR2-GPR56 chimeric receptor tagged with eYFP acted as the photon acceptor and 16 different RLuc tagged β-arrestin (β-arrestin 1 and 2) and G-protein ($G_{12}$, $G_{13}$, $G_q$, $G_{11}$, $G_{15}$, $G_{i1}$, $G_{i2}$, $G_{i3}$, $G_{oA}$, $G_{oB}$, $G_z$, $G_{gustducin}$, $G_{sS(short)}$, $G_{sL(Long)}$) effectors acted as the photon donor. For β-arrestin recruitment assays PAR2-GPR56 chimeric receptors were transiently expressed in PAR2 KO HEK293 cells and treated for 20 minutes with 0.3-300nM trypsin. GPR56 was able to cause dose-dependent increases in the BRET ratio of eYFP fluorescence/RLuc luminescence for both β-arrestin 1 ($EC_{50}$=25.00nM) and 2 ($EC_{50}$=24.41nM). For G-protein recruitment assays PAR2-GPR56 chimeric receptors were transiently expressed in PAR2-KO HEK293 cells and treated with 0.3-300nM trypsin. GPR56 was also able to cause dose-dependent increases in the BRET ratio of

eYFP fluorescence/RLuc luminescence for $G_{12}$ ($EC_{50}$=59.14nM), $G_{13}$ ($EC_{50}$=78.16nM), $G_q$ ($EC_{50}$=85.33nM), $G_{11}$ ($EC_{50}$=65.99nM), $G_{15}$ ($EC_{50}$=17.79nM), $G_{i1}$ ($EC_{50}$=148.5nM), $G_{i2}$ ($EC_{50}$=841.5nM), $G_{i3}$ ($EC_{50}$=151.5nM), $G_{oA}$ ($EC_{50}$=47.23nM), $G_{oB}$ ($EC_{50}$=69.99nM), $G_z$ ($EC_{50}$=892.0nM), $G_{gustducin}$ ($EC_{50}$=702.3nM), $G_{sL(Long)}$ ($EC_{50}$=52.52nM), and $G_{sS(short)}$ ($EC_{50}$=49.84nM).

### 3.1.7  BAI1 β-arrestin and G-protein recruitment profile

BRET1 assays with eYFP tagged PAR2-BAI1 chimeric receptor as the photon acceptor and 16 different RLuc tagged β-arrestin (β-arrestin 1 and 2) and G-protein ($G_{12}$, $G_{13}$, $G_q$, $G_{11}$, $G_{15}$, $G_{i1}$, $G_{i2}$, $G_{i3}$, $G_{oA}$, $G_{oB}$, $G_z$, $G_{gustducin}$, $G_{sS(short)}$, $G_{sL(Long)}$) effectors as the photon donor were done to determine the effector coupling of BAI1 (Fig 16). When treated with increasing concentrations of trypsin BAI1 was able to cause dose-dependent increases in the BRET ratio of eYFP fluorescence/RLuc luminescence for both β-arrestin 1 ($EC_{50}$=37.42nM) and 2 ($EC_{50}$=25.72nM). When treated with increasing concentrations of trypsin BAI1 was also able to cause dose-dependent increases in the BRET ratio of eYFP fluorescence/RLuc luminescence for $G_{12}$ ($EC_{50}$=73.79nM), $G_{13}$ ($EC_{50}$=39.60nM), $G_q$ ($EC_{50}$=179.4nM), $G_{11}$ ($EC_{50}$=50.66nM), $G_{15}$ ($EC_{50}$=164.3nM), $G_{i1}$ ($EC_{50}$=44.33nM), $G_{i2}$ ($EC_{50}$=82.13nM), $G_{i3}$ ($EC_{50}$=48.37nM), $G_{oA}$ ($EC_{50}$=33.26nM), $G_{oB}$ ($EC_{50}$=47.93nM), $G_z$ ($EC_{50}$=91.97nM), $G_{gustducin}$ ($EC_{50}$=109.5nM), $G_{sL(Long)}$ ($EC_{50}$=178.2nM), and $G_{sS(short)}$ ($EC_{50}$=83.11nM).
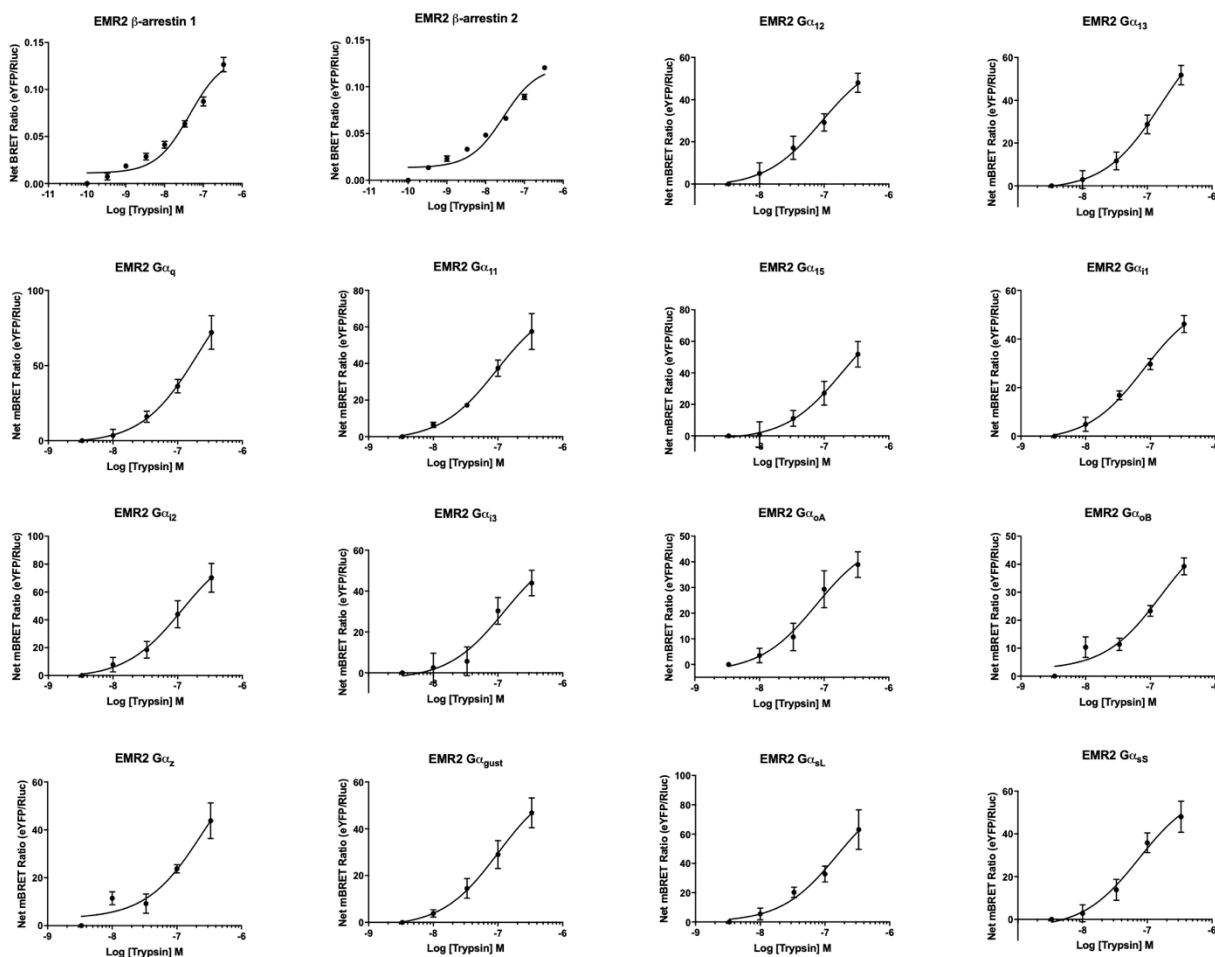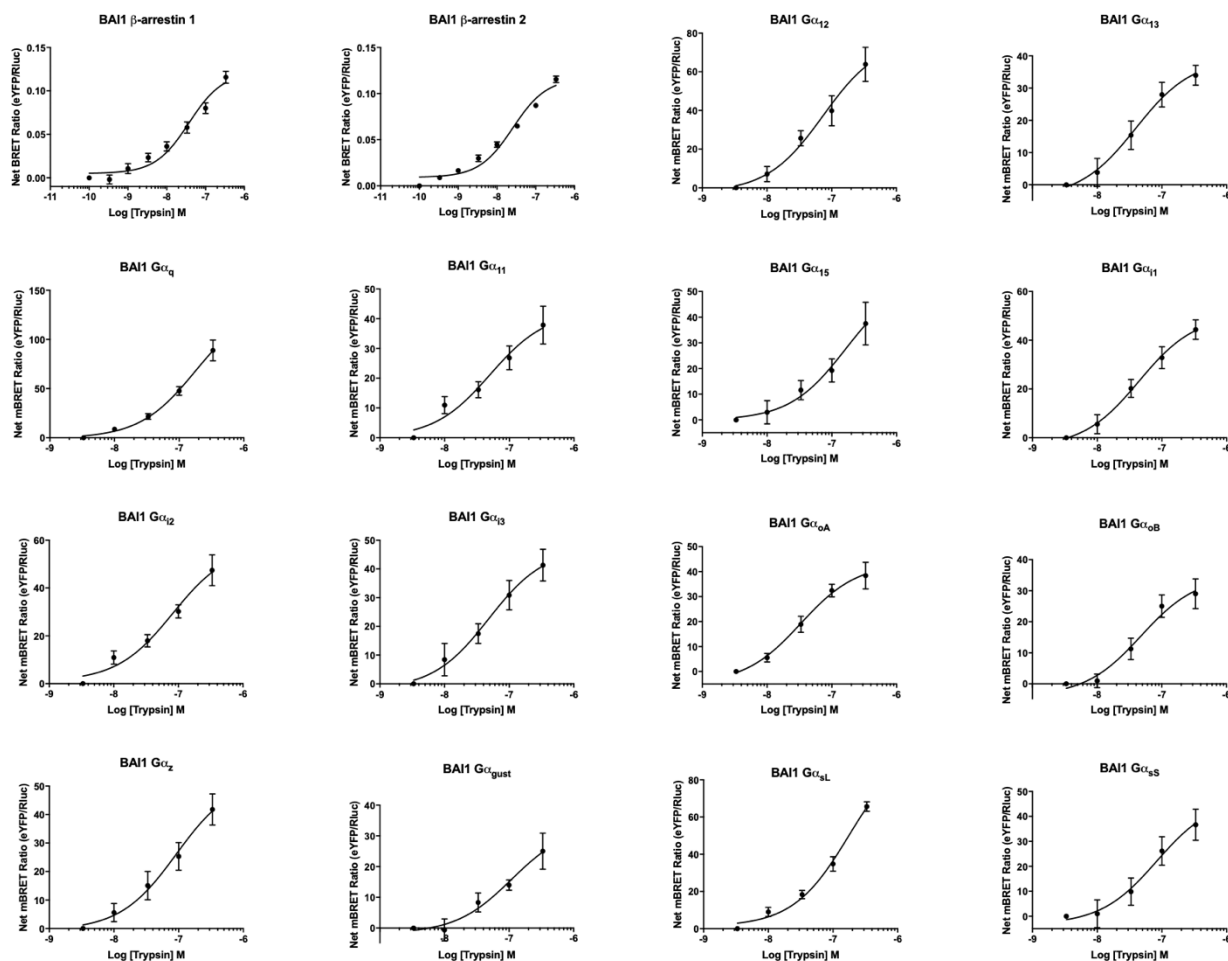
**Figure 16. β-arrestin and G-protein recruitment profile of BAI1** (N=3-5). Bioluminescence resonance energy transfer 1 (BRET1) assays where the PAR2-BAI1 chimeric receptor tagged with eYFP acted as the photon acceptor and 16 different RLuc tagged β-arrestin (β-arrestin 1 and 2) and G-protein ($G_{12}$, $G_{13}$, $G_q$, $G_{11}$, $G_{15}$, $G_{i1}$, $G_{i2}$, $G_{i3}$, $G_{oA}$, $G_{oB}$, $G_z$, $G_{gustducin}$, $G_{sS(short)}$, $G_{sL(Long)}$) effectors acted as the photon donor. For β-arrestin recruitment assays PAR2-BAI1 chimeric receptors were transiently expressed in PAR2 KO HEK293 cells and treated for 20 minutes with 0.3-300nM trypsin. BAI1 was able to cause dose-dependent increases in the BRET ratio of eYFP fluorescence/RLuc luminescence for both β-arrestin 1 ($EC_{50}$=37.42nM) and 2 ($EC_{50}$=25.72nM). For G-protein recruitment assays PAR2-BAI1 chimeric receptors were transiently expressed in PAR2-KO HEK293 cells and treated with 0.3-300nM trypsin. BAI1 was also able to cause dose-dependent increases in the BRET ratio of eYFP fluorescence/RLuc luminescence for $G_{12}$ ($EC_{50}$=73.79nM), $G_{13}$ ($EC_{50}$=39.60nM), $G_q$ ($EC_{50}$=179.4nM), $G_{11}$

(EC$_{50}$=50.66nM), G$_{15}$ (EC$_{50}$=164.3nM), G$_{i1}$ (EC$_{50}$=44.33nM), G$_{i2}$ (EC$_{50}$=82.13nM), G$_{i3}$ (EC$_{50}$=48.37nM), G$_{oA}$ (EC$_{50}$=33.26nM), G$_{oB}$ (EC$_{50}$=47.93nM), G$_{z}$ (EC$_{50}$=91.97nM), G$_{gustducin}$ (EC$_{50}$=109.5nM), G$_{sL(Long)}$ (EC$_{50}$=178.2nM), and G$_{sS(short)}$ (EC$_{50}$=83.11nM).

### 3.1.8 Predicting the sequence of a CD97 tethered ligand mimicking peptide

Synthetic peptides made to mimic a receptors tethered ligand can be used to activate the receptor without the need to expose the receptors tethered ligand, as shown in Figure 6. These tethered ligand mimicking peptides are useful tools when studying receptors activated by the same agonist. For example, both PAR1 and PAR4 are activated by thrombin[48]. Therefore, when studying PAR signaling in platelets, which express both PAR1 and PAR4[113], receptor specific tethered ligand mimicking peptides TFLLR-NH$_2$ for PAR1, and AYPGKF-NH$_2$ for PAR4, can be used[48]. These tethered ligand mimicking peptides have a similar utility when studying aGPCRs, which are all activated by the same mechanism, mechanical force[46,50]. Tethered ligand mimicking peptides have currently been determined for 8 of the 33 aGPCRs[59–61,93,94]. Analyzing these studies gave us valuable insight on how we might generate a peptide that would activate CD97, without having to make peptide library against the CD97 stalk region. The length of agonistic peptides differs greatly between aGPCRs[59–61,93,94]. For example, GPR56 was found to be activated by a peptide corresponding to the first 7 amino acids of its stalk region[59]. GPR110, on the other hand, was activated by peptides corresponding to the first 9-18 amino acids of its stalk region, with the peptide of 12 amino acids found to be the most potent[59]. It was therefore hypothesized that if the stalk region contains a turn element, then this must be included in the peptide for it to be agonistic[46]. Similar to GPR56, CD97 does not contain any turn elements in its stalk region (Fig 9); therefore, we predicted a shorter peptide would be agonistic. Recent structures of aGPCR N-terminal fragments have shown that the β-13 strand, corresponding to the first 9 amino acids of the aGPCR stalk region, is responsible for making the key non-covalent interactions holding the N-terminal and C-terminal fragments together[114]. These 9 amino acids show high sequence conservation across aGPCRs (Fig 9), and 7 of the 8 agonistic aGPCR peptides contain all 9 of these amino acids[59–61,93,94]. Therefore, we generated a peptide corresponding to the first 9 amino acids of the CD97 stalk region, SSFAILMAH-NH$_2$, and tested its ability to activate the receptor.

### 3.1.9 Testing the ability of SSFAILMAH-NH$_2$ to activate CD97

Although TANGO plasmids have been made for over 300 GPCRs, many have not been tested with known receptor agonists[102]. To verify that the TANGO assay was a good method for testing tethered ligand mimicking peptides we used the well documented PAR2 tethered ligand mimicking peptide SLIGRL-NH$_2$ and tested its ability to activate PAR2 using the TANGO assay. SLIGRL-NH$_2$ was able to cause dose-dependent increases in luminescence (EC$_{50}$=10.67μM) with a similar EC$_{50}$ for β-arrestin 2 as we have previously reported (EC$_{50}$=11.1μM)[100] (Fig 17). We next tested the ability of SSFAILMAH-NH$_2$ to activate CD97 using the TANGO assay. SSFAILMAH-NH$_2$ was able to cause dose-dependent increases in luminescence with an EC$_{50}$ of 17.28μM (Fig 17). Next, we used a BRET1 assay with eYFP tagged PAR2-CD97 chimeric receptor as the photon acceptor and RLuc tagged β-arrestin 1 and 2 as the photon donors to test the ability of SSFAILMAH-NH$_2$ to activate CD97. SSFAILMAH-NH$_2$ was able to cause dose-dependent increases in the BRET ratio of eYFP fluorescence/RLuc luminescence for β-arrestin 1 (EC$_{50}$=22.86μM) and 2 (EC$_{50}$=78.29μM) (Fig 17).
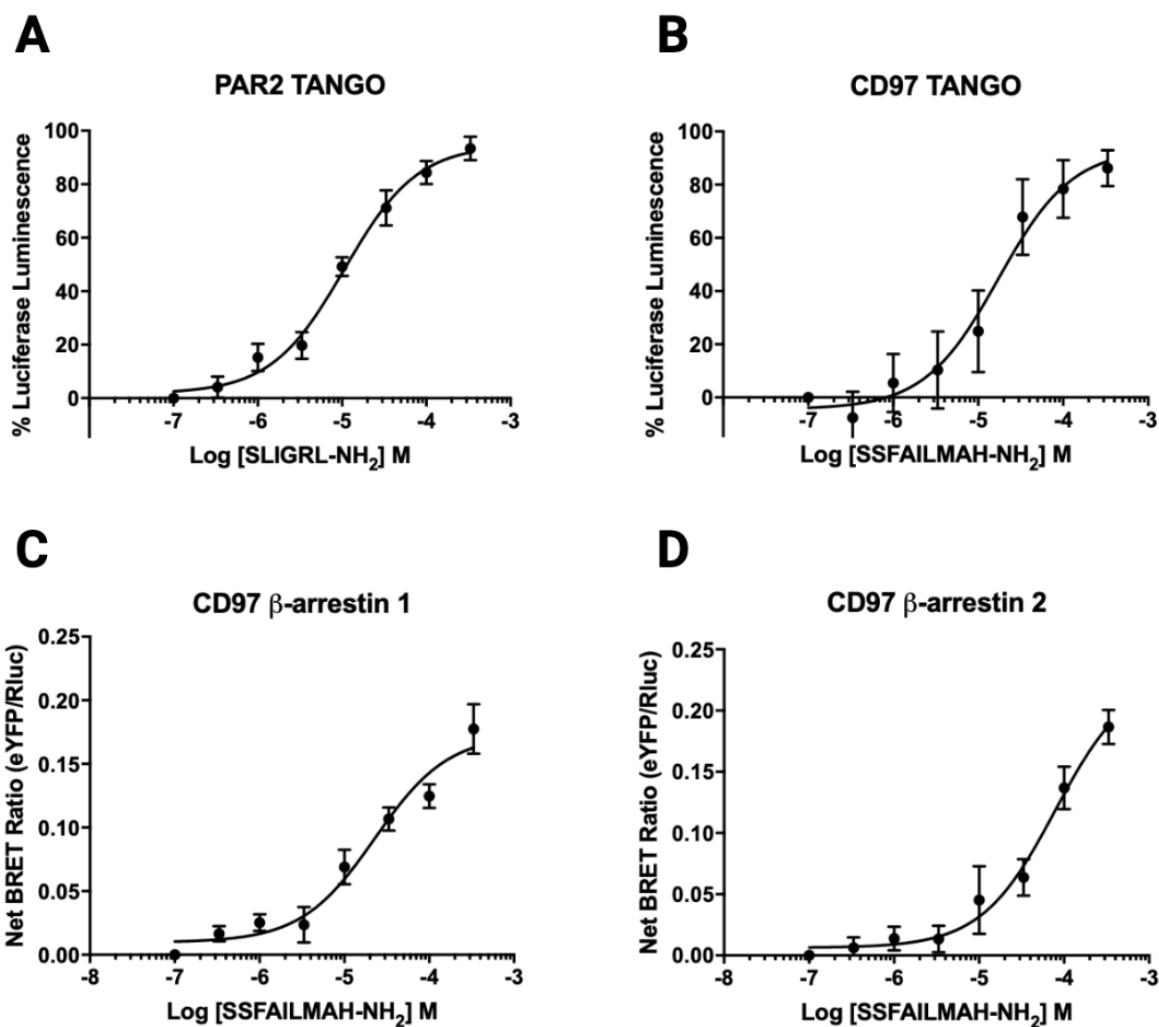
**Figure 17. TANGO and BRET assays testing the ability of tethered ligand mimicking peptide SSFAILMAH-NH$_2$ to activate CD97** (N=3). HTLA cells were transiently transfected with PAR2 or CD97 TANGO constructs and treated with 0.3-300μM PAR2 activating peptide SLIGRL-NH$_2$ or CD97 activating peptide SSFAILMAH-NH$_2$. A) SLIGRL-NH$_2$ was able to cause dose-dependent increases in luminescence (EC$_{50}$=10.67μM) with a similar EC$_{50}$ for β-arrestin 2 as we have previously reported (EC$_{50}$=11.1μM)[100]. B) SSFAILMAH-NH$_2$ was able to cause dose-dependent increases in luminescence with an EC$_{50}$ of 17.28μM. Shown on the bottom graphs are BRET1 assays with eYFP tagged PAR2-CD97 chimeric receptor as the photon acceptor and RLUC tagged β-arrestin 1 and 2 as the photon donors to test the ability of

SSFAILMAH-NH$_2$ to activate CD97. C) and D) SSFAILMAH-NH$_2$ was able to cause dose-dependent increases in the BRET ratio of eYFP fluorescence/RLUC luminescence for β-arrestin 1 (EC$_{50}$=22.86μM) and 2 (EC$_{50}$=78.29μM).

## 3.2   Discussion

### 3.2.1   PAR2-aGPCR chimeric receptor expression

When examined by confocal microscopy our eYFP tagged PAR2-CD97, EMR2, and BAI1 chimeric receptors showed proper cell surface expression (Fig 12). This confirmed that addition of the PAR2 N-terminus allowed proper expression of the receptors and did not result in a constitutively activated receptor that was entirely intracellular as was seen with the truncated receptor method previously used[62]. CD97 showed some intracellular pools of receptor that may reflect a certain level of constitutive activity in this receptor or may be indicative of intracellular pools of this receptor being present in cells to enable rapid repopulation following activation and internalization of cell surface receptors. Such intracellular pools of PAR1 are seen in some cells[115,116]. The expression pattern of the PAR2-GPR56 chimeric receptor is quite puzzling and this receptor appeared to be expressed almost entirely inside the cell (Fig 12). This is odd since the PAR2-GPR56 chimeric receptor dose dependently recruited a variety of effector proteins (Fig 15). It is possible that the observed localization is the normal sub-cellular expression pattern of GPR56 with only a small population of GPR56 present at the cell membrane and the remaining receptors associated with intracellular protein scaffolds. In future experiments we plan to test this hypothesis by analyzing the expression of full length GPR56. The intracellular structures that our PAR2-GPR56 chimeric receptor is associated with look very similar to mitochondria, and there is evidence that GPR56 is involved with mitochondrial function[117]. Therefore, in the future we also plan to examine if GPR56 co-localizes with mitochondria markers.

### 3.2.2   CD97 activation results in the recruitment of β-arrestin and a variety of G-proteins

By creating a chimeric trypsin activated PAR2-CD97 receptor, where the first 36 amino acids of PAR2 were fused to the C-terminal fragment of CD97, we were able to study the recruitment of 16 effector proteins from the 5 major signaling pathways downstream of GPCRs. As shown in figure 13 CD97 dose-dependently recruited both β-arrestin 1 ($EC_{50}$=61.59nM) and 2 ($EC_{50}$=136.5nM). The interaction of CD97 with β-arrestin 1 has been previously shown using co-immunoprecipitation[118]. In this earlier study CD97 was

overexpressed and co-immunoprecipitation with β-arrestin 1 was compared with cells not overexpressing CD97[118]. Even though CD97 is not activated, the overexpression of the receptor results in more basal activity compared to cells not overexpressing the receptor. In this study they also identified a site of interaction between CD97 and β-arrestin 1[118]. Mutation of residues 631 to 641 on intracellular loop 3 (ICL3) and TM6 decreased the interaction of CD97 and β-arrestin 1[118]. They also determined that GRK6 is involved with phosphorylating CD97 following receptor activation creating binding sites for β-arrestins[118]. The rather limited approach of overexpressing the full-length inactive receptor to study aGPCR signaling is common because specific synthetic agonists and other methods of activating aGPCRs were not available. Our chimeric receptors have provided another strategy for tackling this problem and we are the first to report the interaction of CD97 with β-arrestin 2, and to show the dose-dependent interaction of CD97 with β-arrestins 1 and 2.

CD97 dose-dependently recruited both $G_{12}$ ($EC_{50}$=48.85nM) and $G_{13}$ ($EC_{50}$=169.1nM) (Fig 13). The interaction of CD97 with the $G_{12/13}$ family of G-proteins has been previously documented[73,119]. Receptors made to express only the C-terminal fragment of CD97 showed higher levels of SRE reporter gene luminescence and RhoA activation compared to full-length receptors. This signaling was shown to be tethered ligand dependent, as receptors truncated to TM1 and therefore lacking the stalk region, did not show any difference in response compared to full length receptors. Although SRE and RhoA are mainly downstream of $G_{12/13}$, these pathways can also be activated by the $G_{q/11}$ family of G-proteins[27]. This is another example of why the GPCR field is moving away from methods such as gene reporter assays in favor of methods directly measuring the interaction of receptors with effector proteins, as we have done. Recently another study used a yeast cell growth reporter gene assay to show that CD97 interacts with $G_{12}$ and $G_{13}$[119]. In this assay, yeast cell growth is controlled by the $G_{\beta\gamma}$ subunit and all but the $G_{\alpha}$ protein of interest are knocked out[119]. Therefore, the only way for the yeast cells to grow is if your receptor activates the G-protein of interest[119]. Yeast cells expressing $G_{12}$ and $G_{13}$ grew more with CD97 receptors lacking the N-terminal fragment than cells expressing full-length receptors, supporting CD97 activation of both $G_{12}$ and $G_{13}$[119]. Our data supports these observations, and we are the first to show the dose-dependent

interaction of CD97 with $G_{12/13}$. CD97 signaling through $G_{12/13}$ also makes sense as its overexpression in cancer cells increases tumors cell migration and metastasis[53,55,56,70–74], a process that is well established to involve $G_{12/13}$ signaling [120]. Also, CD97 has been shown to be expressed at the leading edge of tumors[56]. CD97 $G_{12/13}$ signaling is also likely involved in its role of regulating immune cell migration and mobilization[50,77–79,121].

CD97 dose-dependently recruited $G_q$ ($EC_{50}$=78.83nM) and $G_{11}$ ($EC_{50}$=87.10nM) (Fig 13). As the $EC_{50}$ of $G_{15}$ recruitment ($EC_{50}$=1092nM) was very high and response so small and variable we conclude that CD97 likely does not couple to $G_{15}$. As mentioned in the last paragraph, a G-protein coupling profile for CD97 was recently reported using a yeast cell growth assay[119]. In this study CD97 was not shown to couple to $G_{16}$[119]. As $G_{15}$ is the mouse homolog of $G_{16}$, these findings are also in agreement with our data[27]. Yeast cells expressing $G_q$ and CD97 without its N-terminal fragment grew more than cells expressing full-length receptor[119]. This supports our data, and we show also that CD97 can dose-dependently recruit $G_q$ and $G_{11}$. Using the yeast cell growth assay, Bhudia et al also showed that CD97 activated $G_{14}$. Unfortunately, we did not have a RLuc tagged $G_{14}$ BRET sensor, therefore future studies will have to be done to support their findings[101]. As the interaction of CD97 with the $G_{q/11}$ family of G-proteins has only recently been determined, the functional outcome of this signaling in physiology and disease is currently unknown. However, effectors such as Phosphoinositide 3-kinase (PI3K), PLC-β/DAG, and RhoA are downstream of $G_{q/11}$ and are important in immune cell migration and mobilization[27,121]. Therefore, CD97 $G_{q/11}$ signaling may also contribute to its role in regulating immune cell migration and mobilization[25–29].

As shown in figure 13 CD97 dose-dependently recruited $G_{i1}$ ($EC_{50}$=65.73nM), $G_{i2}$ ($EC_{50}$=23.10nM), $G_{i3}$ ($EC_{50}$=91.31nM), $G_{oA}$ ($EC_{50}$=110.6nM), $G_{oB}$ ($EC_{50}$=80.90nM), $G_z$ ($EC_{50}$=67.27nM), and $G_{gustducin}$ ($EC_{50}$=155.5nM). Yeast cells expressing $G_{i1}$ and $G_z$, but not $G_{i3}$ and $G_o$, had increased growth when expressed with CD97 without its N-terminal fragment[119]. Our data supports the coupling of CD97 with $G_{i1}$ and $G_z$, however we also show dose-dependent coupling to $G_{i3}$, $G_{oA}$, and $G_{oB}$. This discrepancy in results may be explained by the fact that Bhudia et al were using human CD97 with chimeric yeast G-proteins[119]. The 5 C-terminal amino acids of mammalian G-proteins were added to the

yeast G-protein Gpa1[119] , since these amino acids are the important mammalian receptor interacting residues. Although this yeast-based assay gave very similar results to our BRET assays in mammalian cells, Bhudia et al do discuss the possibility of false positives and negatives, which could explain our differences in results[119]. The coupling of CD97 to $G_{i1-3}$ is in keeping with its role in immune cell function. In leukocytes the $G_{i1-3}$ G-proteins are important for regulating many chemokine and chemoattractant responses involved in immune cell activation and recruitment[121]. $G_{i2}$ knockout mice develop colitis and colorectal cancer due to an increase in $T_H1$ type cytokines such as IL-12, which is constitutively repressed by $G_{i2}$ signaling[27,122,123]. Interestingly, we found that CD97 is a high affinity recruiter of $G_{i2}$. As discussed in chapter 1 the overexpression of CD97 attenuated experimentally induced colitis[71]. Therefore, CD97 signaling through $G_{i2}$ likely reduces inflammatory mediators such as IL-12 associated with the development of colitis. $G_{\beta\gamma}$, which mainly comes from the activation of $G_{i/o}$ G-proteins, can activate PI3K/Protein kinase B (AKT) and inhibit Glycogen synthase kinase 3β (GSK-3β) which stabilizes β-catenin for incorporation into adherens junctions[27,124,125]. CD97 overexpression was shown to protect against colitis by increasing the density of colonic adherens junctions through activation of PI3K/AKT and inhibition of GSK-3β [71]. CD97 has been shown to bind β-catenin through its PDZ domain[126]. Therefore, the sequestering of β-catenin at the membrane by CD97 may be the result of its $G_i$ mediated stabilization of β-catenin which then binds CD97 to remain membrane localized for incorporation in adherens junctions. By determining the signaling partners of CD97 we may have been able to better explain its function in regulating intestinal barrier permeability. The ability of CD97 to dose dependently recruit $G_{oA}$, and $G_{oB}$ is surprising as the receptor is not reported to be expressed in neurons or neuroendocrine cells[50]. However, CD97 is involved in glioblastoma, a brain cancer of the neuronal immune cell astrocytes[53]. Therefore, our results suggest a possible yet undetermined function of CD97 in the CNS. It is not surprising that CD97 is a high affinity recruiter of $G_z$, as this G-protein is expressed in hematopoietic cells and likely contributes to its function in regulating immune cell responses[27,28]. The ability of CD97 to dose-dependently recruit $G_{gustducin}$ is quite interesting. This would suggest a possible role for CD97 in nutrient sensing in the gastrointestinal tract, as the receptor is not known to be expressed in the tongue but is

expressed in the stomach and intestinal resorptive, goblet, Paneth, and enteroendocrine cells[50,69,127].

As the $EC_{50}$ of $G_{sL(Long)}$ ($EC_{50}$=250.0nM), and $G_{sS(short)}$ ($EC_{50}$=568.8nM) recruitment by CD97 was quite high and the magnitude of the responses was small and variable we conclude that CD97 likely doesn't couple to the $G_s$ family of G-proteins (Fig 13). Our data is supported by the fact that yeast cells expressing $G_s$ and CD97 without its N-terminal fragment grew no differently than cells expressing full-length receptors[119].

### 3.2.3 EMR2 activation results in the recruitment of β-arrestin and a variety of G-proteins

By creating a chimeric trypsin activated PAR2-EMR2 receptor, where the first 36 amino acids of PAR2 were fused to the C-terminal fragment of EMR2, we were able to study the recruitment of 16 effector proteins from the 5 major signaling pathways downstream of GPCRs. As shown in figure 14 EMR2 dose-dependently recruited both β-arrestin 1 ($EC_{50}$=44.35nM) and 2 ($EC_{50}$=28.90nM). We are the first to show the dose-dependent interaction of EMR2 with β-arrestins.

EMR2 dose-dependently recruited $G_{12}$ ($EC_{50}$=92.01nM) and $G_{13}$ ($EC_{50}$=162.8nM) (Fig 14). Our results are in keeping with studies in yeast cells where expressing $G_{12/13}$ and EMR2 without its N-terminal fragment resulted in more growth than cell expressing full-length receptor[119]. EMR2 $G_{12/13}$ signaling is likely involved in its role in cell migration and metastasis in various cancers[53]. $G_{12/13}$ signaling is also likely involved in its role in neutrophil migration, degranulation, and cytokine secretion[50,80,81].

As shown in figure 14 EMR2 dose-dependently recruited $G_q$ ($EC_{50}$=209.8nM), $G_{11}$ ($EC_{50}$=95.71nM) and $G_{15}$ ($EC_{50}$=185.4nM). Yeast cells expressing $G_q$, $G_{14}$, and $G_{16}$ and EMR2 without its N-terminal fragment grew more than cells expressing full-length receptor[119]. Our data supports EMR2 recruitment of $G_q$, $G_{11}$, and $G_{15}$, and we are the first to show the dose-dependent recruitment of these G-proteins. Unfortunately, we did not have a $G_{14}$ BRET sensor, therefore future studies will have to be done to support their data[101]. As mentioned in the introductory chapter, $G_{16}$ is the human homolog of the murine G-protein $G_{15}$, therefore it is not surprising EMR2 can couple to both G

proteins[27,28]. EMR2 was previously shown to couple to $G_{16}$, where its signaling was found to be important for macrophage differentiation and proinflammatory responses[128]. Therefore, EMR2 coupling to the $G_{q/11}$ family of G-protein likely contributes to its role in regulating immune cell functions such as macrophage differentiation and proinflammatory responses, and neutrophil migration, degranulation, and cytokine secretion[50,80,81,128].

EMR2 dose-dependently recruited $G_{i1}$ ($EC_{50}$=79.28nM), $G_{i2}$ ($EC_{50}$=115.4nM), $G_{i3}$ ($EC_{50}$=123.9nM), $G_{oA}$ ($EC_{50}$=75.90nM), $G_{oB}$ ($EC_{50}$=144.9nM), $G_z$ ($EC_{50}$=249.5nM) and $G_{gustducin}$ ($EC_{50}$=100.9nM) (Fig 14). Our data are consistent with results from the study showing that yeast cells expressing $G_{i1}$, $G_{i3}$, $G_o$, and $G_z$ and EMR2 without its N-terminal fragment grew more than full-length receptor expressing cells[119]. However, we are the first to show EMR2 coupling to $G_{i2}$, both $G_{oA}$ and $G_{oB}$, and $G_{gustducin}$, as well as the dose-dependent coupling of EMR2 to the $G_{i/o}$ family of G-proteins. EMR2 coupling to $G_{i1-3}$ and $G_z$ likely contribute to its roles in macrophage differentiation and proinflammatory responses, as well as neutrophil migration, degranulation, and cytokine secretion[50,80,81,128]. Similar to CD97, the ability for EMR2 to couple with $G_{oA}$ and $G_{oB}$ is odd as the receptor is not known to be expressed in neurons or neuroendocrine cells[50]. However, EMR2 is also reported to be involved in glioblastoma, a brain cancer of the neuronal immune cell astrocytes[53]. Therefore, our results suggest a possible yet undetermined function of EMR2 in the CNS. The ability of EMR2 to dose-dependently recruit $G_{gustducin}$ is odd considering that the receptor is not known to be expressed in the tongue or in nutrient sensing cells of the gastrointestinal tract[50,127]. Therefore, our results may suggest a possible yet undiscovered role for EMR2 in the gustatory system.

As shown in figure 14 EMR2 dose-dependently recruited $G_{sL(Long)}$ ($EC_{50}$=155.6nM), and $G_{sS(short)}$ ($EC_{50}$=74.45nM). Our data is supported by the fact that yeast cell expressing $G_s$ and EMR2 without its N-terminal fragment grew more than cells expressing full-length receptor[119]. The ability of EMR2 to couple to both the $G_{i/o}$ and $G_s$ families of G-proteins at first may seem odd. However, many other well studied receptors, such as the β2 adrenergic, histamine, serotonin, and glucagon receptors, have been shown to couple to both the $G_{i/o}$ and $G_s$ families of G-proteins[129]. Further, another aGPCR, GPR98

(ADGRV1) can couple to both the $G_{i/o}$ and $G_s$ families of G-proteins[53,130,131]. However, the role of EMR2 $G_s$ coupling remains a mystery as this signaling would likely antagonize many of its known functions in immune cells[50,80,81,128]. Therefore, future experiments will need to be done to determine the relevance of EMR2 $G_s$ signaling.

### 3.2.4    GPR56 activation results in the recruitment of β-arrestin and a variety of G-proteins

By creating a chimeric trypsin activated PAR2-GPR56 receptor, where the first 36 amino acids of PAR2 were fused to the C-terminal fragment of GPR56, we were able to study the recruitment of 16 effector proteins from the 5 major signaling pathways downstream of GPCRs. As shown in figure 15 GPR56 dose-dependently recruited both β-arrestin 1 ($EC_{50}$=25.00nM) and 2 ($EC_{50}$=24.41nM). The interaction of GPR56 with β-arrestin 2 was previously shown using co-immunoprecipitation with GPR56 with and without its N-terminal fragment[62]. These researchers also showed that although removal of the GPR56 stalk region did decrease the interaction of β-arrestin 2 with GPR56, it was still significantly higher than levels seen with the full-length receptor[62]. Therefore, the recruitment of β-arrestin 2 to GPR56 seems to be the result of not only tethered ligand binding but also receptor conformational change[62]. Our data supports GPR56 recruitment of β-arrestin 2, and we are also the first to show the dose-dependent recruitment of β-arrestin 1 and 2.

GPR56 dose-dependently recruited both $G_{12}$ ($EC_{50}$=59.14nM), and $G_{13}$ ($EC_{50}$=78.16nM) (Fig 15). The ability of GPR56 to dose-dependently couple to $G_{12/13}$ has been previous documented[58,59,62]. Using the tethered ligand mimicking peptide TYFAVLM-NH$_2$, Stoveken et al showed that GPR56 dose-dependently activated $G_{13}$. They did so by measuring the rate of exchange of GDP for GTPγS, a non-degradable form GTP, on $G_{13}$[59]. Using the SRE reporter gene assay, Kishore et al showed that GPR56 without its N-terminal fragment produced significantly higher SRE luminescence than cells expressing full-length receptor. They also showed that this increase in SRE luminescence was tethered ligand dependent, as removal of the GPR56 stalk region abolished this signal[62]. However, it should be noted that activation of the SRE reporter gene could also come from activation of the $G_{q/11}$ family of G-proteins[27]. Our data supports GPR56

coupling to $G_{12/13}$, and we also for the first time show the dose-dependent coupling of GPR56 to $G_{12}$. GPR56 coupling to $G_{12/13}$ is likely involved in its metastatic role in various cancers, such as colorectal, melanoma and prostate[53]. $G_{12/13}$ signaling is also likely involved in the role GPR56 plays in platelet activation and immune cell compartmentalization[58,87]. Finally, GPR56 $G_{12/13}$ signaling is also likely involved in its role in the development of the cerebral cortex, where it guides the migration of newly formed neurons to their proper location on the pial membrane[82,83,85].

As shown in figure 15 GPR56 dose-dependently recruited $G_q$ ($EC_{50}$=85.33nM), $G_{11}$ ($EC_{50}$=65.99nM) and $G_{15}$ ($EC_{50}$=17.79nM). The association of GPR56 with $G_{q/11}$ has been previously shown using co-immunoprecipitation and mass spectroscopy[132]. In this study, Little et al showed that the interaction of GPR56 with $G_{q/11}$ was stabilized in a molecular scaffold by the tetraspanins proteins CD9 and CD81. Our data supports the coupling of GPR56 to $G_q$ and $G_{11}$, and we are the first to show the dose-dependent recruitment of these G-proteins. Interestingly, we also show that GPR56 is a high affinity recruiter of $G_{15}$. As mentioned in chapter 1 $G_{15}$ shows expression restricted to hematopoietic cells[27,28]. GPR56 has been shown to be important for platelet activation[58]. As $G_{q/11}$ signaling is important for the activation of platelets it is not surprising GPR56 would signal through $G_q$, $G_{11}$, and the hematopoietic cell restricted G-protein $G_{15}$[27,28,58,113]. However, when Yeung et al applied the GPR56 tethered ligand mimicking peptide TYFAVLM-$NH_2$ to platelets they were not able to see an increase in intracellular $Ca^{2+}$. This may be explained by work done by Kishore et al, where they showed GPR56 receptors without its N-terminal fragment and without its stalk region both had significantly higher NFAT reporter gene luminescence than full-length receptors. This suggests that GPR56 $G_{q/11}$ signaling is mediated by a receptor conformational change explaining why Yeung et al did not see an increase in intracellular $Ca^{2+}$ with TYFAVLM-$NH_2$[62].

GPR56 dose-dependently recruited $G_{i1}$ ($EC_{50}$=148.5nM), $G_{i3}$ ($EC_{50}$=151.5nM), $G_{oA}$ ($EC_{50}$=47.23nM), and $G_{oB}$ ($EC_{50}$=69.99nM) (Fig 15). As the $EC_{50}$'s of $G_{i2}$ ($EC_{50}$=841.5nM), $G_z$ ($EC_{50}$=892.0nM) and $G_{gustducin}$ ($EC_{50}$=702.3nM) were high and response were small and variable we conclude that GPR56 likely does not couple to these

G-proteins (Fig 15). The coupling of GPR56 to the $G_{i/o}$ family of G-proteins was recently shown by Yeung et al. The GPR56 tethered ligand mimicking peptide TYFAVLM-NH$_2$ was able to decrease forskolin elevated levels of cAMP in platelets[58]. GPR56 coupling to $G_{i/o}$ in platelets is consistent with its role in platelet activation[58]. Our data supports GPR56 coupling to $G_{i1}$ and $G_{i3}$, and these G-proteins likely contribute to its role in platelet activation[27,58,113]. We are the first to show GPR56 coupling to $G_{oA}$ and $G_{oB}$, and this coupling is consistent with its role in brain development and expression in oligodendrocytes, gilia cells, microglia, and neural progenitor cells[50,82,83,85].

As shown in figure 15 GPR56 dose-dependently recruited $G_{sL(Long)}$ ($EC_{50}=52.52nM$), and $G_{sS(short)}$ ($EC_{50}=49.84nM$). We are the first to report the coupling of GPR56 to the $G_s$ family of G-proteins. The coupling of GPR56 to $G_s$ is curious as it would seem to antagonize its $G_i$ signaling in platelet activation[27,58,113]. However, as mentioned in the discussion of EMR2 other receptors do display this signaling phenomenon and future studies will need to be done to determine the functional role of GPR56 $G_s$ signaling[119,129–131].

## 3.2.5 BAI1 activation results in the recruitment of β-arrestin and a variety of G-proteins

By creating a chimeric trypsin activated PAR2-BAI1 receptor, where the first 36 amino acids of PAR2 were fused to the C-terminal fragment of BAI1, we were able to study the recruitment of 16 effector proteins from the 5 major signaling pathways downstream of GPCRs. As shown in figure 16 BAI1 dose-dependently recruited both β-arrestin 1 ($EC_{50}=37.42nM$) and 2 ($EC_{50}=25.72nM$). The interaction of BAI1 with β-arrestin 2 has been previously shown using co-immunoprecipitation of BAI1 with and without its N-terminal fragment[62]. These researchers also showed that removal of the BAI1 stalk region did not decrease its interaction with β-arrestin 2[62]. Therefore, the interaction of BAI1 with β-arrestin 2 seems to be the result of a receptor conformational change and not the binding of its tethered ligand[62]. Our data supports the coupling of BAI1 with β-arrestin 2, and we are the first to show the dose dependent coupling to β-arrestin 1 and 2.

BAI1 dose-dependently recruited $G_{12}$ ($EC_{50}$=73.79nM), and $G_{13}$ ($EC_{50}$=39.60nM) (Fig 16). The interaction of BAI1 with $G_{12/13}$ has been previously shown. BAI1 receptors without their N-terminal fragment had increased RhoA activity and SRE reporter gene luminescence compared to cells expressing full-length receptor[62,133]. Kishore et al also showed that removal of the BAI1 stalk region did not decrease SRE reporter gene luminescence. Therefore, the interaction of BAI1 with $G_{12/13}$ seems to be the result of a receptor conformational change and not the binding of its tethered ligand[62]. Kishore et al also showed the direct interaction of BAI1 with $G_{13}$ by immunoprecipitation[62]. Our data supports the coupling of BAI1 to $G_{12/13}$ and we are the first to show the dose-dependent recruitment of these G-proteins. BAI1 $G_{12/13}$ is likely involved in its roles in regulating macrophage phagocytosis of bacterial and apoptotic cells, myoblast fusion in muscle fibers, and synaptogenesis[89–92,133].

As shown in figure 16 BAI1 dose-dependently recruited $G_q$ ($EC_{50}$=179.4nM), $G_{11}$ ($EC_{50}$=50.66nM), and $G_{15}$ ($EC_{50}$=164.3nM). The interaction of BAI1 with $G_{q/11}$ has been inferred, as BAI1 receptors without their N-terminal fragment had increased NFAT reporter gene luminescence than cells expressing full-length receptor[62]. However, it should be noted that activation of the NFAT receptor gene can also occur through activation of the $G_{12/13}$ family of G-proteins[27]. Kishore et. al., also showed that removal of the BAI1 stalk region did not decrease NFAT reporter gene luminescence. Therefore, the interaction of BAI1 with $G_{q/11}$ seems to be the result of a receptor conformational change and not the binding of its tethered ligand[62]. Our data supports the coupling of BAI1 to $G_{q/11}$, and we are the first to show the dose-dependent interaction of BAI1 with $G_q$, $G_{11}$, and $G_{15}$. BAI1 $G_{q/11}$ signaling is likely involved in its roles in regulating macrophage phagocytosis of bacterial and apoptotic cells, myoblast fusion in muscle fibers and synaptogenesis[89–92,133].

BAI1 dose-dependently recruited $G_{i1}$ ($EC_{50}$=44.33nM), $G_{i2}$ ($EC_{50}$=82.13nM), $G_{i3}$ ($EC_{50}$=48.37nM), $G_{oA}$ ($EC_{50}$=33.26nM), $G_{oB}$ ($EC_{50}$=47.93nM), $G_z$ ($EC_{50}$=91.97nM), and $G_{gustducin}$ ($EC_{50}$=109.5nM) (Fig 16). We are the first to show the interaction of BAI1 with the $G_{i/o}$ family of G-proteins. BAI1 $G_i$ signaling is likely involved in its roles in regulating macrophage phagocytosis of bacterial and apoptotic cells, myoblast fusion in

muscle fibers, and synaptogenesis[89–92,133]. BAI1 recruitment of $G_{oA}$ and $G_{oB}$ is not surprising as it is expressed in astrocytes, microglia, and neurons[50]. The ability of BAI1 to dose-dependently recruit $G_{gustducin}$ is odd considering that the receptor is not known to be expressed in the tongue or in nutrient sensing cells of the gastrointestinal tract[50,127]. Therefore, our results may suggest a possible yet undiscovered role for BAI1 in the gustatory system.

As shown in figure 16 BAI1 dose-dependently recruited $G_{sL(Long)}$ ($EC_{50}$=178.2nM), and $G_{sS(short)}$ ($EC_{50}$=83.11nM). We are the first to report the interaction of BAI1 with the $G_s$ family of G-proteins. The coupling of BAI1 to $G_s$ is curious as it would seem to antagonize its $G_i$ signaling in macrophage phagocytosis of bacterial and apoptotic cells, myoblast fusion in muscle fibers and synaptogenesis[89–92,133]. However, as mentioned in the discussion of EMR2 and GPR56 other receptors do display this signaling phenomenon and future studies will need to be done to determine the functional role of BAI1 $G_s$ signaling[119,129–131].

## 3.2.6    Utility of PAR2-aGPCR chimeric receptors

Overall, our results support the idea that our PAR2-aGPCR chimeric receptors can be more broadly used to study the signaling and function of all members of the aGPCR family. By analyzing studies done on trypsin and thrombin cleavage site specificities we were able to predict that the C-terminal fragments of aGPCRs could be unmasked by proteolytic cleavage[108,111]. By fusing the first 36 amino acids of PAR2 to the C-terminal fragment of aGPCRs, the receptors could be time dependently activated by increasing concentrations of trypsin. We tested this hypothesis by creating PAR2-CD97, EMR2, GPR56, and BAI1 chimeric receptors, where 3/4 of these receptors had unique trypsin cleavage sites. We are confident that our four PAR2-aGPCR chimeric receptors were all effectively cleaved by trypsin as they dose dependently recruited a variety of effector proteins. With the lack of synthetic agonists and tools for activating aGPCRs with their natural mechanism of action, our chimeric receptors represent an exciting new method for studying aGPCR signaling and function.

### 3.2.7 SSFAILMAH-NH$_2$ is a potent CD97 activating tethered ligand mimicking peptide

We first validated that the TANGO assay would be a useful screening assay for our lab's purposes. As we were planning on using the assay for testing potential tethered ligand mimicking peptides, we validated the assay by using the well-studied PAR2 tethered ligand mimicking peptide SLIGRL-NH$_2$. As shown in figure 17 SLIGRL-NH$_2$ dose dependently activated PAR2 with a similar EC50 (11.1μM) for β-arrestin 2 recruitment as we have previously reported[100]. Now confident the TANGO assay was an effective screening tool we tested our predicted CD97 activating peptide SSFAILMAH-NH$_2$. As shown in figure 17 SSFAILMAH-NH$_2$ dose dependently activated CD97 with an EC$_{50}$ of 17.28μM. As mentioned in chapter 2, our PAR2-aGPCR chimeric receptors are more ideal screening tools than full-length receptors as they eliminate the uncontrollable N-terminal fragment removal that can occur through regular cellular processes. Therefore, we next used our PAR2-CD97 chimeric receptor to test the ability of SSFAILMAH-NH$_2$ to activate CD97 using the BRET1 assay. As shown in the lower two graphs of figure 17 SSFAILMAH-NH$_2$ was able to cause the dose dependent recruitment of both β-arrestin 1 (EC$_{50}$=22.86μM) and 2 (EC$_{50}$=78.29μM). As the TANGO assay measures β-arrestin 2 recruitment it might seem odd at first that the EC$_{50}$'s of SSFAILMAH-NH$_2$ are different between the TANGO and BRET1 assays but are similar between the two assays for SLIGRL-NH$_2$. However, the TANGO receptor constructs have the tail of the vasopressin receptor 2 to boost β-arrestin recruitment[102,103,106]. Therefore, it would be expected that the TANGO assay would underestimate the EC$_{50}$ of β-arrestin 2 recruitment for receptors, explaining our results for SSFAILMAH-NH$_2$. However, as the PAR receptors are very strong recruiters of β-arrestin this may explain why the EC$_{50}$ of SLIGRL-NH$_2$ β-arrestin 2 recruitment are similar between the two assays. Therefore, both our TANGO assay and BRET1 assay data support that SSFAILMAH-NH$_2$ is a potent CD97 activating tethered ligand mimicking peptide. It also supports that our method for predicting aGPCR tethered ligand mimicking peptides is quite effective, as we were able to predict a very potent CD97 activating peptide on our first attempt. SSFAILMAH-NH$_2$ is now the second most potent tethered ligand mimicking peptide to be reported[59–61,93,94,134].

## 3.2.8    Future experiments

As validating our PAR2-aGPCR chimeric receptor design has been such a success, it opens the door to many years of future study. First, we plan to support the results of our G-protein recruitment data by preforming three second messenger-based assays. As all four of our chimeric receptors dose dependently recruited the $G_{q/11}$ family of G-proteins we plan to use a fluorescence based $Ca^{2+}$ assay to support our observations, as we have done previously[96]. To support our observation that all four chimeric receptors recruited the $G_{i/o}$ family of G-proteins we plan to use the GLO-sensor assay with forskolin to pre-elevate cAMP levels to block the effects of $G_s$[135]. If our observations are correct, then trypsin treatment of our chimeric receptors should be able to elicit a concentration dependent decrease in the rate of cAMP production. We plan to use a similar approach to show that EMR2, GPR56, BAI1 can recruit the $G_s$ family of G-proteins. However, we will use pertussis toxin to inhibit $G_i$ and see if our chimeric receptors can dose dependently increase the rate of cAMP production[135]. The final second messenger assay we plan to do is measuring the activation of ERK/MAPK, as we have done previously[100]. We plan to measure the ability of our chimeric receptors to dose dependently increase the amount of phosphorylated ERK using western blots[100].

Another exciting project we plan on pursuing is the study of aGPCR internalization. As control of receptor activation has been difficult to achieve, little study has been done on aGPCR internalization. Having this future project in mind when designing our chimeric receptors, we added restriction enzyme cut sites to put in an N-terminal red fluorescent protein (RFP) tag. Therefore, by using receptors N-terminally tagged with RFP and C-terminally tagged with YFP we can specifically track receptors being activated by our trypsin treatment through the different stages of their internalization pathway. Further, this N-terminal RFP tag on our chimeric receptors can also be used as another way of proving they are being properly cleaved by trypsin. As the activation of aGPCRs is irreversible, similar to the PARs, we would expect them to traffic in a similar manner. PARs are known to traffic almost exclusively to the lysosomes for degradation and not back to the membrane for further rounds of activation[136]. Therefore, we would hypothesize that aGPCRs would follow a similar internal trafficking pathway.

An ongoing interest of our lab is to understand where and how β-arrestin interacts with tethered ligand activated receptors. In the past we have determined important PAR2 and PAR4 β-arrestin interacting residues through the mutation of predicted phosphorylation sites and interactions predicted by molecular modeling[97,100]. We plan to use a similar approach to attempt to determine important β-arrestin interacting residues in CD97, EMR2, GPR56, and BAI1 by using our chimeric receptors.

Our lab is also interested in identifying the exact residues forming the tethered ligands of aGPCRs[96]. Therefore, we plan on doing a series of mutations to the stalk regions of our PAR2-CD97, EMR2, GPR56, and BAI1 chimeric receptors to determine the sequence of these receptors tethered ligands. In a recent book chapter (Mirka and Ramachandran, In press) we were able to predict a number of conserved molecular switches involved in aGPCR activation, which were determined through analysis of the recently solved structure of GPR97[65]. In brief, the toggle switch residue $W^{6.48}$ was found to serve a similar function as $W^{6.53}$ and is conversed in 31/33 aGPCRs[65]. The PIF motif was found to be replaced with a $F^{3.44}M^{3.47}xW^{6.53}$ upper quaternary core motif that was found to serve an important role in aGPCR activation[65]. The D(E)RY motif was found to be replaced with a $H^{3.53}L^{3.54}Y^{3.55}$ motif that was also found to serve an important role in aGPCR activation[65]. However, mutational studies testing the importance of these residues in receptor activation have only been done on GPR97 and GPR126, two members of the G subfamily[65]. Therefore, we plan to perform similar mutations on members of the E subfamily CD97 and EMR2, on GPR56 which is a member of the G subfamily, and on BAI1 which is a member of the B subfamily using our chimeric receptors. These mutational studies will show whether these conserved residues have important functions in aGPCR activation in general or if their importance is restricted to the G subfamily.

Our work here with four aGPCRs also provides guidance for creating the full panel of 33 trypsin activated PAR2-aGPCR chimeric receptors. We hope to develop this as an open-source platform of constructs that us and other labs can use to study aGPCR signaling and function. This panel of constructs will also be useful for future small molecule library drug screens. This is because full length aGPCRs can be activated by uncontrollable cellular processes, which could cause a lot of false positives in drug screening. Unlike

full length aGPCRs our chimeric receptors can only be activated by trypsin mediated proteolytic cleavage, therefore removing this uncontrollable error.

The polycystin family of receptors share a similar structure and mechanism of action to aGPCRs[137]. The receptors are autoproteolytically cleaved during biosynthesis into N-terminal and C-terminal fragments, which remain non covalently associated through the interaction of the β-13 strand with the GAIN domain[137]. As they share a similar structure and mechanism of action this family of 5 atypical GPCRs are also difficult to study[137]. Therefore, another future application of our approach could be to make PAR2-polycystin chimeric receptors to study the signaling and function of this receptor family.

In the future we plan to use our CD97 tethered ligand mimicking peptide SSFAILMAH-NH$_2$ in the same G-protein recruitment and second messenger assays to support our results with trypsin activation. The use of the peptide will also allow us to determine which signaling pathways are tethered ligand dependent and which ones may instead be due to a receptor conformational change.

We also plan on using our method of predicting tethered ligand mimicking peptides to create agonists for other receptors, such as BAI1 and EMR2. Similar to GPR56 and CD97, BAI1 does not have any predicted turn elements in its stalk region (Fig 9). Therefore, a peptide corresponding to the first 9 amino acids of the BAI1 stalk region, STFAILAQL-NH$_2$, could be the sequence of a future BAI1 tethered ligand mimicking peptide. EMR2 does have a predicted turn element in its stalk region and would therefore likely require a longer peptide, SSFAILMAHYDVQEED-NH$_2$, which includes this turn element.

The use of our PAR2-aGPCR chimeric receptors in in-vitro and in-vivo studies are limited by the fact that PAR1 and PAR2 are also activated by trypsin and must therefore be either inhibited or knocked out[48]. However, as long as our tethered ligand mimicking peptides do not cross react with other aGPCRs they can be used in functional in-vitro and in-vivo studies. The tethered ligand mimicking peptides of receptors in the same subfamily have been shown to cross react[60]. Therefore, we plan to use the TANGO assay

to screen SSFAILMAH-NH$_2$, TYFAVLM-NH$_2$, and our future BAI1 and EMR2 tethered ligand mimicking peptides against all 33 aGPCRs to test for specificity.

Another project we plan on pursuing in the near future is the development of aGPCR antagonists. Due to the difficulty of studying tethered ligand activated receptors, a class of compounds known as pepducins were designed to help study the PARs[138–140]. Pepducins are intracellular targeting palmitoylated peptides derived from a receptors intracellular loops or transmembrane domains[138–140]. By mimicking the intracellular domains of a receptor, they are able to bind and stabilize the inactive state[138–140]. Although pepducins were originally developed to study the PARs, they have since been used to study many GPCRs[138–140]. Therefore, in the future we plan on making pepducins to study the signaling and function of our four aGPCRs of interest.

### 3.2.9    Limitations

The PAR2-aGPCR chimeric receptors have enabled us to study receptor proximal signaling events for four different adhesion GPCRs for the first time. There are however some limitations to our approach. Firstly, several concentration effect curves do not saturate, limiting our ability to quantitatively compare coupling of the different signaling pathways. We used up to 300nM trypsin as concentrations higher than this cause non-specific responses due to the lifting and proteolytic lysis of cells[141] and can result in activation of PAR1. Nevertheless, these constructs will enable us to develop additional pharmacological tools targeting each receptor that will allow such quantitative assessment.

The main limitation of aGPCR tethered ligand mimicking peptides is their solubility, and SSFAILMAH-NH$_2$ is no exception[59–61,93,94]. Due to the cytotoxic effects of DMSO it is recommended to limit its concentration to less than 0.1% in most cellular assays[142]. However, most aGPCR tethered ligand mimicking peptides require at least 3-5% DMSO to remain soluble in solution[59–61,93,94]. Therefore, in the future we plan to optimize the sequence of SSFAILMAH-NH$_2$, TYFALM-NH$_2$, and our future BAI1 and EMR2 tethered ligand mimicking peptides to improve their solubility and activity. Recently the GPR64 tethered ligand mimicking peptide, TSFGILLDLSRTSLP-NH$_2$, was optimized to

improve its activity 170-fold[134]. The only changes made were substitution of the first residue, T to V, and the third residue, F to Phe(4-Me)[134]. Although these modification did not improve the solubility of the peptide, they did drastically improve its activity from the high to low µM range[134]. Therefore, when optimizing our peptides, we will keep these modifications in mind. When designing the tethered ligand mimicking peptides for the PARs it was found that peptides mimicking the murine tethered ligand were more potent than ones mimicking the human sequence[48]. However, no one has tried mimicking the murine tethered ligand sequence when generating aGPCR tethered ligand mimicking peptides. Therefore, in the future when optimizing our tethered ligand mimicking peptides, we will test if mimicking the murine sequence improves activity.

# References

1.      Heldin C-H, Lu B, Evans R, Gutkind JS. Signals and Receptors. *Cold Spring Harb Perspect Biol*. 2016;8(4). doi:10.1101/cshperspect.a005900

2.      Cooper GM. *The Cell: A Molecular Approach*. 2. ed. ASM Press [u.a.]; 2000.

3.      Klezovitch O, Vasioukhin V. Cadherin signaling: keeping cells in touch. *F1000Research*. 2015;4:550. doi:10.12688/f1000research.6445.1

4.      Perrais M, Chen X, Perez-Moreno M, Gumbiner BM. E-Cadherin Homophilic Ligation Inhibits Cell Growth and Epidermal Growth Factor Receptor Signaling Independently of Other Cell Interactions. Schwarzbauer J, ed. *Mol Biol Cell*. 2007;18(6):2013-2025. doi:10.1091/mbc.e06-04-0348

5.      Long M, Adler AJ. Cutting Edge: Paracrine, but Not Autocrine, IL-2 Signaling Is Sustained during Early Antiviral CD4 T Cell Response. *J Immunol*. 2006;177(7):4257-4261. doi:10.4049/jimmunol.177.7.4257

6.      Santo S, Widmer H. Paracrine factors for neurodegenerative disorders: special emphasis on Parkinson′s disease. *Neural Regen Res*. 2016;11(4):570. doi:10.4103/1673-5374.180739

7.      Goel R, Raju R. A Signaling Network of Thyroid-Stimulating Hormone. *J Proteomics Bioinform*. 2011;04(10). doi:10.4172/jpb.1000195

8.      Vhora I, Patil S, Bhatt P, Gandhi R, Baradia D, Misra A. Receptor-targeted drug delivery: current perspective and challenges. *Ther Deliv*. 2014;5(9):1007-1024. doi:10.4155/tde.14.63

9.      Purves D, Williams SM, eds. *Neuroscience*. 2nd ed. Sinauer Associates; 2001.

10.     Alexander S, Mathie A, Peters J. LIGAND-GATED ION CHANNELS: Ligand-gated ion channels. *Br J Pharmacol*. 2011;164:S115-S135. doi:10.1111/j.1476-5381.2011.01649_4.x

11.      Siegel GJ, ed. *Basic Neurochemistry: Molecular, Cellular, and Medical Aspects*. 6th ed. Lippincott Williams & Wilkins; 1999.

12.      Alberts B, ed. *Molecular Biology of the Cell*. 4th ed. Garland Science; 2002.

13.      De Meyts P. The Insulin Receptor and Its Signal Transduction Network. In: Feingold KR, Anawalt B, Boyce A, et al., eds. *Endotext*. MDText.com, Inc.; 2000. Accessed August 19, 2021. http://www.ncbi.nlm.nih.gov/books/NBK378978/

14.      Fuentes N, Silveyra P. Estrogen receptor signaling mechanisms. In: *Advances in Protein Chemistry and Structural Biology*. Vol 116. Elsevier; 2019:135-170. doi:10.1016/bs.apcsb.2019.01.001

15.      Fredriksson R, Schiöth HB. The Repertoire of G-Protein–Coupled Receptors in Fully Sequenced Genomes. *Mol Pharmacol*. 2005;67(5):1414-1425. doi:10.1124/mol.104.009001

16.      Lagerström MC, Schiöth HB. Structural diversity of G protein-coupled receptors and significance for drug discovery. *Nat Rev Drug Discov*. 2008;7(4):339-357. doi:10.1038/nrd2518

17.      Bockaert J. Molecular tinkering of G protein-coupled receptors: an evolutionary success. *EMBO J*. 1999;18(7):1723-1729. doi:10.1093/emboj/18.7.1723

18.      Sriram K, Insel PA. G Protein-Coupled Receptors as Targets for Approved Drugs: How Many Targets and How Many Drugs? *Mol Pharmacol*. 2018;93(4):251-258. doi:10.1124/mol.117.111062

19.      Hille B. G protein-coupled receptor. *Scholarpedia*. 2009;4(12):8214. doi:10.4249/scholarpedia.8214

20.      Hilger D, Masureel M, Kobilka BK. Structure and dynamics of GPCR signaling complexes. *Nat Struct Mol Biol*. 2018;25(1):4-12. doi:10.1038/s41594-017-0011-7

21.    Thal DM, Glukhova A, Sexton PM, Christopoulos A. Structural insights into G-protein-coupled receptor allostery. *Nature*. 2018;559(7712):45-53. doi:10.1038/s41586-018-0259-z

22.    Weis WI, Kobilka BK. The Molecular Basis of G Protein–Coupled Receptor Activation. *Annu Rev Biochem*. 2018;87(1):897-919. doi:10.1146/annurev-biochem-060614-033910

23.    Latorraca NR, Venkatakrishnan AJ, Dror RO. GPCR Dynamics: Structures in Motion. *Chem Rev*. 2017;117(1):139-155. doi:10.1021/acs.chemrev.6b00177

24.    Trzaskowski B, Latek D, Yuan S, Ghoshdastider U, Debinski A, Filipek S. Action of Molecular Switches in GPCRs - Theoretical and Experimental Studies. *Curr Med Chem*. 2012;19(8):1090-1109. doi:10.2174/092986712799320556

25.    Wacker D, Stevens RC, Roth BL. How Ligands Illuminate GPCR Molecular Pharmacology. *Cell*. 2017;170(3):414-427. doi:10.1016/j.cell.2017.07.009

26.    Ballesteros JA, Weinstein H. Integrated methods for the construction of three-dimensional models and computational probing of structure-function relations in G protein-coupled receptors. In: Sealfon SC, ed. *Methods in Neurosciences*. Vol 25. Receptor Molecular Biology. Academic Press; 1995:366-428. doi:10.1016/S1043-9471(05)80049-7

27.    Wettschureck N, Offermanns S. Mammalian G Proteins and Their Cell Type Specific Functions. *Physiol Rev*. 2005;85(4):1159-1204. doi:10.1152/physrev.00003.2005

28.    Syrovatkina V, Alegre KO, Dey R, Huang X-Y. Regulation, Signaling, and Physiological Functions of G-Proteins. *J Mol Biol*. 2016;428(19):3850-3868. doi:10.1016/j.jmb.2016.08.002

29.    van Gastel J, Hendrickx JO, Leysen H, et al. β-Arrestin Based Receptor Signaling Paradigms: Potential Therapeutic Targets for Complex Age-Related Disorders. *Front Pharmacol*. 2018;9:1369. doi:10.3389/fphar.2018.01369

30.     Gurevich VV, Gurevich EV. GPCR Signaling Regulation: The Role of GRKs and Arrestins. *Front Pharmacol*. 2019;10:125. doi:10.3389/fphar.2019.00125

31.     Cheng Z, Garvin D, Paguio A, Stecha P, Wood K, Fan F. Luciferase Reporter Assay System for Deciphering GPCR Pathways. *Curr Chem Genomics*. 2010;4:84-91. doi:10.2174/1875397301004010084

32.     Suzuki N, Hajicek N, Kozasa T. Regulation and Physiological Functions of G12/13-Mediated Signaling Pathways. *Neurosignals*. 2009;17(1):55-70. doi:10.1159/000186690

33.     Pierce KL, Lefkowitz RJ. Classical and new roles of β-arrestins in the regulation of G-PROTEIN-COUPLED receptors. *Nat Rev Neurosci*. 2001;2(10):727-733. doi:10.1038/35094577

34.     Luttrell LM, Lefkowitz RJ. The role of β-arrestins in the termination and transduction of G-protein-coupled receptor signals. *J Cell Sci*. 2002;115(3):455-465. doi:10.1242/jcs.115.3.455

35.     Rosenbaum DM, Rasmussen SGF, Kobilka BK. The structure and function of G-protein-coupled receptors. *Nature*. 2009;459(7245):356-363. doi:10.1038/nature08144

36.     Garelja ML, Au M, Brimble MA, et al. Molecular Mechanisms of Class B GPCR Activation: Insights from Adrenomedullin Receptors. *ACS Pharmacol Transl Sci*. 2020;3(2):246-262. doi:10.1021/acsptsci.9b00083

37.     Vizurraga A, Adhikari R, Yeung J, Yu M, Tall GG. Mechanisms of Adhesion G protein Coupled Receptor Activation. *J Biol Chem*. Published online August 6, 2020:jbc.REV120.007423. doi:10.1074/jbc.REV120.007423

38.     Møller TC, Moreno-Delgado D, Pin J-P, Kniazeff J. Class C G protein-coupled receptors: reviving old couples with new partners. *Biophys Rep*. 2017;3(4-6):57-63. doi:10.1007/s41048-017-0036-9

39.     Kozielewicz P, Turku A, Schulte G. Molecular Pharmacology of Class F Receptor Activation. *Mol Pharmacol*. 2020;97(2):62-71. doi:10.1124/mol.119.117986

40.     Nichols AS, Floyd DH, Bruinsma SP, Narzinski K, Baranski TJ. Frizzled receptors signal through G proteins. *Cell Signal*. 2013;25(6):1468-1475. doi:10.1016/j.cellsig.2013.03.009

41.     Arensdorf AM, Marada S, Ogden SK. Smoothened Regulation: A Tale of Two Signals. *Trends Pharmacol Sci*. 2016;37(1):62-72. doi:10.1016/j.tips.2015.09.001

42.     Venkatakrishnan AJ, Deupi X, Lebon G, Tate CG, Schertler GF, Babu MM. Molecular signatures of G-protein-coupled receptors. *Nature*. 2013;494(7436):185-194. doi:10.1038/nature11896

43.     Adams MN, Ramachandran R, Yau M-K, et al. Structure, function and pathophysiology of protease activated receptors. *Pharmacol Ther*. 2011;130(3):248-282. doi:10.1016/j.pharmthera.2011.01.003

44.     Purcell RH, Hall RA. Adhesion G Protein–Coupled Receptors as Drug Targets. *Annu Rev Pharmacol Toxicol*. 2018;58(1):429-449. doi:10.1146/annurev-pharmtox-010617-052933

45.     Coughlin SR. How the protease thrombin talks to cells. *Proc Natl Acad Sci*. 1999;96(20):11023-11027. doi:10.1073/pnas.96.20.11023

46.     Liebscher I, Schöneberg T. Tethered Agonism: A Common Activation Mechanism of Adhesion GPCRs. In: Langenhan T, Schöneberg T, eds. *Adhesion G Protein-Coupled Receptors*. Vol 234. Handbook of Experimental Pharmacology. Springer International Publishing; 2016:111-125. doi:10.1007/978-3-319-41523-9_6

47.     Heuberger DM, Schuepbach RA. Protease-activated receptors (PARs): mechanisms of action and potential therapeutic modulators in PAR-driven inflammatory diseases. *Thromb J*. 2019;17(1):4. doi:10.1186/s12959-019-0194-8

48.     Ramachandran R, Noorbakhsh F, DeFea K, Hollenberg MD. Targeting proteinase-activated receptors: therapeutic potential and challenges. *Nat Rev Drug Discov*. 2012;11(1):69-86. doi:10.1038/nrd3615

49.     Nakanishi-Matsui M, Zheng Y-W, Sulciner DJ, Weiss EJ, Ludeman MJ, Coughlin SR. PAR3 is a cofactor for PAR4 activation by thrombin. *Nature*. 2000;404(6778):609-613. doi:10.1038/35007085

50.     Hamann J, Aust G, Araç D, et al. International Union of Basic and Clinical Pharmacology. XCIV. Adhesion G Protein–Coupled Receptors. Ohlstein EH, ed. *Pharmacol Rev*. 2015;67(2):338-367. doi:10.1124/pr.114.009647

51.     Scholz N, Langenhan T, Schöneberg T. Revisiting the classification of adhesion GPCRs. *Ann N Y Acad Sci*. 2019;1456(1):80-95. doi:10.1111/nyas.14192

52.     Bassilana F, Nash M, Ludwig M-G. Adhesion G protein-coupled receptors: opportunities for drug discovery. *Nat Rev Drug Discov*. 2019;18(11):869-884. doi:10.1038/s41573-019-0039-y

53.     Gad AA, Balenga N. The Emerging Role of Adhesion GPCRs in Cancer. *ACS Pharmacol Transl Sci*. 2020;3(1):29-42. doi:10.1021/acsptsci.9b00093

54.     Langenhan T, Piao X, Monk KR. Adhesion G protein-coupled receptors in nervous system development and disease. *Nat Rev Neurosci*. 2016;17(9):550-561. doi:10.1038/nrn.2016.86

55.     Lin H-H, Hsiao C-C, Pabst C, Hébert J, Schöneberg T, Hamann J. Adhesion GPCRs in Regulating Immune Responses and Inflammation. In: *Advances in Immunology*. Vol 136. Elsevier; 2017:163-201. doi:10.1016/bs.ai.2017.05.005

56.     Safaee M, Clark AJ, Ivan ME, et al. CD97 is a multifunctional leukocyte receptor with distinct roles in human cancers. *Int J Oncol*. 2013;43(5):1343-1350. doi:10.3892/ijo.2013.2075

57.    Araç D, Leon K. Structure, function and therapeutic potential of adhesion GPCRs. In: *GPCRs*. Elsevier; 2020:23-41. doi:10.1016/B978-0-12-816228-6.00002-7

58.    Yeung J, Adili R, Stringham EN, et al. GPR56/ADGRG1 is a platelet collagen-responsive GPCR and hemostatic sensor of shear force. *Proc Natl Acad Sci*. 2020;117(45):28275-28286. doi:10.1073/pnas.2008921117

59.    Stoveken HM, Hajduczok AG, Xu L, Tall GG. Adhesion G protein-coupled receptors are activated by exposure of a cryptic tethered agonist. *Proc Natl Acad Sci*. 2015;112(19):6194-6199. doi:10.1073/pnas.1421785112

60.    Demberg LM, Winkler J, Wilde C, et al. Activation of Adhesion G Protein-coupled Receptors. *J Biol Chem*. 2017;292(11):4383-4394. doi:10.1074/jbc.M116.763656

61.    Liebscher I, Schön J, Petersen SC, et al. A Tethered Agonist within the Ectodomain Activates the Adhesion G Protein-Coupled Receptors GPR126 and GPR133. *Cell Rep*. 2014;9(6):2018-2026. doi:10.1016/j.celrep.2014.11.036

62.    Kishore A, Purcell RH, Nassiri-Toosi Z, Hall RA. Stalk-dependent and Stalk-independent Signaling by the Adhesion G Protein-coupled Receptors GPR56 (ADGRG1) and BAI1 (ADGRB1). *J Biol Chem*. 2016;291(7):3385-3394. doi:10.1074/jbc.M115.689349

63.    Salzman GS, Zhang S, Gupta A, Koide A, Koide S, Araç D. *Stachel* -independent modulation of GPR56/ADGRG1 signaling by synthetic ligands directed to its extracellular region. *Proc Natl Acad Sci*. 2017;114(38):10095-10100. doi:10.1073/pnas.1708810114

64.    Huang BX, Hu X, Kwon H-S, et al. Synaptamide activates the adhesion GPCR GPR110 (ADGRF1) through GAIN domain binding. *Commun Biol*. 2020;3(1):109. doi:10.1038/s42003-020-0831-6

65.     Ping Y-Q, Mao C, Xiao P, et al. Structures of the glucocorticoid-bound adhesion receptor GPR97–Go complex. *Nature*. Published online January 6, 2021. doi:10.1038/s41586-020-03083-w

66.     Lee J-W, Huang BX, Kwon H, et al. Orphan GPR110 (ADGRF1) targeted by N-docosahexaenoylethanolamine in development of neurons and cognitive function. *Nat Commun*. 2016;7(1):13123. doi:10.1038/ncomms13123

67.     Stoveken HM, Larsen SD, Smrcka AV, Tall GG. Gedunin- and Khivorin-Derivatives Are Small-Molecule Partial Agonists for Adhesion G Protein-Coupled Receptors GPR56/ADGRG1 and GPR114/ADGRG5. *Mol Pharmacol*. 2018;93(5):477-488. doi:10.1124/mol.117.111476

68.     Hamann J, Petrenko AG. Introduction: History of the Adhesion GPCR Field. In: Langenhan T, Schöneberg T, eds. *Adhesion G Protein-Coupled Receptors*. Vol 234. Handbook of Experimental Pharmacology. Springer International Publishing; 2016:1-11. doi:10.1007/978-3-319-41523-9_1

69.     Veninga H, Becker S, Hoek RM, et al. Analysis of CD97 Expression and Manipulation: Antibody Treatment but Not Gene Targeting Curtails Granulocyte Migration. *J Immunol*. 2008;181(9):6574-6583. doi:10.4049/jimmunol.181.9.6574

70.     Yin Y, Xu X, Tang J, et al. CD97 Promotes Tumor Aggressiveness Through the Traditional G Protein–Coupled Receptor–Mediated Signaling in Hepatocellular Carcinoma. *Hepatology*. 2018;68(5):1865-1878. doi:10.1002/hep.30068

71.     Becker S, Wandel E, Wobus M, et al. Overexpression of CD97 in Intestinal Epithelial Cells of Transgenic Mice Attenuates Colitis by Strengthening Adherens Junctions. Bereswill S, ed. *PLoS ONE*. 2010;5(1):e8507. doi:10.1371/journal.pone.0008507

72.     Hilbig D, Dietrich N, Wandel E, et al. The Interaction of CD97/ADGRE5 With β-Catenin in Adherens Junctions Is Lost During Colorectal Carcinogenesis. *Front Oncol*. 2018;8:182. doi:10.3389/fonc.2018.00182

73. Ward Y, Lake R, Yin JJ, et al. LPA Receptor Heterodimerizes with CD97 to Amplify LPA-Initiated RHO-Dependent Signaling and Invasion in Prostate Cancer Cells. *Cancer Res*. 2011;71(23):7301-7311. doi:10.1158/0008-5472.CAN-11-2381

74. Hsiao C-C, Keysselt K, Chen H-Y, et al. The Adhesion GPCR CD97/ADGRE5 inhibits apoptosis. *Int J Biochem Cell Biol*. 2015;65:197-208. doi:10.1016/j.biocel.2015.06.007

75. Rioux JD, Silverberg MS, Daly MJ, et al. Genomewide Search in Canadian Families with Inflammatory Bowel Disease Reveals Two Novel Susceptibility Loci. *Am J Hum Genet*. 2000;66(6):1863-1870. doi:10.1086/302913

76. Mathew CG. Genetics of inflammatory bowel disease: progress and prospects. *Hum Mol Genet*. 2004;13(90001):161R - 168. doi:10.1093/hmg/ddh079

77. Leemans JC, te Velde AA, Florquin S, et al. The Epidermal Growth Factor-Seven Transmembrane (EGF-TM7) Receptor CD97 Is Required for Neutrophil Migration and Host Defense. *J Immunol*. 2004;172(2):1125-1131. doi:10.4049/jimmunol.172.2.1125

78. Capasso M, Durrant LG, Stacey M, Gordon S, Ramage J, Spendlove I. Costimulation via CD55 on Human CD4 [+] T Cells Mediated by CD97. *J Immunol*. 2006;177(2):1070-1077. doi:10.4049/jimmunol.177.2.1070

79. van Pel M, Hagoort H, Hamann J, Fibbe WE. CD97 is differentially expressed on murine hematopoietic stem-and progenitor-cells. *Haematologica*. 2008;93(8):1137-1144. doi:10.3324/haematol.12838

80. Yona S, Lin H, Dri P, et al. Ligation of the adhesion-GPCR EMR2 regulates human neutrophil function. *FASEB J*. 2008;22(3):741-751. doi:10.1096/fj.07-9435com

81. Huang Y-S, Chiang N-Y, Hu C-H, et al. Activation of Myeloid Cell-Specific Adhesion Class G Protein-Coupled Receptor EMR2 via Ligation-Induced Translocation and Interaction of Receptor Subunits in Lipid Raft Microdomains. *Mol Cell Biol*. 2012;32(8):1408-1420. doi:10.1128/MCB.06557-11

82.     Chiang N-Y, Hsiao C-C, Huang Y-S, et al. Disease-associated GPR56 Mutations Cause Bilateral Frontoparietal Polymicrogyria via Multiple Mechanisms. *J Biol Chem*. 2011;286(16):14215-14225. doi:10.1074/jbc.M110.183830

83.     Singer K, Luo R, Jeong S-J, Piao X. GPR56 and the Developing Cerebral Cortex: Cells, Matrix, and Neuronal Migration. *Mol Neurobiol*. 2013;47(1):186-196. doi:10.1007/s12035-012-8343-0

84.     Piao X. G Protein-Coupled Receptor-Dependent Development of Human Frontal Cortex. *Science*. 2004;303(5666):2033-2036. doi:10.1126/science.1092780

85.     Li S, Jin Z, Koirala S, et al. GPR56 Regulates Pial Basement Membrane Integrity and Cortical Lamination. *J Neurosci*. 2008;28(22):5817-5826. doi:10.1523/JNEUROSCI.0853-08.2008

86.     Luo R, Jeong S-J, Jin Z, Strokes N, Li S, Piao X. G protein-coupled receptor 56 and collagen III, a receptor-ligand pair, regulates cortical development and lamination. *Proc Natl Acad Sci*. 2011;108(31):12925-12930. doi:10.1073/pnas.1104821108

87.     Saito Y, Kaneda K, Suekane A, et al. Maintenance of the hematopoietic stem cell pool in bone marrow niches by EVI1-regulated GPR56. *Leukemia*. 2013;27(8):1637-1649. doi:10.1038/leu.2013.75

88.     Chen G, Yang L, Begum S, Xu L. GPR56 is essential for testis development and male fertility in mice. *Dev Dyn*. 2010;239(12):3358-3367. doi:10.1002/dvdy.22468

89.     Park D, Tosello-Trampont A-C, Elliott MR, et al. BAI1 is an engulfment receptor for apoptotic cells upstream of the ELMO/Dock180/Rac module. *Nature*. 2007;450(7168):430-434. doi:10.1038/nature06329

90.     Das S, Owen KA, Ly KT, et al. Brain angiogenesis inhibitor 1 (BAI1) is a pattern recognition receptor that mediates macrophage binding and engulfment of Gram-negative bacteria. *Proc Natl Acad Sci*. 2011;108(5):2136-2141. doi:10.1073/pnas.1014775108

91.     Hochreiter-Hufford AE, Lee CS, Kinchen JM, et al. Phosphatidylserine receptor BAI1 and apoptotic cells as new promoters of myoblast fusion. *Nature*. 2013;497(7448):263-267. doi:10.1038/nature12135

92.     Duman JG, Tzeng CP, Tu Y-K, et al. The Adhesion-GPCR BAI1 Regulates Synaptogenesis by Controlling the Recruitment of the Par3/Tiam1 Polarity Complex to Synaptic Sites. *J Neurosci*. 2013;33(16):6964-6978. doi:10.1523/JNEUROSCI.3978-12.2013

93.     Demberg LM, Rothemund S, Schöneberg T, Liebscher I. Identification of the tethered peptide agonist of the adhesion G protein-coupled receptor GPR64/ADGRG2. *Biochem Biophys Res Commun*. 2015;464(3):743-747. doi:10.1016/j.bbrc.2015.07.020

94.     Nazarko O, Kibrom A, Winkler J, et al. A Comprehensive Mutagenesis Screen of the Adhesion GPCR Latrophilin-1/ADGRL1. *iScience*. 2018;3:264-278. doi:10.1016/j.isci.2018.04.019

95.     Ramachandran R, Mihara K, Mathur M, et al. Agonist-Biased Signaling via Proteinase Activated Receptor-2: Differential Activation of Calcium and Mitogen-Activated Protein Kinase Pathways. *Mol Pharmacol*. 2009;76(4):791-801. doi:10.1124/mol.109.055509

96.     Thibeault PE, LeSarge JC, Arends D, et al. Molecular basis for activation and biased signaling at the thrombin-activated GPCR proteinase activated receptor-4 (PAR4). *J Biol Chem*. 2020;295(8):2520-2540. doi:10.1074/jbc.RA119.011461

97.     Ramachandran R, Mihara K, Thibeault P, et al. Targeting a Proteinase-Activated Receptor 4 (PAR4) Carboxyl Terminal Motif to Regulate Platelet Function. *Mol Pharmacol*. 2017;91(4):287-295. doi:10.1124/mol.116.106526

98.     Ramachandran R, Mihara K, Chung H, et al. Neutrophil Elastase Acts as a Biased Agonist for Proteinase-activated Receptor-2 (PAR2). *J Biol Chem*. 2011;286(28):24638-24648. doi:10.1074/jbc.M110.201988

99.     Griesbeck O, Baird GS, Campbell RE, Zacharias DA, Tsien RY. Reducing the Environmental Sensitivity of Yellow Fluorescent Protein. *J Biol Chem*. 2001;276(31):29188-29194. doi:10.1074/jbc.M102815200

100.    Thibeault PE, Ramachandran R. Role of the Helix-8 and C-Terminal Tail in Regulating Proteinase Activated Receptor 2 Signaling. *ACS Pharmacol Transl Sci*. 2020;3(5):868-882. doi:10.1021/acsptsci.0c00039

101.    Olsen RHJ, DiBerto JF, English JG, et al. TRUPATH, an open-source biosensor platform for interrogating the GPCR transducerome. *Nat Chem Biol*. 2020;16(8):841-849. doi:10.1038/s41589-020-0535-8

102.    Kroeze WK, Sassano MF, Huang X-P, et al. PRESTO-Tango as an open-source resource for interrogation of the druggable human GPCRome. *Nat Struct Mol Biol*. 2015;22(5):362-369. doi:10.1038/nsmb.3014

103.    Barnea G, Strapps W, Herrada G, et al. The genetic design of signaling cascades to record receptor activation. *Proc Natl Acad Sci*. 2008;105(1):64-69. doi:10.1073/pnas.0710487105

104.    Pfleger KDG, Eidne KA. Illuminating insights into protein-protein interactions using bioluminescence resonance energy transfer (BRET). *Nat Methods*. 2006;3(3):165-174. doi:10.1038/nmeth841

105.    Ayoub MA, Pin J-P. Interaction of Protease-Activated Receptor 2 with G Proteins and β-Arrestin 1 Studied by Bioluminescence Resonance Energy Transfer. *Front Endocrinol*. 2013;4. doi:10.3389/fendo.2013.00196

106.    Laroche G, Giguère PM. Measurement of β-Arrestin Recruitment at GPCRs Using the Tango Assay. In: Tiberi M, ed. *G Protein-Coupled Receptor Signaling*. Vol 1947. Methods in Molecular Biology. Springer New York; 2019:257-267. doi:10.1007/978-1-4939-9121-1_14

107.    Waugh DS. An overview of enzymatic reagents for the removal of affinity tags. *Protein Expr Purif*. 2011;80(2):283-293. doi:10.1016/j.pep.2011.08.005

108.    Le Bonniec BF, Myles T, Johnson T, Knight CG, Tapparelli C, Stone SR. Characterization of the P $_2$ ' and P $_3$ ' Specificities of Thrombin Using Fluorescence-Quenched Substrates and Mapping of the Subsites by Mutagenesis ·. *Biochemistry*. 1996;35(22):7114-7122. doi:10.1021/bi952701s

109.    Schechter I, Berger A. On the size of the active site in proteases. I. Papain. *Biochem Biophys Res Commun*. 1967;27(2):157-162. doi:10.1016/S0006-291X(67)80055-X

110.    Mathiasen S, Palmisano T, Perry NA, et al. G12/13 is activated by acute tethered agonist exposure in the adhesion GPCR ADGRL3. *Nat Chem Biol*. 2020;16(12):1343-1350. doi:10.1038/s41589-020-0617-7

111.    Gosalia DN, Salisbury CM, Ellman JA, Diamond SL. High Throughput Substrate Specificity Profiling of Serine and Cysteine Proteases Using Solution-phase Fluorogenic Peptide Microarrays. *Mol Cell Proteomics*. 2005;4(5):626-636. doi:10.1074/mcp.M500004-MCP200

112.    Liu B, Lee G, Wu J, et al. The PAR2 signal peptide prevents premature receptor cleavage and activation. Vaudry H, ed. *PLOS ONE*. 2020;15(2):e0222685. doi:10.1371/journal.pone.0222685

113.    Thibeault PE, Ramachandran R. Biased signaling in platelet G-protein coupled receptors. *Can J Physiol Pharmacol*. 2021;99(3):255-269. doi:10.1139/cjpp-2020-0149

114.    Araç D, Leon K. Structure, function and therapeutic potential of adhesion GPCRs. In: *GPCRs*. Elsevier; 2020:23-41. doi:10.1016/B978-0-12-816228-6.00002-7

115.    Hein L, Ishii K, Coughlin SR, Kobilka BK. Intracellular targeting and trafficking of thrombin receptors. A novel mechanism for resensitization of a G protein-coupled receptor. *J Biol Chem*. 1994;269(44):27719-27726. doi:10.1016/S0021-9258(18)47045-7

116.    Shapiro MJ, Trejo J, Zeng D, Coughlin SR. Role of the Thrombin Receptor's Cytoplasmic Tail in Intracellular Trafficking. *J Biol Chem*. 1996;271(51):32874-32880. doi:10.1074/jbc.271.51.32874

117.    White JP, Wrann CD, Rao RR, et al. G protein-coupled receptor 56 regulates mechanical overload-induced muscle hypertrophy. *Proc Natl Acad Sci*. 2014;111(44):15756-15761. doi:10.1073/pnas.1417898111

118.    Yin Y, Xu X, Tang J, et al. CD97 Promotes Tumor Aggressiveness Through the Traditional G Protein–Coupled Receptor–Mediated Signaling in Hepatocellular Carcinoma. *Hepatology*. 2018;68(5):1865-1878. doi:10.1002/hep.30068

119.    Bhudia N, Desai S, King N, et al. G Protein-Coupling of Adhesion GPCRs ADGRE2/EMR2 and ADGRE5/CD97, and Activation of G Protein Signalling by an Anti-EMR2 Antibody. *Sci Rep*. 2020;10(1):1004. doi:10.1038/s41598-020-57989-6

120.    Juneja J, Casey PJ. Role of G12 proteins in oncogenesis and metastasis. *Br J Pharmacol*. 2009;158(1):32-40. doi:10.1111/j.1476-5381.2009.00180.x

121.    Lämmermann T, Kastenmüller W. Concepts of GPCR -controlled navigation in the immune system. *Immunol Rev*. 2019;289(1):205-231. doi:10.1111/imr.12752

122.    Hörnquist CE, Lu X, Rogers-Fani PM, et al. G(alpha)i2-deficient mice with colitis exhibit a local increase in memory CD4+ T cells and proinflammatory Th1-type cytokines. *J Immunol Baltim Md 1950*. 1997;158(3):1068-1077.

123.    Rudolph U, Finegold MJ, Rich SS, et al. Ulcerative colitis and adenocarcinoma of the colon in Gαi2-deficient mice. *Nat Genet*. 1995;10(2):143-150. doi:10.1038/ng0695-143

124.    Shevtsov SP, Haq S, Force T. Activation of β-catenin Signaling Pathways by Classical G-Protein-Coupled Receptors: Mechanisms and Consequences in Cycling and Non-cycling Cells. *Cell Cycle*. 2006;5(20):2295-2300. doi:10.4161/cc.5.20.3357

125.    Laprise P, Chailler P, Houde M, Beaulieu J-F, Boucher M-J, Rivard N. Phosphatidylinositol 3-Kinase Controls Human Intestinal Epithelial Cell Differentiation by Promoting Adherens Junction Assembly and p38 MAPK Activation. *J Biol Chem*. 2002;277(10):8226-8234. doi:10.1074/jbc.M110235200

126.    Hilbig D, Sittig D, Hoffmann F, et al. Mechano-Dependent Phosphorylation of the PDZ-Binding Motif of CD97/ADGRE5 Modulates Cellular Detachment. *Cell Rep*. 2018;24(8):1986-1995. doi:10.1016/j.celrep.2018.07.071

127.    Depoortere I. Taste receptors of the gut: emerging roles in health and disease. *Gut*. 2014;63(1):179-190. doi:10.1136/gutjnl-2013-305112

128.    I K-Y, Huang Y-S, Hu C-H, et al. Activation of Adhesion GPCR EMR2/ADGRE2 Induces Macrophage Differentiation and Inflammatory Responses via Gα16/Akt/MAPK/NF-κB Signaling Pathways. *Front Immunol*. 2017;8. doi:10.3389/fimmu.2017.00373

129.    Kilts JD, Gerhardt MA, Richardson MD, et al. $\beta_2$-Adrenergic and Several Other G Protein–Coupled Receptors in Human Atrial Membranes Activate Both $G_s$ and $G_i$. *Circ Res*. 2000;87(8):705-709. doi:10.1161/01.RES.87.8.705

130.    Hu Q-X, Dong J-H, Du H-B, et al. Constitutive Gαi Coupling Activity of Very Large G Protein-coupled Receptor 1 (VLGR1) and Its Regulation by PDZD7 Protein. *J Biol Chem*. 2014;289(35):24215-24225. doi:10.1074/jbc.M114.549816

131.    Shin D, Lin S-T, Fu Y-H, Ptacek LJ. Very large G protein-coupled receptor 1 regulates myelin-associated glycoprotein via $G_s$/$G_q$-mediated protein kinases A/C. *Proc Natl Acad Sci*. 2013;110(47):19101-19106. doi:10.1073/pnas.1318501110

132.    Little KD, Hemler ME, Stipp CS. Dynamic Regulation of a GPCR-Tetraspanin-G Protein Complex on Intact Cells: Central Role of CD81 in Facilitating GPR56-Gα$_{q/11}$ Association. *Mol Biol Cell*. 2004;15(5):2375-2387. doi:10.1091/mbc.e03-12-0886

133.    Stephenson JR, Paavola KJ, Schaefer SA, Kaur B, Van Meir EG, Hall RA. Brain-specific Angiogenesis Inhibitor-1 Signaling, Regulation, and Enrichment in the Postsynaptic Density. *J Biol Chem*. 2013;288(31):22248-22256. doi:10.1074/jbc.M113.489757

134.    Sun Y, Zhang D, Ma M-L, et al. Optimization of a peptide ligand for the adhesion GPCR ADGRG2 provides a potent tool to explore receptor biology. *J Biol Chem*. 2021;296:100174. doi:10.1074/jbc.RA120.014726

135.    Kim BH, Pereverzev A, Zhu S, Tong AOM, Dixon SJ, Chidiac P. Extracellular nucleotides enhance agonist potency at the parathyroid hormone 1 receptor. *Cell Signal*. 2018;46:103-112. doi:10.1016/j.cellsig.2018.02.015

136.    Trejo J, Coughlin SR. The Cytoplasmic Tails of Protease-activated Receptor-1 and Substance P Receptor Specify Sorting to Lysosomes versusRecycling. *J Biol Chem*. 1999;274(4):2216-2224. doi:10.1074/jbc.274.4.2216

137.    Maser RL, Calvet JP. Adhesion GPCRs as a paradigm for understanding polycystin-1 G protein regulation. *Cell Signal*. 2020;72:109637. doi:10.1016/j.cellsig.2020.109637

138.    O'Callaghan K, Kuliopulos A, Covic L. Turning Receptors On and Off with Intracellular Pepducins: New Insights into G-protein-coupled Receptor Drug Development. *J Biol Chem*. 2012;287(16):12787-12796. doi:10.1074/jbc.R112.355461

139.    Ortiz Zacarías NV, Lenselink EB, IJzerman AP, Handel TM, Heitman LH. Intracellular Receptor Modulation: Novel Approach to Target GPCRs. *Trends Pharmacol Sci*. 2018;39(6):547-559. doi:10.1016/j.tips.2018.03.002

140.    Chaturvedi M, Schilling J, Beautrait A, Bouvier M, Benovic JL, Shukla AK. Emerging Paradigm of Intracellular Targeting of G Protein-Coupled Receptors. *Trends Biochem Sci*. 2018;43(7):533-546. doi:10.1016/j.tibs.2018.04.003

141.    Huang H-L, Hsing H-W, Lai T-C, et al. Trypsin-induced proteome alteration during cell subculture in mammalian cells. *J Biomed Sci*. 2010;17(1):36. doi:10.1186/1423-0127-17-36

142.    Nguyen ST, Nguyen HT-L, Truong KD. Comparative cytotoxic effects of methanol, ethanol and DMSO on human cancer cell lines. *Biomed Res Ther*. 2020;7(7):3855-3859. doi:10.15419/bmrat.v7i7.614

# Curriculum Vitae

| | |
|---|---|
| **Name:** | Victor Mirka |
| **Post-secondary Education and Degrees:** | The University of Western Ontario<br>London, Ontario, Canada<br>Masters of science<br>Degree planned to be conferred October 2021<br>2019-2021 |
| | The University of Western Ontario<br>London, Ontario, Canada<br>Bachelor of Medical Science<br>Honors specialization: Physiology and Pharmacology<br>Degree conferred June 2019<br>2015-2019 |
| **Honours and Awards:** | Province of Ontario Graduate Scholarship<br>2019-2021 |
| **Related Work Experience:** | Teaching Assistant<br>The University of Western Ontario<br>Pharm 3620<br>2020-2021 |
| | Teaching Assistant<br>The University of Western Ontario<br>PhysPharm 3000E<br>2019-2020 |

**Publications:**

Mirka V, Ramachandran R. (2021) Allosteric modulation of tethered ligand activated receptors. ELSEVIER. In press.